



# Design of a Novel Propulsion Mechanism for Flexible Endoscopes Inspired by Plant Root Growth.

A Bio-Inspired Solution to Propagation through the Human Colon.



Daan Verheijen





# Design of a Novel Propulsion Mechanism for Flexible Endoscopes Inspired by Plant Root Growth.

A Bio-Inspired Solution to Propagation through the Human Colon

To obtain the degree of Master of Science in Mechanical Engineering.  
An electronic version of this thesis is available at <http://repository.tudelft.nl/>.



DELFT UNIVERSITY OF TECHNOLOGY

MASTER THESIS

Master: Mechanical Engineering  
Track: BioMechanical Design (BMD)  
Specialization: BioInspired Technology (BITE)

|                              |  |
|------------------------------|--|
| <i>Student Name:</i>         | <i>Daan Verheijen</i>  |
| <i>Student Number:</i>       | <i>4232356</i>   |
| <i>Supervisors:</i>          | <i>Prof. dr. ir. P. Breedveld</i><br><i>Dr. ir. A. Sakes</i> |
| <i>Graduation committee:</i> | <i>Dr. J. Zhou</i>   |





# ABSTRACT

When inserting a flexible endoscope into a human colon during colonoscopy, limitations in the endoscope design can cause medical implications such as excessive colon stretching and buckling of the endoscope shaft. This thesis proposes a novel propulsion mechanism design for flexible endoscopes which changes the method of insertion as a way to prevent these implications. As inspiration for the design an analogy is drawn between plant roots growing through tortuous cracks in soil and flexible endoscopes moving through a tortuous human colon. The analogy was found to be relevant, resulting in eight biological features of which seven were suitable as a potential solution in the development of a flexible endoscope. Of these seven suitable solutions, apical extension and variable stiffness were implemented as functions in the proposed propulsion mechanism. The focus of the design process on these two functions ultimately culminated in a proof of concept flexible, extending endoscope design dubbed the Flextendoscope. The Flextendoscope consists of an inverted tube mechanism which can propel the endoscope through apical extension combined with a fiber jamming mechanism that can vary the bending stiffness. The concept design is found very promising as it theoretically allows insertion of a highly compliant shaft which is also able to provide the high tip rigidity required at the surgical location after insertion. Although evaluation of the Flextendoscope prototype validated the feasibility of the proposed proof of concept design, the performance of the apical extension function was of a more limited success. Due to internal frictional resistances the prototype shaft only extended under the lowest evaluated pressure (0.5 bar) and required a high manual force (up to 119 Newtons) to do so. The behavior of the variable stiffness function on the other hand was found to be very desirable. The bending stiffness of the prototype increased with internal pressure level as well as radial deflection, showing initial elastic deformation followed by hysteresis. It showed considerable stiffening at a convenient threshold pressure of 0.7 bar, slightly above the pressure at which the shaft is extended. Future iterations of the Flextendoscope design should focus on overcoming the internal frictional resistances that limit the apical extension of the current design. They can do so by multiplying the number of inverted tubes inside the shaft. This multiplication would enclose the sliding shaft material of each inverted tube within their own central lumen thus avoiding contact between the sliding shaft material and other stationary components in the design, preventing frictional interactions. If the frictional resistance is overcome the Flextendoscope design could prevent colon stretching during insertion of an flexible endoscope and inherently prevent shaft buckling. The prevention of these implications by the Flextendoscope design could ultimately lead to colonoscopy becoming an easier, safer and less painful procedure with a higher success rate.

# CONTENTS

|  |           |
|--|-----------|
| <b>1 Introduction .....</b>  | <b>1</b>  |
| 1.1 Background .....   | 1         |
| 1.2 Problem Statement .....  | 2         |
| 1.3 Scope .....  | 4         |
| 1.4 Goal .....   | 4         |
| 1.5 Structure .....  | 4         |
| <b>2 Biological Inspiration .....</b>  | <b>5</b>  |
| 2.1 Introduction .....   | 5         |
| 2.2 Plant Root Growth .....  | 5         |
| 2.3 From Biology to Technology .....   | 7         |
| 2.4 State of the Art in Plant Root Growth Inspired Propulsion Mechanisms ..... | 9         |
| 2.5 Conclusion .....   | 10        |
| <b>3 Conceptual Design .....</b>   | <b>12</b> |
| 3.1 Design Focus .....   | 12        |
| 3.2 Design Requirements .....  | 12        |
| 3.3 Theoretical Solution Areas .....   | 13        |
| 3.3.1 Apical Extension .....   | 13        |
| 3.3.2 Variable Stiffness in Bending .....                                      | 14        |
| 3.4 Concept Generation .....   | 15        |
| 3.5 Concept Designs .....  | 18        |
| 3.5.1 Concept One .....  | 18        |
| 3.5.2 Concept Two .....  | 19        |
| 3.5.3 Concept Three .....  | 20        |
| 3.6 Selection of Final Concept .....   | 20        |
| <b>4 Final Design .....</b>  | <b>23</b> |
| 4.1 From Concept to Final Design .....   | 23        |
| 4.2 Design Detailing .....   | 25        |
| 4.2.1 Shaft .....  | 25        |
| 4.2.2 Housing .....  | 27        |
| 4.3 Initial Prototype .....  | 27        |
| 4.4 Flextendoscope .....   | 31        |
| <b>5 Evaluation .....</b>  | <b>33</b> |
| 5.1 Experiments .....  | 33        |
| 5.1.1 Experimental Goal .....  | 33        |
| 5.1.2 Experimental Methods .....   | 33        |

|  |           |
|--|-----------|
| 5.2 Results.....                                   | 35        |
| 5.3 Discussion of the Results .....                | 38        |
| <b>6 Discussion .....</b>                          | <b>40</b> |
| 6.1 Overview .....                                 | 40        |
| 6.2 Prototype Behavior .....                       | 40        |
| 6.3 Design Limitations and Recommendations .....   | 41        |
| 6.4 Scientific Relevance and Future Research ..... | 44        |
| <b>7 Conclusion.....</b>                           | <b>45</b> |
| Bibliography .....                                 | 46        |
| Appendix A: Technical Design Drawings .....        | 48        |
| Appendix B: MATLAB Data Analysis Scripts .....     | 57        |
| Appendix C: Concept Design Ideation.....           | 61        |
| Appendix D: Steerable Flexendoscope Concepts ..... | 63        |



# 1 INTRODUCTION

## 1.1. BACKGROUND

### Flexible Endoscopes

Over the last century, innovations in endoscopic instrumentation have greatly expanded the ability of physicians to diagnose and treat afflictions inside the human body [1]. One of these innovations is the development of endoscopes with a flexible shaft as an addition to previously rigid ones. A state of the art flexible endoscope, shown in Figure 1.1, consists of a long, thin and flexible tube that has a steerable tip at its anterior end and a control handle at its posterior end. Endoscopes are designed this way so that they can be inserted deep into a patient's body through a small natural orifice.

The tip of an endoscope contains LED lights and a small camera to record video images of the patient's internal tissue, which can be displayed live on a screen outside a patient's body. The handle contains one or two controls that enable a physician to control the direction of the tip from outside the body through single or multidirectional steering. The flexible shaft has a central hollow space, or lumen, which consists of multiple separate channels. These channels allow for the delivery or removal of gasses, fluids and surgical instruments to and from the site of surgical interest, near the inserted endoscope tip. Lastly, Bowden cables and electronic wiring are implemented through the shaft to actuate the steering mechanism and electronic equipment inside the tip.

The design of flexible endoscopes varies slightly depending on the organ system for which they are intended to be used, for example colonoscopes for use in the colon and bronchoscopes for use in the lungs. Flexible endoscopes generally have a length up to approximately 1.8 meters and range from about 5 to 15 millimeters in width [2].

### Endoscopic Interventions

The innovation of endoscopes with a flexible shaft has allowed for non-invasive exploration of tortuous, tubular organs by means of endoluminal interventions through a natural orifice, such as the mouth, anus and vagina. This has made previously hard to reach locations in the human body more easily accessible. Nowadays, flexible endoscopes have become indispensable and are commonplace in most hospitals [1]. There, they are used to



Figure 1.1: A state of the art flexible endoscope with a tip on the anterior end (right), a control handle on the posterior end (left) and a flexible tube or shaft, connecting the two. From: E.D. Rozeboom, et al. [3].

perform a range of both diagnostic and therapeutic interventions. The purpose of these interventions entail actions such as checking for cancers, taking biopsy samples or removing earlier identified polyps and other abnormalities. Flexible endoscopes are most commonly used to perform interventions in the human gastrointestinal tract, where the shape and flexibility of the endoscope are optimal to traverse the long and tubular organs that form the tract. An overview of the gastrointestinal tract is given in Figure 1.2.

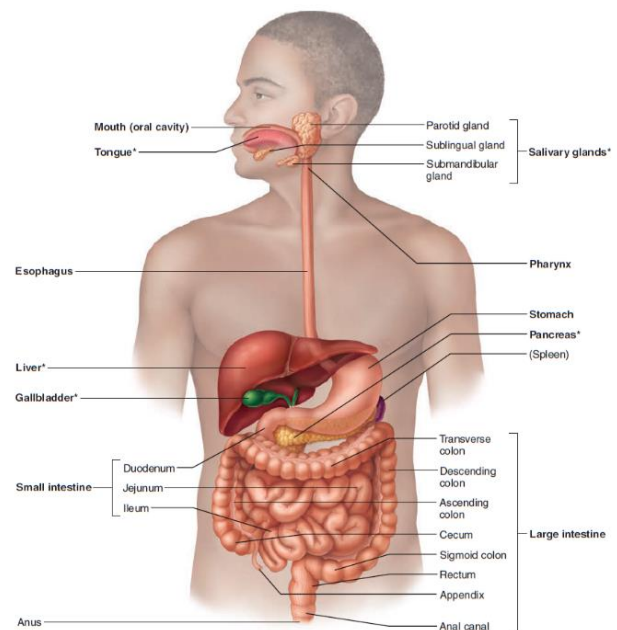


Figure 1.2: Overview of the human gastrointestinal tract and its internal organs, running all the way from the mouth to the anus. From: E.N. Marieb and K. Hoehn, 2016 [4].

## Gastrointestinal Tract

The gastrointestinal tract runs through the body from the mouth to the anus, consisting of the *pharynx*, *esophagus*, *stomach*, as well as the small and large *intestine*. The walls of the gastrointestinal cavity and its organs consist of four layers. From inside to outside these are the *mucosa*, *submucosa*, *muscularis externa* and *serosa*, as depicted in Figure 1.3. The *mucosa* is a mucous membrane that mainly serves to secrete digestive enzymes and protect against infectious disease [4]. The protective lining is very sensitive and excessive contact can result in ulceration, irritation and inflammation, which can be very painful. The remaining three layers around the mucosa respectively contain a large amount of blood vessels and nerve fibers, muscle cells and finally connective tissue [4].

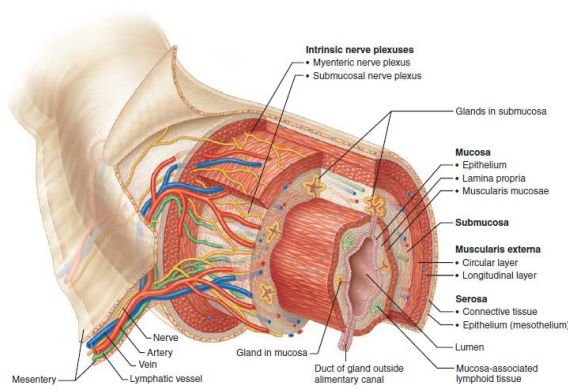


Figure 1.3: Section view of the four layers in the gastrointestinal tract wall, which from inside to outside are the mucosa, submucosa, muscularis externa and the serosa. From: E.N. Marieb and K. Hoehn, 2016 [4].

## Colonoscopy

A colonoscopy is the performance of an endoscopic procedure inside a specific region of the gastrointestinal tract, namely the large intestine or colon, which can be accessed via entry through the anus. The colon gives the least amount of support and guidance to an endoscope compared to the other organs in the gastrointestinal tract that are frequently traversed by flexible endoscopes. This is because the colon is the most compliant and relatively tortuous [2]. This makes colonoscopies one of the most difficult types of endoscopic interventions to perform, requiring specialized and frequently trained maneuvers to insert an endoscope successfully into the colon [5]. Figure 1.4 shows a flexible endoscope that is fully inserted into a human colon and gives an overview of some of the

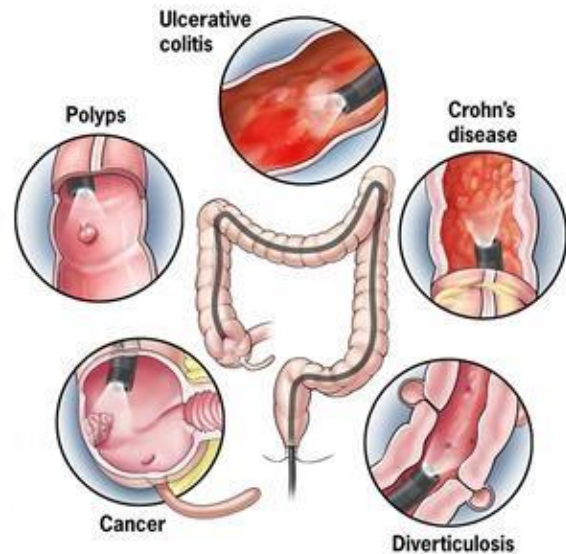


Figure 1.4: Center: Image of a flexible endoscope that is fully inserted into the colon. Outside: Multiple abnormalities that can be encountered during a colonoscopy.

abnormalities that might be detected during a colonoscopy.

## 1.2. PROBLEM STATEMENT

### Problem introduction

When performing a colonoscopy, a gastroenterologist inserts a flexible endoscope through the patient's anus. It is manually pushed through the colon from the entry point to the area of medical interest, which can be located at any point along the tortuous cavity. The manual pushing forces, applied at the posterior handle, can have a magnitude of up to approximately 29 N. Additionally, the gastroenterologist actively steers the tip of the endoscope to maneuver it around bends in the colon. The shaft that follows, however, is passively guided by the surrounding colon walls while relying on its own (limited) flexibility to maneuver through bends in the colon. As a consequence, the endoscope shaft partially transfers the manually applied insertion forces to the colon wall tissue in the form of normal forces up to a magnitude of around 13 N (depending on the bending stiffness of the endoscope shaft). [6]. This contact establishment and subsequent transmission of normal forces has a number of implications, which are shown in Figure 1.5.

### Implication 1: Colon Stretching

Firstly, these contact normal forces stretch the colon wall at the bend. This continues until the stress that is built up in the colon wall tissue is large

enough to deflect the flexible endoscope shaft around that bend. This increases the radius of the colon's bend considerably compared to its radius in an undisturbed state. Although the colon is very elastic, this excessive stretching can cause considerable pain, complicate the insertion process and increase the chance of wall perforation [5].

### Implication 2: Shaft Buckling

Secondly, the endoscope's shaft can buckle if its tip is pressed into the close-lying colon wall when pushed beyond the bend [5]. The subsequent reaction force at the tip in combination with the posterior insertion pushing force result in an axially compressive load on the shaft. The endoscope shaft is highly vulnerable to these compressive stresses due to the long, slender and flexible nature of its design, making it susceptible to buckling. The buckling adds a force at the contact point in the colon bend in addition to the previously transferred insertion push forces. This further increases stretching and the chance of wall perforation at the contact point in the colon bend.

### Implication 3: Shaft Sliding

Finally, excessive contact between the manually pushed endoscope shaft and the colon wall can result in the transmission of shear forces. This is due to the frictional nature of the contact interaction between the sliding shaft and the stationary colon wall. Initially, transmission of these shear forces is prevented (through the secretion of mucous by membranes inside the colon) but will still occur in the case of continued excessive contact. Similar to the transferred normal forces, shear forces further increase colon wall stretching and thereby also increase the change of complications such as wall perforation occurring.

### Consequent Problems

To successfully and safely insert a flexible endoscope into a patient's colon, the occurrence of aforementioned implications has to be prevented. This currently requires the performance of highly skilled endoscope maneuvers such as N-loops and  $\alpha$ -loops. These maneuvers require many training runs to master. This makes colonoscopy very difficult, expensive, time consuming, painful and of limited success as avoidance of the implication can not be fully guaranteed [5]. Therefore, in order to improve the patient's experience, reduce training

costs and increase the procedural ease and success-rate, research should look at redesigning state of the art flexible endoscopes to overcome the following limitations in their current design.

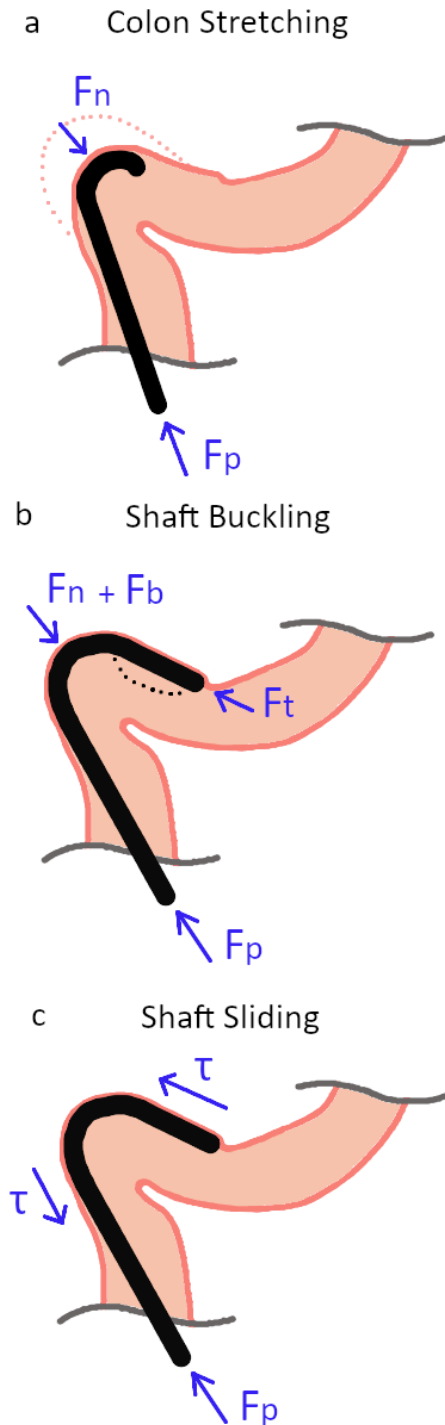


Figure 1.5: a) Colon stretching due to partial transmission of the endoscope's push insertion forces ( $F_p$ ) applied to the colon in the form of normal forces ( $F_n$ ) at the contact point. b) Shaft buckling and the subsequent transmission of buckling forces ( $F_b$ ) due to the combination of reaction forces at the tip ( $F_t$ ) and push insertion forces at the handle ( $F_p$ ). c) Transmission of shear forces ( $\tau$ ) due to the frictional nature of the contact interaction between the sliding endoscope shaft and the stationary colon wall.



### Limitations of Current Flexible Endoscope Design

The previously stated implications and consequent problems can be attributed to three limitations in current state of the art flexible endoscope design:

1. *The steering capability of current flexible endoscopes is limited to the tip.*

Firstly, the steering capability being limited to only the tip is what causes the endoscope shaft to come in contact with the colon tissue.

2. *The existence of paradoxical bending stiffness requirements force a tradeoff to be made in the degree of flexibility of current endoscope shafts.*

Secondly, contradictory stiffness requirements force a tradeoff to be made in the degree of flexibility of an endoscope shaft. On the one hand, the endoscope shaft needs to be stiff in bending to 1) facilitate the tip stability required to accurately perform a medical procedure at the site of surgical interest and to 2) be able to transmit the posteriorly applied push forces through the shaft to the tip. On the other hand, the shaft needs to be compliant in bending to allow passive deflection around bends in the colon without transmitting excessive forces to wall tissue at the contact points.

3. *The flexible endoscope tip and shaft have to be inserted by sliding through the posterior application of manual push forces.*

Lastly, the current push insertion method results in undesirable sliding contact interaction between the endoscope and the colon wall and additionally requires the endoscope shaft to have some degree of stiffness in bending during the insertion process.

### 1.3. SCOPE

In order to overcome these limitations in state of the art flexible endoscopes and improve colonoscopic procedures, multiple aspects of the current flexible endoscope design will have to be reconsidered. To make a start in that process, this thesis will focus on the method of endoscope insertion and propose a proof of concept design of a novel propulsion mechanism for flexible endoscopes.

Changing the method of insertion to something other than sliding insertion through posterior push forces has the potential to overcome all three

limitations in current flexible endoscope design. Additionally, the manner of flexible endoscope insertion into a colon is interesting as it has so far remained largely unexplored. The research in this thesis is aimed to serve as an initial stepping stone for further exploration into this topic. Therefore, it will focus on assessment of the proof of concept's rudimentary functionality as well as the potential and suitability of the solution it provides. Consequently, readiness of the design for application in a human colon is outside the scope of this thesis.

Finally, endoscope steerability is left outside the scope of this thesis. Including it would greatly complicate the design while it could still be added in later stages of the development. Furthermore, the Bio-Inspired Technology research group (BITE) from the Delft University of Technology, already has a lot of experience in making steerable instruments and adding steerability functionality to previously passive instruments [7,8,9].

### 1.4. GOAL

The goal of the research is to design and evaluate a proof of concept prototype of a passively steered propulsion mechanism for the purpose of propagating a flexible endoscope through a colon-shaped cavity in a manner that inherently prevents both shaft buckling and the transmission of excessive contact forces (related to colon stretching and shaft sliding).

### 1.5. STRUCTURE

This thesis describes the design and evaluation of a novel flexible endoscope propulsion mechanism. The rest of this thesis will be structured as follows: Chapter two discusses plant root growth, which forms a biological inspiration for the mechanism design. It subsequently translates the biological features of plant root growth into technical principles and discusses the state of the art in plant root inspired mechanisms. Chapter three considers the design focus and design requirements. It leads into the initial design process, resulting in multiple concept mechanisms and ending with the selection of one of them. Chapter four describes the continued development of the chosen concept into a detailed final design and the prototype production. Chapter five evaluates the prototype through a series of experiments. It entails both the experiment design and the obtained results. Finally, chapters six and seven contain the discussion and conclusion.

## 2 BIOLOGICAL INSPIRATION

### 2.1. INTRODUCTION

This chapter will look at plant root growth as a source of inspiration for the design proposed in this thesis. Biological inspiration proves valuable because an analogy can be drawn between a mechanical design problem and an organism in nature that deals with a mechanically comparable situation within its natural habitat. Through that analogy, it is then possible to observe what traits, morphologies and behaviors the analogous organism has developed and consequently improve the proposed design by adapting it based on the made observations. In this chapter, such an analogy is drawn between the movement of a flexible endoscope through the tortuous tubular colon inside a human body and the movement of a plant root through a narrow, tortuous crack inside the earth's soil.

First, the plant root growth mechanism is analyzed to identify the key features that make a plant root function the way it does. These biological features are then translated into the underlying core mechanical principles. These principles are judged on whether they would be suitable as a solution for endoscope propulsion into the human colon and if that solution would be within the scope of this thesis. Finally this chapter looks at the state of the art in plant root growth inspired propulsion mechanisms as an additional source of inspiration. The identified mechanical principles that allow roots to move through soil so efficiently (and are suitable for colonoscopy) will be used in future chapters as a basis for the development of the proposed propulsion mechanism design.

Plant roots are chosen as the source of inspiration because they are able to propagate through cracks in soil under a greatly reduced frictional resistance compared to mechanically pushed shafts. They are also able to actively avoid resistive normal forces from being applied on their tip while finding a path of least resistance through the soil and actively avoiding buckling of their body.

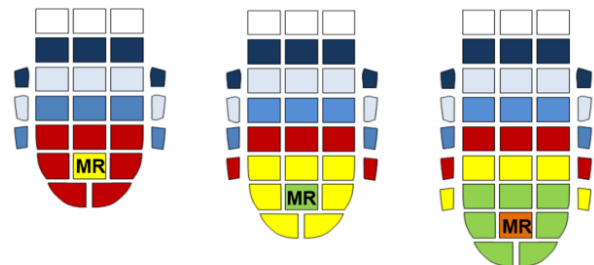
### 2.2. PLANT ROOT GROWTH

#### Phases of the root growth cycle

Plant root growth, schematically represented in Figure 2.1, is a cyclical process that consists of two

phases, primary growth and secondary growth. In the primary growth phase, the root elongates axially at the tip. In the secondary growth phase, the previously axially elongated section of the root is radially thickened. Plant roots are flexible organs and their geometry depends on the relative magnitudes of the primary and secondary growth phases. These magnitudes can change based on interactions of the root with surrounding soil as shown in Figure 2.2.

Primary growth will slow or cease completely if the resistance of the surrounding soil on the root tip exceeds the growth pressure that the root itself can generate [10]. In response the root will thicken by increasing the magnitude of its secondary growth phase. The radial thickening increases the surface area with which the root can exert pressure on the surrounding soil. Additionally, the radial expansion causes tensile stresses to build up in the surrounding soil. This ultimately results in a weakening of the anterior soil as a zone of stress relief is created in front of the tip. As the resistance of the anterior soil on the root tip decreases the magnitude of the primary growth phase is increased and the root continues to elongate through the weakened soil. The cycle of reduced primary growth, increased secondary growth, anterior stress relief and continued primary growth is repeated continually. Although it remains unknown how plant roots are able to moderate their growth cycles, it is speculated that growth substances such as auxin play a role in shaping the expanding cells and altering the morphology of mechanically impeded roots [11,12].



*Figure 2.1: The movement of cells over time (from left to right) during plant root growth. Segments of the same color represent cells that proliferated around the same moment in time at the meristematic region (MR). After proliferation cells move backward to form the mature zone of the root or move forward to form the root cap. Cells continuously slough from the root cap, sloughed cells do not move with respect to the surrounding soil as the tip grows further into the soil. From A. Sadeghi, et al., 2014 [13]*

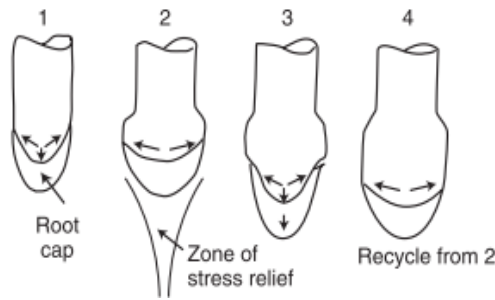


Figure 2.2: The process of growth in an impeded root shown in four stages. 1) slowed axial growth. 2) increased radial growth and subsequent axial stress relief 3) continued axial growth until further impedance. 4) further radial growth and stress relief. From: A.M. Abdalla, et al., 1969 [14]

### Plant root zones

The root of a plant is divided into multiple zones as shown in Figure 2.3. Plant root growth originates near the tip of the root in the meristematic zone. In this zone new cells are created through cell division. After division, some cells move anteriorly to regenerate the root cap, however, most new cells move posteriorly to the elongation zone. There they expand driven by the internal turgor pressure [10]. Although cell division in the apical meristem is essential for growth, the largest increase in the root's volume is due to the later cell expansion [11]. After the expansion, the meristematic cells differentiate to become the main tissue of the root. This forms a mature zone behind the root tip. The mature zone remains stationary to the surrounding soil as the meristematic zone and tip continue to elongate in axial direction. Root hairs and secondary lateral roots will eventually grow from this mature zone to fixate the roots to its surroundings. The mature zone gives the root a foundation to oppose the growth pressure at its tip, allowing the root to grow into the anterior soil without slipping.

### Altering growth direction

The tip of a plant root is able to sense the resistive forces applied to it by the surrounding soil and consequently alter the growth direction of the root. By altering direction the root avoids denser patches in the soil, minimizing the pressure that the root tip has to exert to continue growing. This allows the root to follow least-resistance pathways through the soil such as naturally occurring cracks. The alteration of direction is accomplished through a combination of active movements of the root

apex, such as circumnutation, and passive deflection through bending of the flexible tip.

### Protection of the root tip

As the root propagates through the soil, the meristematic zone is protected by the root cap on the tip. Sloughing border cap cells and mucigel (a slimy substance secreted from the root tip) form a sheath around the root tip. This separates the elongation zone of the root from the abrasive surrounding soil. The sheath remains stationary relative to the surrounding soil, reducing the friction experienced by the growing root with a factor 3 to 5 [15]. The root cap is continuously regenerated by a small portion of meristematic cells that move anteriorly after cell division and that differentiate into cap cells to compensate for the deformation of the root cap due to cell sloughing.

### High energetic cost

Propagation through soil has a very high energetic cost compared to terrestrial, aquatic or aerial locomotion, given the high resistance to penetration of the medium [16]. The interaction of the biological features found within the plant root growth mechanism is what allows the root to adapt to the surrounding soil and propagate itself effectively.

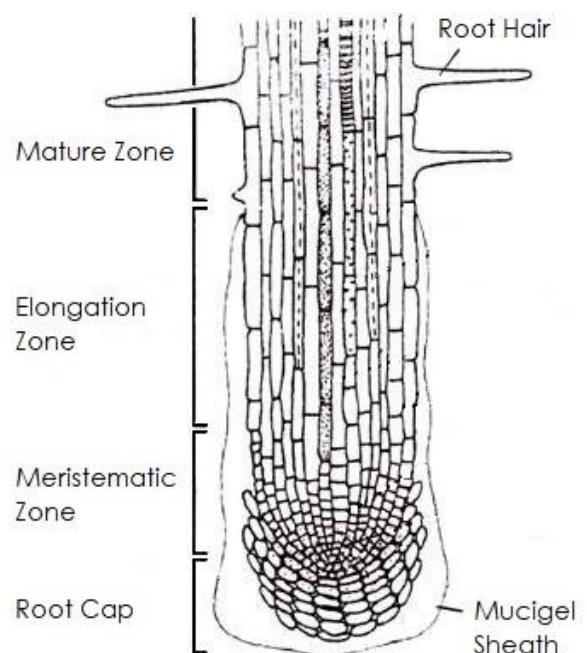


Figure 2.3: Schematic section view of a growing root tip indicating the different zones that together make up a plant root.



## 2.3. FROM BIOLOGY TO TECHNOLOGY

### Interpretation of the biological inspiration

When using nature as an inspirational source for technological development, it is important to interpret the behavior and functionality of the inspirational source in a way that is most beneficial to the design. This involves picking and choosing the properties of the biological phenomenon that are favorable to the design. The goal of the analogy drawn between flexible endoscope propagation and plant root growth is not to design an endoscope that like a plant root proliferates cells. Rather, the goal is to replicate the effects of the inner workings such as cell proliferation to design a propagation mechanism with a comparable external mechanical functionality. In this section, the previously discussed functionality of the plant root growth mechanism is dissected into separate biological features. Of each feature the exact function or purpose is pinpointed, the underlying core mechanical principle is described and the suitability of the principle's offered solution is determined. This results in a list of core mechanical principles that can assist in finding a solution to the design problem of this thesis. A summarized overview of this list is shown in Table 2.1.

#### Biological feature 1: Primary growth

The first biological feature to be addressed is primary growth initiated from the meristematic zone in the root apex. The main function of this feature is to propel the root tip in axial direction. However, by initiating growth from the root apex exclusively, an inherent secondary functionality emerges, which is the creation of a stationary, mature zone behind the root apex. The underlying

mechanical principle is elongation of the body through the addition of material at the apex. This specific action is from now on referred to as "apical extension" [17].

Firstly, the principle of apical extension could serve as a way to propel an endoscope tip into the colon. Secondly, it is a potential solution to the transmission of excessive shear forces during endoscope insertion because it would limit the sliding movement along the colon wall to the endoscope tip as the rest of the endoscope body remains stationary. Finally, it offers a solution to endoscope shaft buckling. The application of propulsion forces at the tip of the endoscope, rather than at the posterior handle, would inherently prevent the build up of axial compressive stresses inside the endoscope shaft, making buckling impossible.

#### Biological feature 2: Secondary growth

The function of secondary growth is to actively thicken the plant root. The underlying mechanical principle is an active variability of a body's second moment of area. This allows a root to actively control its critical buckling load as well as the normal force that is exerted by its body or tip before deforming in bending. Actively decreasing the second moment of area of a flexible endoscope could be a suitable solution to prevent excessive normal force transmission and thus prevent colon stretching. Actively increasing the second moment of area of a flexible endoscope to prevent shaft buckling would, however, not be a suitable solution. The increase would prevent shaft bending and ultimately result in perforation of the colon wall.

*Table 2.1: Overview of the eight biological features of the plant root growth mechanism, with their function, underlying mechanical principle, their part in the potential solution, suitability of that solution for MIS and if that solution falls within the scope of this thesis.*

| Biological Feature   | Function in Root Growth | Underlying Mechanical Principle              | Potential Solution to                                     | Suitable  | Within Scope |
|----------------------|-------------------------|--|---|-----------|--------------|
| Primary Growth       | Root Tip Propulsion     | Apical Extension                             | Probe Tip Propulsion, Buckling & Shear Force Transmission | Yes       | Yes          |
| Secondary Growth     | Root Body Thickening    | Change in Second Moment of Area              | Buckling<br>Normal Force Transmission                     | No<br>Yes | Yes          |
| Cell Differentiation | Root Body Stiffening    | Change in Young's Modulus                    | Buckling<br>Normal Force Transmission                     | No<br>Yes | Yes          |
| Root Hair Growth     | Root Body Anchoring     | Change in Unsupported Length                 | Buckling<br>Normal Force Transmission                     | No        | Yes          |
| Tip Sensing          | Reducing Tip Forces     | Sensor-Actuator Feedback Loop                | Buckling<br>Normal Force Transmission                     | Yes       | No           |
| Circumnutation       | Root Tip Orientation    | Actuated Helical Movement                    | Buckling & Normal Force Transmission                      | Yes       | No           |
| Root Cap Sloughing   | Root Tip Shielding      | Placement of an Intermediate layer or Sheath | Shear Force Transmission                                  | Yes       | Yes          |
| Mucilage Excretion   | Root Tip Shielding      | Wet Lubrication of Contact Surfaces          | Shear Force Transmission                                  | Yes       | Yes          |

### **Biological feature 3: Cell differentiation**

The main (mechanical) function of cell differentiation is to stiffen and maintain the shape of the root body by developing a woody internal structure. The mechanical principle underlying this feature is an active variability in the Young's Modulus of the bodily material. Similar to the previous biological feature, this feature also allows a root to actively control its critical buckling load and the normal force that is exerted by its body or tip before deforming in bending. Actively reducing the Young's Modulus of a flexible endoscope shaft could therefore also serve as a suitable way to prevent excessive normal force transmission and thus prevent colon stretching. Actively increasing the Young's Modulus of a flexible endoscope shaft to prevent buckling is, however, not a suitable solution because it would also ultimately prevent shaft bending and thus result in perforation of the colon wall.

### **Biological feature 4: Root hair growth**

The main (mechanical) function of root hair growth is to anchor the mature root to its surroundings. The underlying mechanical principle is a decrease in the effective unsupported length of a body (as measured from its tip) by creating fixation points to the surrounding environment closer to the tip. Similar to the previous two biological features, This feature allows a root to control its critical buckling load as well as the normal force that is exerted by its body or tip before deforming in bending [18,19]. This principle would not be suitable as a solution to prevent buckling or to reduce the normal force transmission during flexible endoscope insertion. The anchoring would ultimately induce the very colon wall penetration that is to be avoided.

### **Biological feature 5: Tip sensing**

The function tip sensing is to communicate the axial resistive forces on the root tip to the meristematic zone. The underlying technical principle is a feedback loop communication between a force sensor and actuator. This feature allows a root to actively avoid excessive force transmission at its tip. A sensor - actuator feedback loop would be suitable solution to actively prevent excessive normal force transmission and buckling caused by the contact of an endoscope tip with the colon wall. However, the underlying principle is outside the thesis scope because active steering of

the endoscope tip as a potential solution is not explored in this thesis for reasons explained in Section 1.3.

### **Biological feature 6: Circumnutation**

The function of circumnutation is to continuously move the root tip in a helical motion to enable tactile exploration of the surroundings by the tip. The mechanical principle behind circumnutation is a continuously actuated change in tip orientation. This feature allows the sensing root tip to find the point of lowest resistance in the anterior growth medium. This principle is a suitable solution to the prevention of shaft buckling and excessive normal force transmission. However, like the previous principle, the solution falls outside the scope of this thesis as it would also require active steering of the endoscope tip.

### **Biological feature 7: Root cap sloughing**

The main (mechanical) function of root cap sloughing is to isolate the root tip from the surrounding soil by creating an intermediate layer of cells between the tip and the soil. The mechanical principle behind this biological feature is a change of the frictional interaction between to layers through the placement of an intermediate layer or sheath. This feature allows a root to move through soil under a greatly reduced frictional resistance because the layer of sloughed cells has a lower coefficient of friction than the surrounding soil. The release of loose particles into a colon is highly undesired and as such not a suitable solution to prevent shear force transmission caused by excessive shaft sliding. However, the placement of an intermediate layer that remains attached to the flexible endoscope body would be a suitable alternative.

### **Biological feature 8: Mucilage excretion**

The function of mucilage excretion is to reduce the friction between the root tip and its surroundings by releasing a slimy gel from sloughed cap cells. The underlying mechanical principle is the lowering of the frictional coefficient between two sliding contact surfaces through wet lubrication. This allows a root to grow through soil under a reduced frictional resistance. Wet lubrication would be a suitable solution to prevent transmission of shear forces to a colon wall caused by excessive sliding of a flexible endoscope.

### The essence of plant root growth

Of the features discussed above, primary growth, or apical extension, is the most iconic feature of plant root growth and forms the essence of the plant root growth mechanism. This feature is what allows the root to extend through the soil with a flexible body to avoid denser patches of soil and thus lowers its penetration resistance. Furthermore, it reduces the frictional interaction by establishing a stationary mature zone behind the apex. Primary growth would serve as a solution to shear force transmission as well as normal force transmission of a flexible endoscope and would also inherently prevent shaft buckling. Additionally, the underlying mechanical principle, apical extension, was found to be suitable for use in colonoscopy and within the scope of this thesis. Therefore, the next section will look into the state of the art in apical extension mechanisms that were inspired by plant root growth to further inspire the design process of this thesis.

## 2.4. STATE OF THE ART IN PLANT ROOT GROWTH INSPIRED PROPULSION MECHANISMS

### Method of database exploration

To identify the range of existing plant root growth inspired mechanisms, a semi systematic search of the Scopus database was conducted through an iterative process using several different search queries combining keywords such as: *root, vine, hyphae, grow\*, propul\*, elong\*, extent\*, apical, inspired, mechanism, tool, device and instrument*. After this initial sweep of the database, Scopus was searched again based on new keywords, identified in previous relevant search results, such as: *inverted-tube* and *eversion*. Additionally, the database was searched on the names of authors of relevant previous search results.

The search yielded fifteen records that describe mechanisms which are either consciously inspired on plant root growth or that use of apical extension as the method for propulsion. The identified records describe twelve separate mechanisms, shown in Figure 2.4, each using one of five fundamental underlying concepts to translate the mechanical principle into a functional propulsion mechanism. In the following sections each of these fundamental concept types is discussed separately.

### Mechanism type 1: Inverted tube mechanisms

The largest group of growth inspired mechanisms, identified during the database exploration, is that of inverted tubes. An inverted tube consists of a soft, flexible and thin-walled hollow tube, often made of plastics such as LDPE, which is inverted into itself. The inverted section of the tube is spooled up and stored posteriorly. This results in an enclosed volume between the external, everted, and internal, inverted walls of the tube as can be seen in the designs in Figures 2.4-A to E.

Increasing the pressure inside the enclosed volume causes the tube to evert at its tip. This increasing the length of the tube at its apex while the previously everted tubing (forming the outside layer) remains stationary. The internal pressure is generally pneumatically controlled as is the case in mechanisms 2.4-A to D. It can, however, also be hydraulically controlled as in mechanism shown in Figure 2.4-E.

The direction of apical extension in these mechanisms is controlled through passive, active or mechanically programmed steering. Passive steering (used by mechanisms A and E) relies on the flexibility of the extending continuum body to deflect the mechanism around surrounding obstacles upon contact. The mechanism by J.D. Greer et al. (Figure 2.4-C) actively controls the direction of its tip with static pneumatic chambers positioned in series around the circumference of the tube. By inflating these chambers on one side of the everted tube that side is shortened in length compared to the opposing side. This causes the inverted tube to bent towards its the inflated side. The direction of extension in the mechanism by P. Slade, *et al.*, in Figure 2.4-B is mechanically programmed into the tube prior to inversion. The shape of the tube is longer on one side compared to the other side in certain sections of the tube to create bends in the tube when everted.

Inverted tube mechanisms can only extend for the length of tubing that is stored on the spool and is thus finite in length.

### Mechanism type 2: Additive layering mechanisms

The growth inspired additive layering mechanisms developed by Sadeghi, A. et al. can be seen in Figures 2.4-F and 2.4-G. These mechanisms extend anteriorly using an additive layering technique similar to that seen in FDM printing. In the tip of these mechanisms, a rotatable deposition head 3D

prints a circular layer of material on top of the surface behind the tip. As the deposition head rotates, the helical shape of the tip pushes itself onto the newly printed material. This causes the deposition head, which is connected to the tip, to also move upwards, thus freeing up space underneath the printing nozzle. By continuing this process layer by layer, a helical tubular structure is created.

The mechanism in Figure 2.4-G can control the direction of extension by continuously changing the direction of rotation at the deposition head. This increases the layer count on one side of the tube compared to that of the other side. This ultimately results in the tip tilting to the side with the lower layer count, thus creating a bend. The extension of these mechanisms is irreversible as the layers fuse together. Bends created in the tubular body are therefore permanent.

#### **Mechanism type 3: Skin eversion mechanisms**

Sadeghi, A. et al. also designed skin eversion mechanisms that consist of a solid hollow shaft, with a flexible and soft “continuum skin” stored inside the shaft [20]. The front of the skin is everted around the anterior tip of the shaft and externally fixed to the surroundings. As the rigid shaft is pushed forward, the skin is forced to evert anteriorly. The extension is limited to the length of the internally stored skin as well as the length of the solid shaft. Because the solid shaft is pushed into the continuum skin, the extension is created at the posterior end of the mechanism rather than at its apex. However, the skin imitates the function of apical cell sloughing, causing a reduction of friction and shear forces between the rigid shaft and the surroundings as it extends [20]. Furthermore, as the everted skin remains stationary relative to the surroundings, a mature region is created by the skin posterior to the region of extension.

The first device developed by Sadeghi, A. et al., shown in figure 2.4-H, is not steerable as the inserted shaft is fully rigid. The second mechanism in figure 2.4-I consists of multiple rigid segments (which can swivel relative to each other) enabling discrete passive steering. These mechanisms are similar to the inverted tube mechanisms discussed above but have a solid internal body driving the eversion of the inverted skin instead of a gas or liquid.

#### **Mechanism type 4: Unwinding tube mechanisms**

Similar to inverted tube mechanisms, the unwinding tube mechanism developed by Dehgahni, H. et al. also consists of a soft and flexible thin-walled polymer tube, the extension of which is controlled using pneumatic actuation at the posterior end of the device. As the pressure within the tube increases, new tubing is released from the spool causing lengthening at the tip of the mechanism. However, instead of the tubing being stored posteriorly and everting at the tip, the material is stored in the tip of the device, resulting in a radial expansion of the tubing as it inflates after rolling from the spool. Extension of the mechanism is finite as all material for future lengthening has to be stored in the tip of the device. Steering of the mechanism is once more passive, relying on the soft inflated continuum body to deflect upon contact of the tip with the surrounding environment. The mechanism developed by Dehgahni, H. et al., can be seen in figure 2.4-J.

#### **Mechanism type 5: Concentric tube mechanisms**

Although not consciously based or inspired on root growth, concentric tube mechanisms do extend in a manner similar to continuous apical extension. These mechanisms consist of pre-curved, semi-rigid, hollow, concentric tubes of consecutively decreasing diameter, nested inside each other. After the outermost hollow tube has been fully extended it forms an axially stationary base. The next concentric segment can then be extended forward, emerging from the tip of the previous hollow tube. This process can continue cyclically where the maximum extension length of the mechanism is limited by the length of the individual segments, the external diameter and the wall thickness of the consecutive hollow tubes.

Steering is accomplished by predetermining the shape of each consecutive segment during the design, referred to as mechanical programming. By rotating the pre-curved segments relative to each other, several different bends and shapes can be achieved during the extension. An example of a concentric tube mechanism designed by Morimoto, T.K. et al. is shown in Figure 2.4-K.

## **2.5 CONCLUSION**

The exploration of plant root growth resulted in identification of eight biological features and their underlying mechanical principles. Of these eight

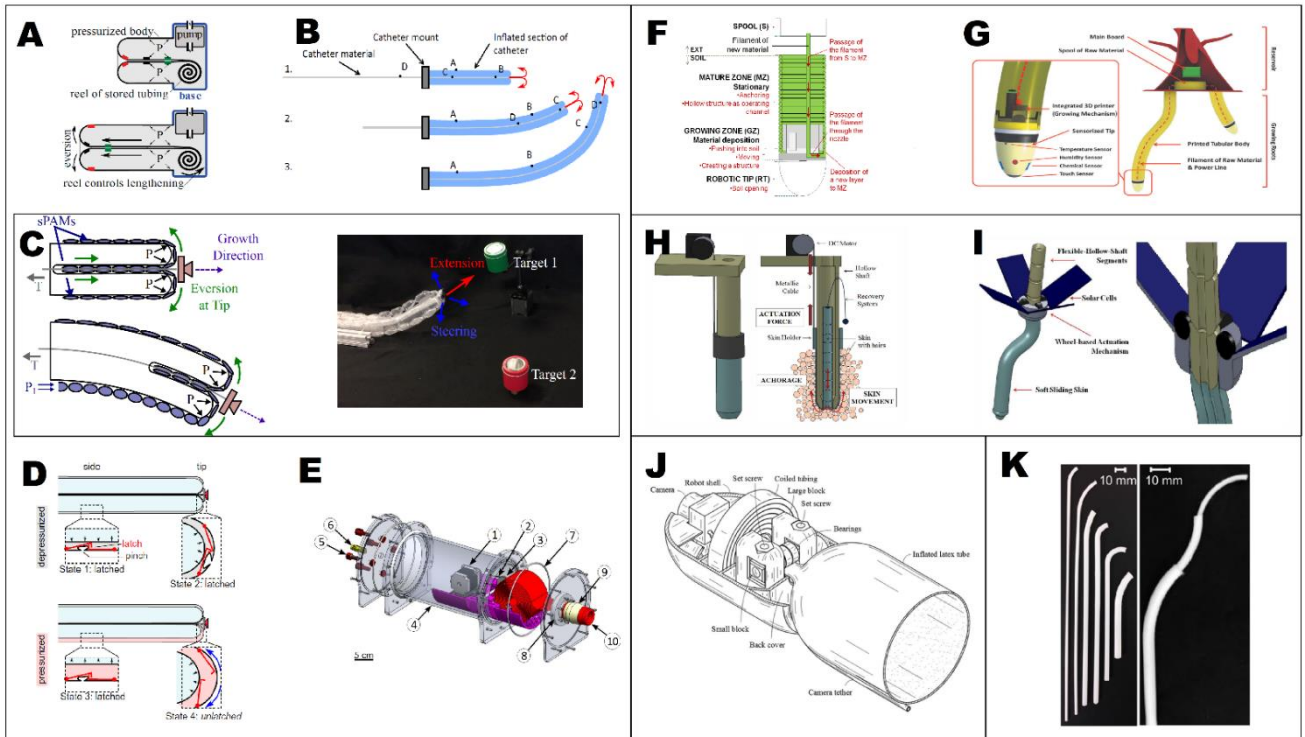


Figure 2.4: Collection of the state of the art in root growth inspired propulsion mechanisms. (A) J.D. Greer, et al. [21]. (B) P. Slade, et al. [17]. (C) by J.D. Greer et al. [22]. (D) E.W. Hawkes, et al. [23] (E) J. Luong, et al. [24]. (F) A. Sadeghi, et al. [13]. (G) A. Sadeghi, et al. [25]. (H) A. Sadeghi, et al. [20]. (I) A. Sadeghi, et al. [20]. (J) H. Dehgahni, et al. [26]. (K) T.K. Morimoto, et al. [17].

mechanical principles, seven were found suitable as a solution to (at least) one of the problems faced during flexible endoscope insertion into a colon. Of these seven suitable solutions, six were found to also be within the scope of this thesis. As such, the analogy between flexible endoscope insertion and plant root growth is shown to be very appropriate, relevant and useful to the design process in this thesis.

To extend the endoscope tip apical extension is found suitable and within the scope of the thesis. To prevent buckling of the endoscope shaft, apical extension of the endoscope shaft is found to be both suitable and within the scope of the thesis. To prevent excessive normal force transmission by a flexible endoscope, actively changing either the Young's modulus or the second moment of area is found to be suitable and within the scope of the thesis. To prevent excessive transmission of shear forces by a flexible endoscope, apical extension, placement of an intermediate layer and wet lubrication are all found suitable and within the scope of the thesis.

Of the plant root growth inspired mechanisms identified in the state of the art, the group of inverted tube mechanisms is most suitable for the design of a flexible endoscope, closely followed by unwinding tube mechanisms and skin eversion

mechanisms. Inverted tube mechanisms are the most suitable for multiple reasons. Firstly, they consist of a very simple structure and are therefore easily scaled down in size. Secondly, they are generally soft upon contact and relatively flexible in bending, which allows them to passively adapt to the internal structure of a colon. Finally, their extension and material supply can be controlled from the posterior side, outside a patient's body.



## 3 CONCEPTUAL DESIGN

### 3.1. DESIGN FOCUS

In this chapter, a conceptual design for the flexible endoscope propulsion mechanism is proposed based on the goal of this thesis and the existing biological solutions, which were discussed in previous chapters. The proposed design has two focus points: apical extension and variable stiffness in bending.

Firstly, it focuses on a propulsion mechanism that can insert a flexible endoscope into a colon-shaped cavity by means of apical extension. Insertion through apical extension will herein replace the design limitation of posterior push insertion. This allows the design to overcome its current medical implications of shaft buckling and shaft sliding as compressive stresses can no longer build up in the endoscope shaft and the shaft remains stationary relative to the surrounding colon wall. Moreover, apical extension no longer requires the endoscope shaft to maintain a high degree of stiffness in bending to successfully insert the endoscope tip, as was the case with posterior push insertion. This allows the design to maintain a very compliant shaft during insertion and overcome the medical implication of colon stretching due to excessive normal force transmission.

Secondly, the design will focus on variability in stiffness of the extended endoscope shaft through for example a change in the shafts second moment of area or Young's modulus as seen in plant root growth. This is because the endoscope shaft still requires a high stiffness in bending after the insertion process. This is required because the tip needs sufficient rigidity to precisely and successfully perform surgical procedures such as taking biopsies or removing polyps from the colon wall.

### 3.2. DESIGN REQUIREMENTS

#### Functional Requirements

The functional requirements form the set of conditions to which the functionality of the design must conform in order for it to be considered satisfactory. They serve as a guideline for the design phase but also as a way to differentiate between the expected performance of multiple design concepts and evaluate the performance of

a physical prototype. The functional requirements are based on the basic functionalities of a colonoscope with addition of the two new design aspects mentioned in the design focus.

1. **Insertion through Apical Extension:** *The endoscope must be insertable into a colon-shaped cavity through apical extension of the endoscope's shaft in such a way that compressive stresses cannot build up inside the shaft, the process is repeatable and that results in a stationary zone behind the endoscope tip.*
2. **Manual propulsion force control:** *The forces used to propel the endoscope must be manually controllable from a handle outside the colon-shaped cavity.*
3. **Self-Propulsion:** *The endoscope must be able to propagate through a colon-shaped cavity without relying on external forces generated through contact with the cavity wall.*
4. **Retraction:** *The endoscope must be retractable out of a colon-shaped cavity through reversal of the apical extension method used during the endoscope insertion process.*
5. **Shaft Flexibility:** *The endoscope's shaft must be able to maintain a low degree of stiffness in bending during the insertion process, such that it can be passively deflected by a colon wall without excessively stretching it.*
6. **Variability of Shaft Stiffness:** *The endoscope's shaft must be able to actively vary its degree of stiffness in bending through variation of one or more of the controlling parameters once extended to the site of surgical interest.*

#### Geometrical Requirements

The geometrical requirements form a guideline for the physical properties of the flexible endoscope design such as its shape and size. In this design, these requirements are based on the functionality of a flexible endoscope, the geometry of the

human colon and the desired interaction with a colon upon contact.

1. **Shaft Shape:** *The cross section of the shaft must be circular in shape to avoid sharp edges and conform to the shape of the colon.*
2. **Shaft Size:** *The external diameter of the endoscope shaft may not exceed 30 mm.*

Although a colonoscope usually has a diameter of up to 15 mm, a maximum diameter of 30 mm is chosen as this size has previously been assumed within the BITE group for other colonoscope proof of concept prototypes.

3. **Tip Shape:** *The tip must be circular in cross section and rounded or blunted to create a dome or half donut shape. It may contain no sharp edges and may not exceed the shaft diameter.*
4. **Lumen:** *The design must allow space for a circularly shaped lumen along the center line of the shaft with a diameter of at least 10 mm.*

Having available space for the placement of a lumen is essential to eventually function as an endoscope. A diameter of 10 mm is chosen to allow enough space for the contents of a conventional endoscope, such as Bowden cables, power cables, glass fibers and lumina for the supply or removal of fluids, gasses and surgical equipment.

### Wishes

Some features are desirable (or essential) in the design of a flexible endoscope but considered too ambitious or too creatively limiting for the current proof of concept stage of the design proposed in this thesis. These properties are therefore expressed as design wishes instead.

1. **Maintain Shape:** *It is desirable for the extended endoscope shaft to maintain its shape when varied in stiffness instead of forcing itself into a straight-line configuration.*

2. **Biocompatibility:** *It is desirable that the design can be constructed entirely out of biocompatible materials.*
3. **Disposable or Reusable:** *It is desirable for the design to be either cheap to produce and therefore suitable for single-use and disposal or be easy to disassemble, sterilize and reassemble (without degrading in quality) to be suitable for reuse.*
4. **Smooth and Soft:** *It is desirable for the exterior surface of the prototype to be completely smooth and soft to protect the colon wall upon contact.*
5. **Suitable in Colonoscopy:** *It is desirable that the key working principles of the design are suitable and save for use in a human colon.*

## 3.3. THEORETICAL SOLUTION AREAS

This section will divide the solution spaces of both design focusses, apical extension and variable stiffness, into a set of theoretical solution areas. This method of analysis helps to ensure that every area, in which a solution to the design focus can theoretically be found, is considered.

### 3.3.1. APICAL EXTENSION

To create an overview of the theoretical ways in which apical extension can be achieved, this analysis divides the solution space into areas based on how material supply to the tip is handled. Initially the solution space can be split into two possible methods for supplying material to the tip for extension. The material can either be:

1. fully stored inside the tip, prior to the extension process.
2. or, transported through the shaft from the posterior end to the tip when required during the extension process.

Next, these two solution areas can be further subdivided based on the state in which the material that is used for the apical extension process is stored or transported. The material can either be:

1. raw, requiring at least some form of processing or assembly inside the tip before being used to extend the shaft.
2. or, fully constructed as a functional shaft ready to be extended from the tip without further processing.

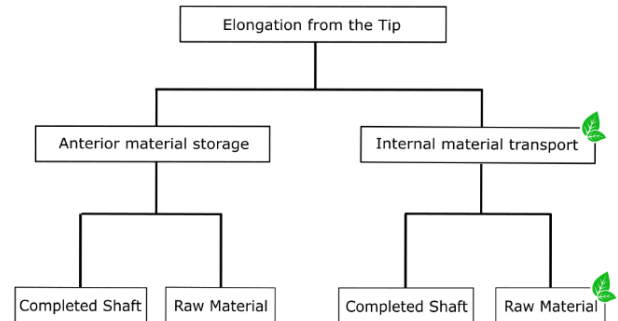
This results in a total of four different solution areas to apical extension an overview of which is shown in Figure 3.1. Each of these solution areas has its own characteristics and as such has specific advantages and disadvantages for use in a flexible endoscope. The most relevant advantages and disadvantages are discussed below.

Firstly, storing all of the material inside the tip results in a finite extension length and a tip volume that scales with the maximum achievable length. On the other hand, transporting the material from the posterior end requires a free internal volume inside the shaft (through which the material can travel) and a material driving force. Therefore, storage in the tip complicates tip design and increases tip size whilst internal transport complicates shaft design and increases the required free space inside the shaft. Which area is more suitable for the design of a flexible endoscope seems to depend on the nature of the shaft design and the material that is used.

Secondly, using raw materials results in the need for some type of processing mechanism in the tip and the provision of energy to that mechanism for the material transformation. This complicates the tip design and likely increases the size of the tip. An example of such a design is the plant root robot designed by A, Sadeghi, discussed in Section 2.4. Raw material might, however, be more compactly stored or transported than a fully assembled shaft which might, contrastingly, ultimately decrease the complexity and volume of the tip or shaft design. Whether it is more practical and efficient to use raw or processed material therefore seems to depend once more on the nature of the shaft design and the material that is used which can vary between concept designs.

To complete the overview, the biological solution to apical extension (which is used by the plant root growth mechanism) is sorted into one of the four theoretical solution areas. As discussed in Chapter 2, the root internally transports raw materials (mostly water) from the base to the

apical meristem. Consequently, the apical extension method used by plant root growth is sorted into the “internal material transport using raw materials” solution area. This is indicated in Figure 3.1 with a green icon.



*Figure 3.1: Overview of the theoretical solution space for apical extension divided into four solution areas. Solution areas with a green leaf icon contain a solution that is used by the biological inspiration, plant root growth, to apically extend.*

### 3.3.2. VARIABLE STIFFNESS IN BENDING

The solution space of the second design focus, variable stiffness, is divided into areas using the theoretical formulas that dictate the bending stiffness and bending moment of a slender beam according to elementary beam theory. The division of the areas is herein based on the physical property that is manipulated by the design to vary the bending stiffness of the shaft.

A beam's bending stiffness is defined as its resistance to deformation through bending and relates the applied force to the resultant deflection of the beam.

$$F = K * \omega \quad (1)$$

This follows from equation one, in which  $K$  is the bending stiffness,  $F$  the applied force and  $\omega$  the resultant deflection. It is first assumed that the deflection of the shaft, induced by the physician to propel the endoscope through the colon, is constant. It can then be seen that an increase in stiffness will result in a subsequent increase of the applied force. According to classic beam theory, the applied force induces a bending moment inside the beam. The relation between this bending moment and the beam's deflection is described by equation two and graphically represented in Figure 3.2. Equation five then follows from the substitution of equations three and four into equation two.

$$M = E * I * \kappa \quad (2)$$

$$\kappa = \frac{\partial^2 \omega}{\partial x^2} \quad (3)$$

$$I = \frac{\pi R^4}{2} \quad (4)$$

$$M = E * \frac{\pi R^4}{2} * \frac{\partial^2 \omega}{\partial x^2} \quad (5)$$

In these equations  $M$  is the bending moment,  $E$  the Young's Modulus,  $I$  the second moment of area of the beam,  $R$  the external radius of the beam,  $\kappa$  the resultant curvature of the beam and  $\omega(x)$  the beam deflection. This deflection has a non-linear relation with the position along the beam,  $x$ , where the force is applied.

From equation five it can be concluded that there are three properties ( $E$ ,  $R$  &  $x$ ) that can be manipulated to vary a beam's internal bending moment (and therefore the applied bending force) when assuming that the deflection,  $\omega$ , induced by the physician still remains constant. This ultimately results in the solution space being divided into three solution areas as shown in Figure 3.3.

Firstly, the actual physical bending stiffness of the beam, or flexural rigidity, can be increased by either increasing the Young's Modulus,  $E$ , or the second moment of area,  $I$ , through manipulation of the beam's external radius,  $R$ .

Alternatively, the bending force required to deflect the shaft can be increased by decreasing the unsupported length of the shaft as measured from point of force application. Even though this approach does not change the mechanical properties of the beam, it does change resistance to bending that is actually experienced at the contact point and therefore results in an increase of the required bending force. Changing the unsupported length is however not a suitable solution in a flexible endoscope as it cannot be achieved without anchoring to the colon. This

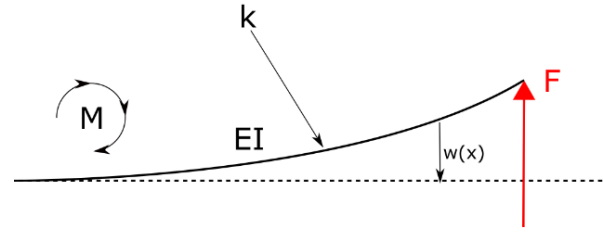


Figure 3.2: Force diagram of a slender beam that is fixed on one side bending under the applied load  $F$ .

theoretical solution therefore does not translate to the scenario of colonoscopy.

To complete the overview, the biological solutions to variable bending stiffness (which is used by the plant root growth mechanism) are sorted into the three theoretical solution areas. In chapter two it is shown that a plant root uses a combination of methods from all of the three theoretical solution areas to vary its bending stiffness. Firstly, a root differentiates its cells to increase its Young's Modulus. Secondly, it increases its external radius to increase its second moment of area. Finally, it anchors itself using root hairs to decrease its unsupported length. Therefore, the plant root growth mechanism is sorted into all three solution areas as indicated by the green leaf icons in Figure 3.3.

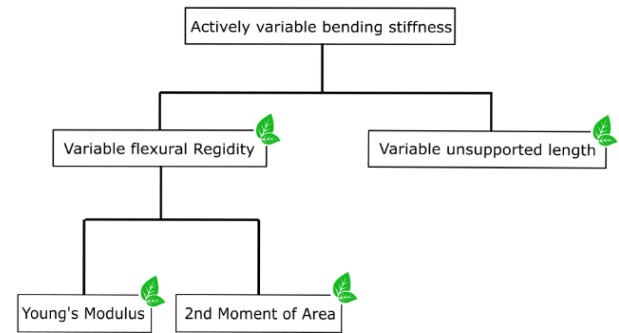


Figure 3.3: Overview of the solution space for variable bending stiffness divided into theoretical solution areas based on elementary beam theory. Solution areas with a green leaf icon contain a solution that is used by the biological inspiration, plant root growth, to vary its bending stiffness.

### 3.4. CONCEPT GENERATION

#### Morphological Chart

In this section, a morphological chart, shown in Table 3.1, is used to generate concept solutions. A morphological chart displays a list of solutions to each subfunction of the design and concepts are generated by picking one solution out of each list. Using this method can result in unexpected

concepts which combined functionality is greater than the sum its sub-functions.

The morphological chart in this thesis consist of two lists of sub-solutions, namely the apical extension and variable stiffness as follows from the design focus. These categories are presented in the form of so called “how to” questions. The solutions in the generated lists are based on the analysis carried out in Section 3.4 and for each solution the underlying theoretical solution area is indicated in the top left corner using one or more letters.

For the first category, apical extension, the letter **S** indicates material storage within the tip and the letter **T** indicates material transport through the shaft. Additionally the letter **C** indicates that the stored or transported material consists of a fully assembled shaft whereas the letter **R** indicates that the material is raw or unprocessed to some degree.

For the variable stiffness functionality, the letter **E** indicates a change in stiffness through variation of the shaft material’s properties, **I** indicates a variation of the shaft’s second moment of area, **X** indicates a change in the force required to achieve a certain degree of bending deformation through variation of the shaft’s unsupported length and  **$\sigma$**  indicates a change in the build up internal stress level.

The color-coded numbers in the top right corner indicate the concept in which the sub solution is used. In the following paragraphs each sub solution chosen from the morphological chart for implication in one of the concepts is discussed.

### Eversion of inverted tube mechanisms

Eversion is the act of a flexible tube turning inside out at its tip. A flexible tube that everts, as shown in Figure 3.4, is often referred to as an inverted tube mechanism. Inverted tube mechanisms consist of a thin-walled tube, which is turned inside-out at the anterior end and is connected to a pressure chamber at its posterior end. The inverted part of the tube is then stored on a spool inside the pressure chamber, creating an enclosed volume. The eversion resistance of the mechanism can be overcome by increasing the pressure inside the enclosed volume. This results in an eversion of the mechanism followed by apical extension at its tip. This extension causes an increase of the internal volume followed by a drop in the internal pressure. The elongation continues until the

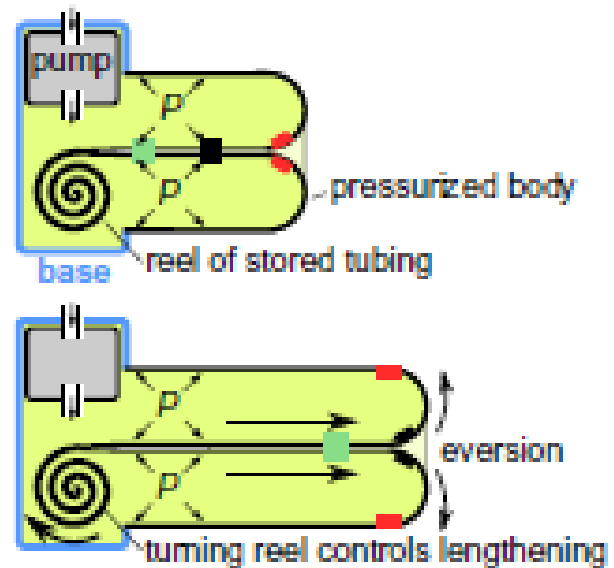


Figure 3.4: Two stages in the lengthening process of an inverted tube mechanism that is extending apically by means of eversion through regulation of the internal pressure level. From: E.W. Hawkes, et al. [23].

posteriorly stored material runs out or until the internal pressure drops below the eversion resistance. By regulating the internal pressure level, the eversion force and subsequent eversion velocity of the tip can be controlled.

### Fiber jamming mechanisms


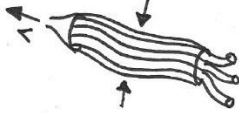

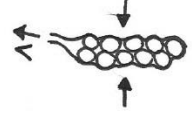
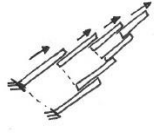
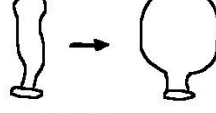


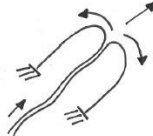




Fiber jamming mechanisms consist of a bundle of longitudinal fibers that are placed within an enclosed volume. When the mechanism is deactivated, the enclosed volume has enough space for the fibers to remain separated. This allows the fibers to move freely relative to each other when bending the mechanism, resulting in a low bending stiffness. When activated, the space around the fibers is compressed, which jams the fibers together. This increases the frictional interaction between the fibers and prevents them from moving relative to each other, essentially forming one thick fiber. This increases the second moment of area of the bundle and as a result its bending stiffness. The bending stiffness is herein dependent on the magnitude of the frictional interaction.

### Granular jamming mechanisms

Granular jamming mechanisms consist of a collection of granules which are placed within an enclosed volume. Their functionality is very comparable to that of the aforementioned fiber



Table 3.1: Morphological table containing two lists of sub-solutions, one for each focus of the design, apical extension and variable stiffness. The letters in the top left corner of each sub solution indicates the theoretical solution area on which the solution is based. S = material stored in the tip, T = material transported through the shaft, C = fully assembled shaft, R = raw shaft material, I = Change in second moment of area, E = Change in Youngs modulus, X = change in unsupported length and finally  $\sigma$  = change in the build up internal stress level. A colored number in a sub solution box indicates that the sub solution has been applied in the corresponding concept.

|            | How to: Axially lengthen the probe's shaft from the tip?  | How to: Actively vary the (experienced) bending stiffness of the probe?   |
|------------|---|---|
| Solution 1 | S C<br><br>Unfolding   | I<br><br>Fiber Jamming <div>1</div>                                 |
| Solution 2 | S C<br><br>Unrolling   | I<br><br>Granular Jamming <div>2</div>                              |
| Solution 3 | T C<br><br>Telescopic Sliding                               | I<br><br>Radial Thickening  |
| Solution 4 | T R<br><br>(3D printed) Layer Stacking                     | X<br><br>Anchoring   |
| Solution 5 | T C<br><br>Eversion <div>1</div> <div>2</div> <div>3</div> | E<br><br>Electro-Active Polymers                                 |
| Solution 6 |   | E<br><br>Temperature Controlled Phase Change                     |
| Solution 7 |   | $\sigma$<br><br>Antagonistic Actuation (w/ Cables)                |
| Solution 8 |   | $\sigma$<br><br>Antagonistic Actuation (w/ Fluidics) <div>3</div> |

jamming mechanisms. When the mechanism is activated the granules are compressed leading to an increased stiffness which is dependent on the magnitude of the frictional interaction between the granules. Granular jamming mechanisms have more freedom in their shape compared to fiber jamming mechanisms and as a result can effectively change their stiffness in multiple directions

#### Fluidic antagonistic actuation mechanisms

Fluidic antagonistic actuation mechanisms use two opposing fluidic actuators to stiffen a joint or structure. When two actuators are placed in an antagonistic configuration, it allows a joint or structure to be actuated in opposite directions. Activating both actuators of the antagonistic pair at the same time fixes the current position of the joint or structure. The stiffness of the fixed position depends on the magnitude of the opposing forces. For example, the muscles in your upper arm form an antagonistic pair allowing you to stiffen your elbow joint through co-contraction and to fix the position of your hand.

### 3.5. CONCEPT DESIGNS

#### 3.5.1. CONCEPT ONE

The first concept, shown in Figure 3.5, arises through the combination of an inverted tube mechanism as the apical extension solution and a fiber jamming mechanism as the variable stiffness solution. The inverted tube in the concept design has three distinct layers. The internal layer is a flexible and expandable tube of silicone rubber. The intermediate layer is made up of fibers which are longitudinally arranged around the circumference of the internal tube. The external layer is made up of a flexible structure that can be inverted whilst also being radially stiff in outward direction beyond a predetermined maximum diameter. An example of such an external layer is a thin plastic bag, which can be crumpled up to become smaller and invert but also has a maximum circumference when inflated. The inverted layers result in an internal volume, which is connected to a pressure chamber at the posterior end to enclose it.

Both of the concept's main functions are controlled through regulation of the pressure

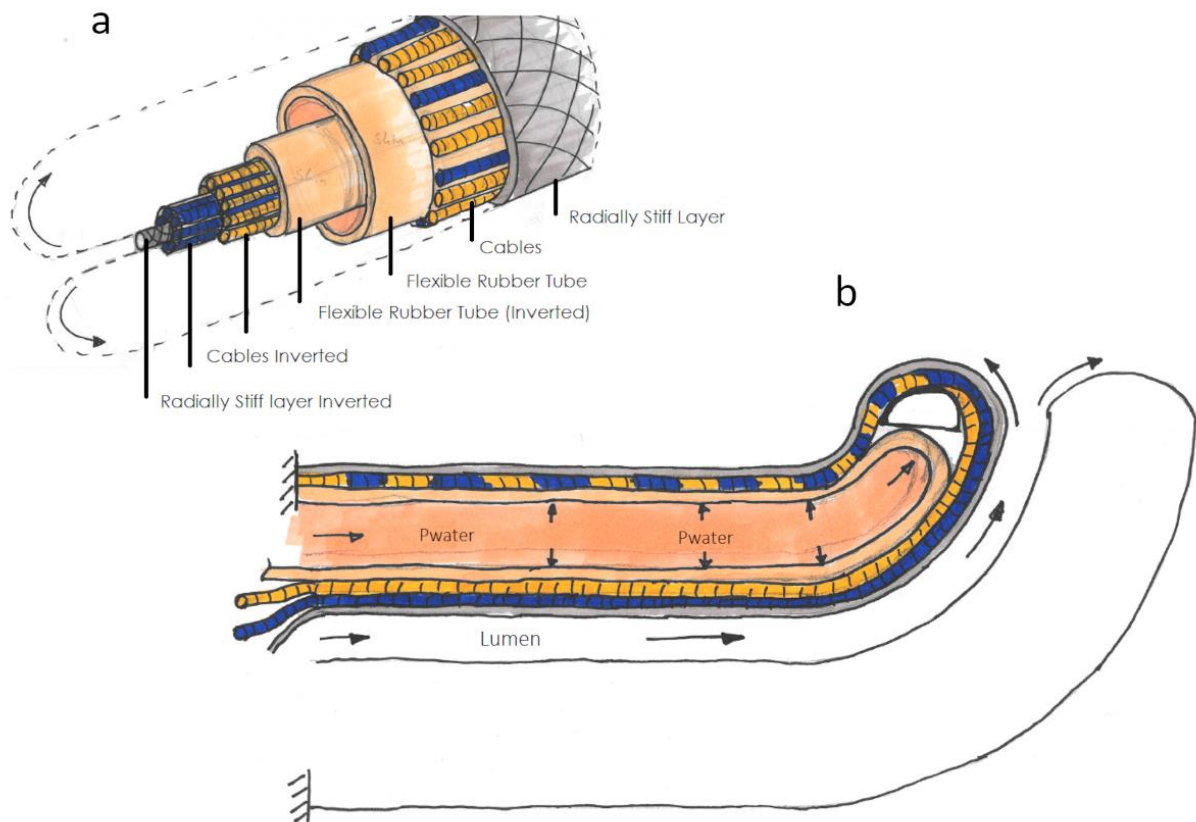


Figure 3.5: Overview of Concept 1 which consist of an inverted tube made up of three layers. An internal flexible rubber tube (beige), an intermediate layers of fibers (yellow & blue) and an external layer consisting of a radially stiff sheath (gray). The inversion of the three layers results in an enclosed internal volume (pink) that can be hydraulically pressurized (P water) from a posterior pressure chamber. a) 3d radial section view b) longitudinal section view.

inside the enclosed, inverted, rubber tube. Pressurizing the tube causes it to both evert all three layers of the tube together in axial direction as well as expand the internal rubber tube (slightly) in radial direction. The eversion in axial direction causes the concept design to apically extend, thus elongating its shaft, similar to conventional inverted tube mechanisms.

Additionally, the (limited) radial expansion of the internal rubber tube compresses the intermediate layer of fibers against the radially stiff external layer. This compression jams the fibers between the internal and external layers, increasing the frictional interaction between the three layers. This results in a fiber jamming mechanism with which the bending stiffness of the everted section of the shaft can be controlled through variation of the internal pressure level. This specific configuration of layers to create a fiber jamming mechanism is based on the FORGUIDE mechanism designed by A.J Loeve, shown in Figure 3.6 [28].

### 3.5.2. CONCEPT TWO

The second concept, shown in Figure 3.7, also uses an inverted tube mechanism as the apical extension solution but now in combination with a granular jamming mechanism as the variable stiffness solution. The concept design consists of two thin layers of inverted plastic tubing that are connected at various points along their length to

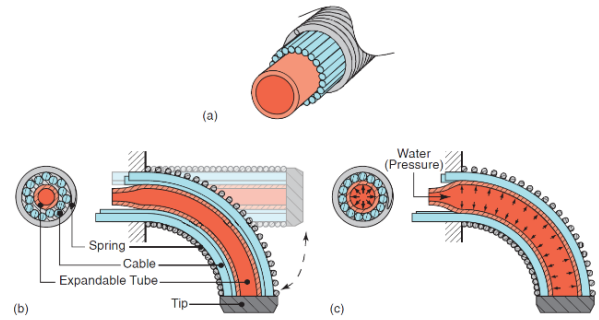


Figure 3.6: (a) 3D view of the FORGUIDE Mechanism. (b) Section view of the FORGUIDE mechanism in its deactivated, compliant, state. (c) Section view of the FORGUIDE mechanism in its activated, stiffened, state. From: A.J. Loeve [28]

create one double-walled inverted tube. The small, enclosed circumferential space between the double walls of the inverted tube is filled with granules and connected to a vacuum pump. The internal volume that results from the inversion of the tube is connected to a pressure chamber at the posterior end to enclose it. Similar to a conventional inverted tube mechanism, the concept design can be everted by increasing the pressure in the enclosed internal volume, lengthening the tube through apical extension.

Additionally, the bending stiffness of the everted tube can be increased by applying a vacuum on the small circumferential volume between the double walls of the tube. This causes the previously free moving granules in the circumferential space to be compressed together

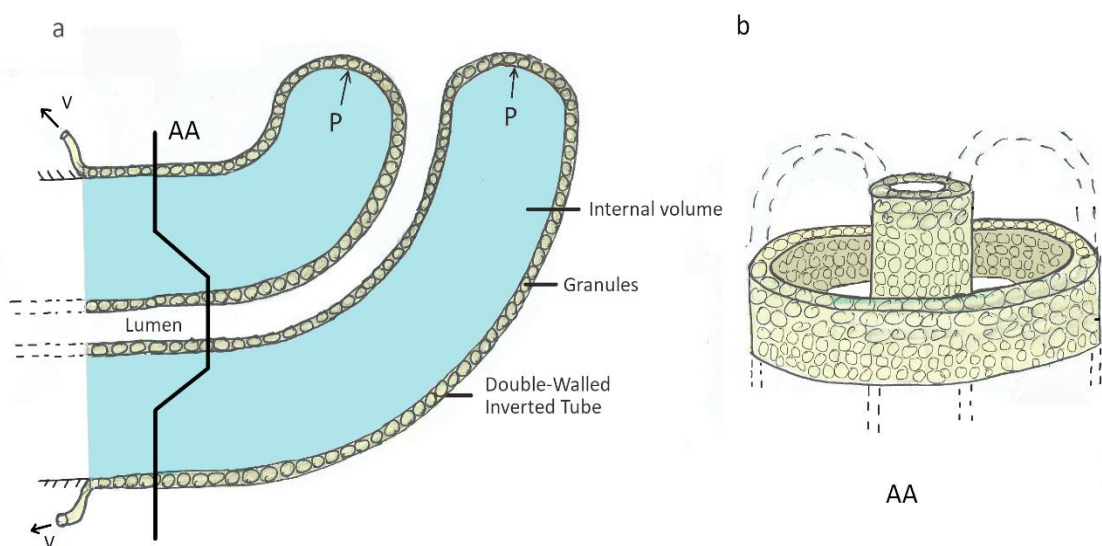


Figure 3.7: Overview of Concept 2 which consist of a double walled inverted tube. The internal volume (blue) can be pressurized (p) by a posteriorly connected pressure chamber to evert and elongate the tube. The circumferential space between the double walls is filled with granules (yellow) and connected to a vacuum pump that can apply a vacuum (v) to jam the granules and increase the tube's bending stiffness. a) longitudinal section view. B) 3d radial section view

increasing their frictional interaction. This results in a granular jamming mechanism with which the bending stiffness of the everted tube can be controlled by varying the extend to which the circumferential space is vacuumed.

### 3.5.3. CONCEPT THREE

The third concept, shown in Figure 3.8, is created through the combination of an inverted tube mechanism as the apical extension solution with an antagonistic hydraulic actuation mechanism to enable variable stiffness. The design consists of one layer of inverted plastic tubing. The volume inside the inverted tube is connected to a pressure chamber and hydraulic pump at the posterior end to enclose it, similar as to the other two concepts. As the pressure inside the tube is increased, the tube everts at the tip, lengthening the shaft.

Around the the circumference of the inverted tube, four linked chains of chambers (each with a fixed volume) are attached along the length of the tube and are connected at the posterior end to a second hydraulic pump. As the inverted tube everts, the chains of external chambers can be activated or pressurized from the posterior end. When pressurizing a chamber, its fixed volume forces the shape of the chamber into a sphere, thickening and shortening it compared to the shape of its deactivated state. The pressure inside the inverted tube is used to extend the tube and the pressure inside the external chambers is used to shorten the

tube. Together they form an antagonistic pair. By activating or pressurizing both parts of the antagonistic pair, a balance of forces is created. This causes a stiffening of the inverted tube, as it attempts to lengthen and shorten at the same time. The stiffness of the tube can be varied by controlling the magnitude of the opposing forces.

### 3.6. SELECTION OF FINAL CONCEPT

#### Harris profile

In this section, the three concepts are evaluated and compared based on the earlier established functional requirements and design wishes using a Harris-profile, shown in Table 3.2. The concepts are given a score from - - to + + for each (equally weighing) selection criterium based on how well the concept is expected to fulfill that criterium. Summation of the plusses and minuses will result in a semi-subjective final score for each concept in which higher scores indicate better concepts. Based on the scores, an argument for which concept to select can be made.

#### Apical extension

All three concepts extent in the same way. However, the eversions of Concepts 1 and 2 are slightly less straightforward as the reciprocal interaction between the three layers in Concept 1 and the movement of the granules in Concept 2 are less predictable during eversion than the single layer tube of Concept 3.

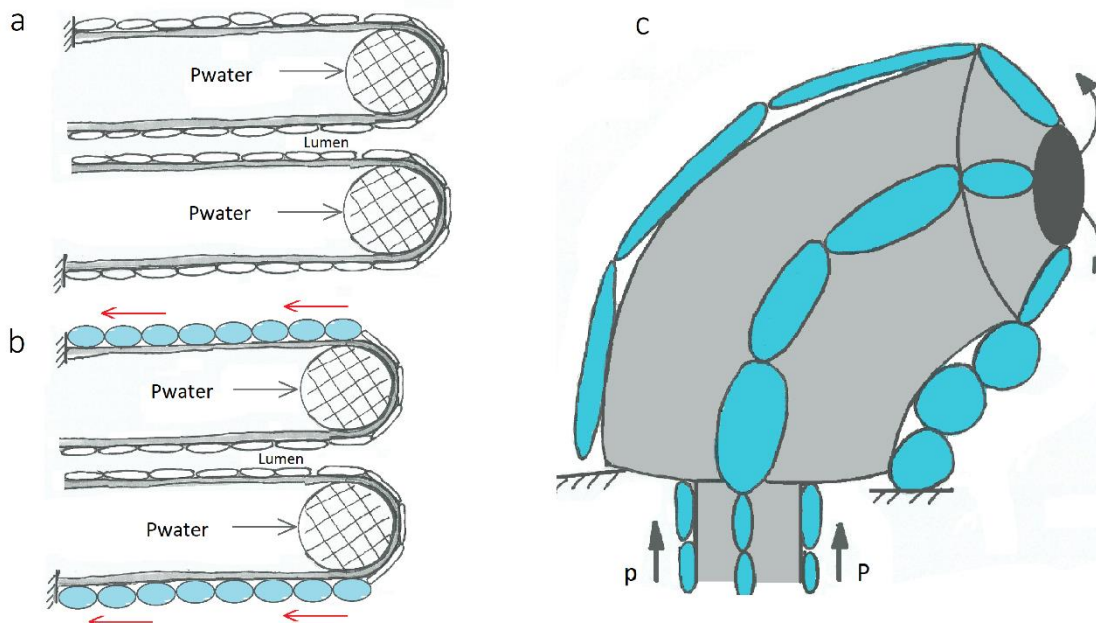


Figure 3.8: Overview of Concept 3 showing an inverted tube (gray) with an internal pressurized volume (white) and external chains of pressurized cells (blue). a) longitudinal section view of the deactivated concept, b) longitudinal section view of the activated concept, c) 3d view of the activated concept whilst in a curved shape.



### Stiffness variability

The stiffness variation of Concept 1 is most likely to work properly as the fibers are well suited to jamming a long shape and because the fiber configuration has been previously validated in the FORGUIDE mechanism. The performance of the stiffness variation in Concept 2 is less certain as a thin layer of granules is less suited to jamming a long shape and the distribution of granules after eversion is uncertain. For Concept 3, the magnitude of the change in bending stiffness (due to the internal build up of tension in axial direction by the antagonistic hydraulic forces) is relatively unknown.

### Propulsion control

The axial propulsion can be controlled the same way in all three concepts: by either lowering the internal pressure or restricting the release of inverted shaft material.

### Self Propulsion

All three concepts need no assistance of their surroundings to propel in axial direction.

### Retraction

Similar to the eversion process, the inversion process is most straightforward in Concept 3, followed by Concept 1 whose interaction between the three layers during inversion is uncertain. Concept 2 is least likely to be successful as the compaction of granules into a smaller volume during inversion might be problematic.

### Shaft Flexibility

The shaft of Concept 1 is likely least compliant during extension because its fiber jamming mechanism might already be active, depending on the internal pressure that is required to evert the shaft. Concept 1 and 2 are equally flexible.

### Maintain Shape

Concepts 1 and 2 are equally likely to maintain their shape during stiffening. The shape maintenance of concept 1 has been validated by the FORGUIDE mechanism [28]. In the stiffening process of Concept 2, there are no forces that might cause it to straighten. Concept three is likely to desire a straightened configuration as a result of the build up of axial stresses in the shaft.

Table 3.2: Harris-Profile of all three concepts indicating their expected fulfillment of the functional requirements (blue) and design wishes (yellow).

| Criteria             | Concept 1 |   |   |    |
|----------------------|-----------|---|---|----|
|                      | --        | - | + | ++ |
| Feasibility          |           |   |   |    |
| Elongation From Tip  |           |   |   |    |
| Variable Stiffness   |           |   |   |    |
| Shaft Flexibility    |           |   |   |    |
| Self-Propulsion      |           |   |   |    |
| Retraction           |           |   |   |    |
| Insertion (velocity) |           |   |   |    |
| Force Control        |           |   |   |    |
| Lumen Placement      |           |   |   |    |
| Shaft Shape / Size   |           |   |   |    |
| Tip Shape / Size     |           |   |   |    |
| Maintain Shape       |           |   |   |    |
| Biocompatibility     |           |   |   |    |
| Novelty              |           |   |   |    |

| Criteria             | Concept 2 |   |   |    |
|----------------------|-----------|---|---|----|
|                      | --        | - | + | ++ |
| Feasibility          |           |   |   |    |
| Elongation From Tip  |           |   |   |    |
| Variable Stiffness   |           |   |   |    |
| Shaft Flexibility    |           |   |   |    |
| Self-Propulsion      |           |   |   |    |
| Retraction           |           |   |   |    |
| Insertion (velocity) |           |   |   |    |
| Force Control        |           |   |   |    |
| Lumen Placement      |           |   |   |    |
| Shaft Shape / Size   |           |   |   |    |
| Tip Shape / Size     |           |   |   |    |
| Maintain Shape       |           |   |   |    |
| Biocompatibility     |           |   |   |    |
| Novelty              |           |   |   |    |

| Criteria             | Concept 3 |   |   |    |
|----------------------|-----------|---|---|----|
|                      | --        | - | + | ++ |
| Feasibility          |           |   |   |    |
| Elongation From Tip  |           |   |   |    |
| Variable Stiffness   |           |   |   |    |
| Shaft Flexibility    |           |   |   |    |
| Self-Propulsion      |           |   |   |    |
| Retraction           |           |   |   |    |
| Insertion (velocity) |           |   |   |    |
| Force Control        |           |   |   |    |
| Lumen Placement      |           |   |   |    |
| Shaft Shape / Size   |           |   |   |    |
| Tip Shape / Size     |           |   |   |    |
| Maintain Shape       |           |   |   |    |
| Biocompatibility     |           |   |   |    |
| Novelty              |           |   |   |    |

### Biocompatibility

At this stage of the development, there is no reason to think that any of the concepts are unsuited for construction from a biocompatible material.

### Disposable or Reusable

Concepts 2 and 3 are equally simple in design and therefore equally suited for single-use or reuse. The design of Concept 1 is more complex and thus

less suited for single-use. The multiple layers of Concept 1 make it also more difficult to sterilize for reuse.

### **Smooth and Soft**

The external layers of concepts 1 and 3 are expected to be equally soft, although the surface of Concept 3 is not smooth due to the external hydraulic chambers. Concept 2 is less smooth and soft due to the hard granules underneath its thin external layer.

### **Suitable in Colonoscopy**

Concept 2 is least suitable for colonoscopy. In the case of a leak in the double wall, a vacuum might be applied to the colon or granules could escape into the colon. Both are highly undesirable. Concept 3 is more suitable for colonoscopy. However, the presence of the external pressure chambers and the Concept's desire to straighten upon stiffening are slightly undesirable. Therefore, Concept 1 is most suitable for colonoscopy.

### **Chosen Concept**

Concept 2 has nine points whereas Concept 1 and 3 both have thirteen points. As Concept 2 is also least suitable for colonoscopy, this concept is not chosen to develop further. Although the scores for Concept 1 and 3 are equal, it can be argued that Concept 1 is the better choice. This opinion stems from the fact that the higher suitability for colonoscopy and better shape maintenance of Concept 1 outweigh the higher simplicity and more predictable apical extension and retraction of Concept 3. As a result, Concept 1 is chosen to be developed further into a physical proof of concept prototype design.

## 4 FINAL DESIGN

### 4.1. FROM CONCEPT TO FINAL DESIGN

#### Introduction

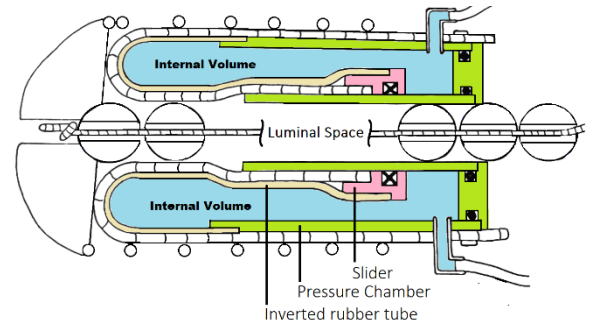
In the previous chapter, Concept 1 was selected to be developed further. In this chapter, that conceptual idea is elevated into a final design. In this section, four additional sub functions are implemented in the design that are required to carry out the two main functions: apical extension and variable stiffness. Additionally, the interaction between segments of the design and the role of friction therein is discussed. In Section 4.2 the design is split into a collection of individual parts, which are then dimensioned in CAD software and materialized so that they can be purchased as off-the-shelf parts or be custom produced from a technical drawing. This ultimately results in an initial prototype in Section 4.3 and an iteration thereof (based on identified flaws) as final design in Section 4.4.

#### Additional function 1: Pressurize internal volume

The volume inside the shaft's inverted tube mechanism has to be enclosed at the posterior end so that it can be pressurized for actuating the apical extension and stiffness variation of the shaft. This is achieved by connecting both the inverted and everted layer of the shaft's inverted flexible rubber tube to a pressure chamber as shown in Figure 4.1. This pressure chamber is then connected to an external pneumatic pump that can regulate the internal pressure level. The pressure chamber has to be designed in such a way that:

1. the inverted layers of the shaft can be stored inside the pressure chamber prior to apical extension;
2. the pressure seal around the enclosed internal volume is maintained during the apical extension process;
3. the central luminal space through the shaft is accessible from the posterior end of the design.

To do so, the pressure chamber is designed as a double walled hollow tube enclosed at the posterior side. This results in an enclosed circumferential space between the double walls of the tube in which the inverted shaft material can



*Figure 4.1: Longitudinal section view showing the shape of pressure chamber (green) to allow storage of the inverted tube (beige) on a slider (pink) such that the internal volume is enclosed whilst retaining access to the central luminal space.*

be stored, leaving a central hollow space inside the inner wall from which the lumen can be accessed.

#### Additional function 2: Store shaft material

In conventional inverted tube mechanisms, the inverted material is stored in the pressure chamber on a spool (as was shown in Figure 3.4 of the previous chapter). This manner of storage would pinch shut the central luminal space, restricting the posterior access. Therefore, the shaft material is stored as a single straight line in and around the pressure chamber. The shaft material is made up of three layers: the internal flexible rubber tube, the intermediate layer of fibers and the external radially stiff layer. The rubber tube and the layer of fibers are both able to invert and are therefore stored inside the pressure chamber. The external layer is, however, not flexible enough to invert and is therefore stored around the outside of the pressure chamber as shown in Figure 4.2.

The posterior end of the two inverted layers is connected to a slider around the inner pressure chamber wall. This is required in order to maintain a pressure seal between the stored material and the inner pressure chamber wall and to keep the internal volume fully enclosed whilst the stored material slides forward to evert at the tip.

#### Additional function 3: Maintain luminal space

The shaft's flexible rubber tube has the tendency to pinch shut the central luminal space of the extending shaft by radially expanding inwards as the internal pressure is increased. A row of beads, connected via a string through their middle, is therefore placed inside the central luminal space of the shaft, as shown in Figure 4.3, to prevent the inwards expansion of the flexible rubber tube after leaving the pressure chamber. A string of beads is

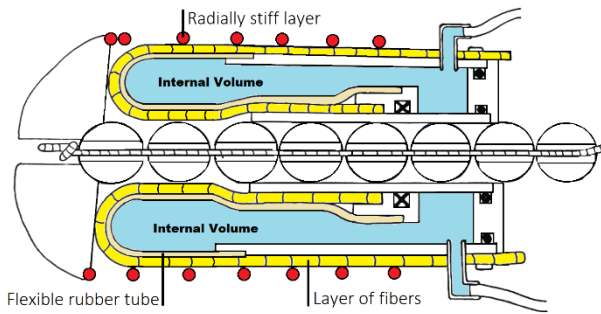


Figure 4.2: Longitudinal section view showing the three layers of the shaft. The internal inverted flexible rubber tube (beige) the intermediate layer of fibers (yellow) and the external radially stiff spring (red).

chosen because they are able to fill the entire luminal space without increasing the (deactivated / unjammed) bending stiffness of the shaft, allowing the shaft to remain as flexible as possible. The string of beads only serves as a proof of concept placeholder for a functional lumen of a future endoscope down the line and it currently has no further functional requirements.

#### Additional function 4: Tip propulsion control

The apical extension of the tip has to be actively controllable from the posterior side of the design. This requires both: 1) keeping the three layers of the shaft together and properly arranged at the tip as the shaft extends, as well as 2) the ability to stop the forward propulsion at the tip. To do so, a dome shaped cap is placed on top of the shaft's apex as shown in Figure 4.3. This cap is then connected to the string that runs through the central lumen. The propulsion of the cap can now be controlled from the posterior end by managing the outflow of the string. Additionally, the cap is connected to the external radially stiff layer of the shaft so that the external shaft layer can follow the cap and slide forwards when the two other layers evert.

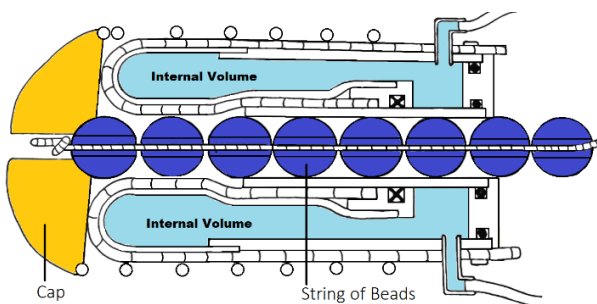


Figure 4.3: Longitudinal section view showing the placement of both a cap (orange) on the apex of the shaft and a string of beads (blue) through the center of the shaft.

#### Interaction between components in the design

The integration of the four additional supporting functions has resulted in a better defined version of the concept, more resemblant of a final design. Figure 4.4 gives an overview of how individual components of the design interact with each other during actuation of the two main functions.

During apical extension, the two inverted layers of the shaft, the flexible rubber tube and the ring of fibers evert because of the forwards force applied on the apex of the inverted rubber tube by the internal pressure. The everting apex in turn applies a forward force on the cap causing it to propel forwards. The cap then applies a pulling force on the external layer of the shaft (the spring) and the central string of beads. This causes the spring and the string of beads to both slide forward along the shaft as it extends. Additionally, the eversion causes the internally stored inverted shaft layers to slide out of the pressure chamber over its inner wall along with the slider. This increases the enclosed internal volume resulting in a decrease of the internal pressure. The apical extension continues until either: 1) the string through the central lumen is manually restrained from moving forwards or 2) the internal pressure in axial direction (driving the extension) drops below the internal resistance to apical extension.

At the same time, the (limited) radial expansion of the inverted rubber tube (caused by the internal pressure in radial direction) jams the intermediate layer of fibers against the external spring and the central string of beads. This causes an increase of

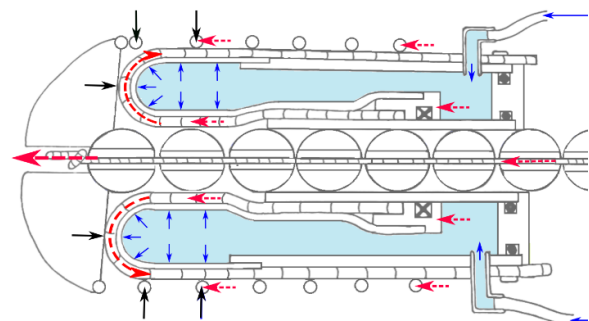


Figure 4.4: Overview of internal forces and the resultant movement and interaction between components during actuation of the apical extension and variable stiffness mechanisms in the design. Internal air pressure (blue), movement direction of individual components (red), reaction forces (black)



the shaft's stiffness in bending relative to the magnitude of the internal pressure level.

### Role of friction in the design

To initiate apical extension of the shaft, the internal pressure in axial direction (driving the extension) has to exceed the internal resistance to that same extension. This internal resistance is mainly caused by the frictional interaction of components moving relative to each other within the design, such as:

1. the slider and the inner pressure chamber wall;
2. the stored inverted layer of fibers and the inner pressure chamber wall;
3. the inverted layer of fibers and the string of beads;
4. the everted layer of fibers and the spring;
5. the apex of the layer of fibers and the cap.

The higher this internal resistance is, the higher the internal pressure has to be to extend the shaft. A higher internal pressure also results in an increased radial fiber jamming and thus increased stiffness in bending of the extending shaft. For colonoscopy, it is desired to extent the shaft with as low a stiffness as possible. Therefore, it is also desired that the internal friction between components remains as low as possible so that the shaft can be extended with a minimal amount of internal pressure and thus minimal bending stiffness.

## 4.2.DESIGN DETAILING

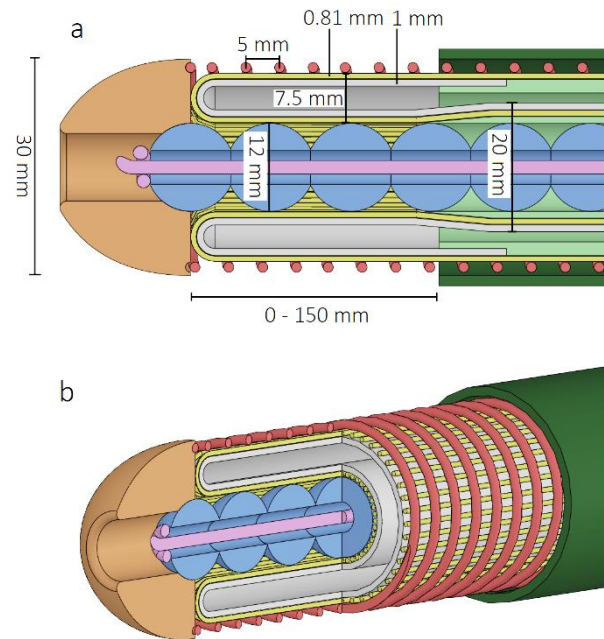
### 4.2.1. SHAFT

#### Design Overview

Figure 4.5 gives an overview of the shaft design and its individual parts (which are discussed below) along with the most important dimensions.

#### Shaft center: String of Beads

The beads are placed in a row along the entire length of the central luminal space and have a diameter of 12 mm to ensure a free luminal space of at least 10 mm as dictated by the geometrical requirements in Section 3.2. At the tip, the first bead is form-fitted and glued into the cap. The string through the beads is made of Dyneema fiber and fitted with a handle at the posterior end so that it can be manually pulled to limit propulsion of the cap. The beads are held in place on the string



**Figure 4.5: Overview of the shaft and its most important dimensions.** a) Longitudinal section view of the shaft (center) additionally showing the cap (orange) and part of the housing (dark and light green). b) 3D double section view of the shaft. Shaft colors: String of beads (pink & blue), layer of fibers (yellow), rubber tube (beige) and spring (red).

by a knot at either end so that the entire row has enough room to bend around its axis but not for individual beads to slide freely along the string. The wooden beads are store-bought. This is a cheap and easy solution for the proof of concept prototype and wood has a relatively low dynamic friction coefficient with the surrounding steel components at around 0.4.

#### Internal shaft layer: Flexible inverted tube

The flexible rubber tube is connected to both the outer pressure chamber wall (at its everted side) and the slider (at its inverted side) using glue to create an airtight seal. The tube is made of rubber so that it can radially expand and has a high friction coefficient with the layer of fibers (made of steel) to effectively jam the mechanism. The tube has a natural, unexpanded, external diameter of 20 mm and a thickness of 1 mm. This diameter is selected for the inverted section of the tube to be stored between the walls of the pressure chamber whilst retaining its natural diameter. Additionally, the (everted) layer of fibers can move freely between the rubber tube and external spring until the internal pressure forces the everted tube to expand all the way to 26 mm. The relatively high thickness of 1 mm is chosen in order to increase the internal pressure required to expand the tube

to the point where fiber jamming initiates, while allowing the shaft to retain a lower stiffness in bending for as long as possible. Furthermore, the high thickness prevents the rubber tube from bulging between the fibers in the intermediate layer and from making contact with the external spring, which would cease the apical extension of the design.

#### **Intermediate shaft layer: Inverted layer of fibers**

There are three central parameters that dictate the design of the layer of fibers: 1) the arrangement of the longitudinal fibers around the circumference of the shaft before, during and after eversion at the tip, shown in Figure 4.6, 2) the fiber material and 3) their diameter of the individual fibers.

The arrangement of the individual fibers around the circumference of the inverted and everted layers is shown in Figure 4.5b (yellow component). The fibers are placed around the inverted layer in a fully filled arrangement (so, no free tangential space). This is to both prevent contact between the inverted flexible rubber tube and the inner pressure chamber wall during storage (which would greatly increase the frictional interaction) and to maximize the amount of fibers in the everted layer. Maximizing the amount of fibers in the everted layer improves jamming and decreases the free space between fibers through which the internal rubber tube could escape its radial confinement. For the same reason, the fibers are arranged around the everted circumference with equal spacing between the fibers.

The fibers will be made of steel, to minimize the dynamic friction with the spring and the string of beads that slide past the fibers in the intermediate layer. Furthermore, the steel fibers will be Incompressible. Incompressibility of the fibers is desirable to limit the expansion of the internal tube and to prevent bulging of the fibers between the beads and the spring. The strands of the steel fibers will be woven in a 7x7 configuration to increase bending flexibility and decrease the radius required for eversion of the individual fibers, at the tip.

For the diameter of the individual fibers, a tradeoff had to be made. A large fiber diameter is desired to decrease the number of fibers required to completely fill the circumference of the inverted layer and increase the distance between the internal and external layers. This improves the tangential stability of the fibers within the layer

(preventing them from slipping over each other) and prevents contact between the rubber tube and spring. On the other hand, a small fiber diameter is desired because it decreases the bending diameter of the fiber, preventing plastic deformation and bending fatigue of the fiber during eversion at the tip. This tradeoff inherently results in an imperfect design but a compromise was found at a diameter of 0.81 mm. This diameter fiber still fits inside the pressure chamber's storage space and is commonly available in the desired 7x7 strand configuration. As a result of the chosen fiber diameter 50 fibers need to be placed around the circumference of the inverted layer to completely fill it.

#### **External shaft layer: Spring**

A custom steel spring is chosen as the external shaft layer. Its main function is to enable fiber jamming by limiting the radial expansion of the shaft. A spring is chosen as it has a high flexibility in bending while also having a high stiffness in circumferential direction. This choice does result in the external layer of the shaft being unable to invert. This requires the spring to slide along the shaft as it extends rather than everting from the tip.

Whereas this appears to be counterproductive to the goal of the design to prevent the medical implication of shear force transmission to the colon wall (due to sliding contact), this is not entirely the case. The highly flexible shaft of the final design, in combination with the mucous naturally present in the colon, should be sufficient to overcome the excessive transmission of shear forces to the colon. Additionally, this shortcoming resulting from the design choice is considered acceptable for the because the design is in its proof of concept stage and temporary medical limitations can be addressed in future iterations.

The spring is form-fitted and glued to the cap. It has an external diameter of 30 mm as dictated by the geometrical requirements and a thread thickness of 1.5 mm with a pitch of 5mm. An intermediate amount of pitch between the threads is selected to both maintain a high level of flexibility in bending while preventing bulging of the underlying layer of fibers between the threads during jamming. Moreover, the pitch allows for preloading of the spring should this be found necessary to smoothly slide along the shaft during extension.

#### 4.2.1. HOUSING

##### Design Overview

Figure 4.6 gives an overview of the housing design and its individual parts (which are discussed below) along with the most important dimensions.

##### Pressure chamber

The pressure chamber is constructed from three parts. Two tubes (the inner and outer pressure chamber walls), one inside the other are connected by an endcap at the end. The inner wall is made of stainless steel and has an external diameter of 26 mm and a wall thickness of 2 mm. The outer wall is made of aluminum and has an external diameter of 15 mm and a wall thickness of 1 mm. This results in a pressurized circumferential space with a width of 3.5 mm in which the inverted shaft material can be stored. Two pressure valves are screwed into the posterior end of the outer pressure chamber wall for the inflow of air from the external pump.

The inner wall is made of stainless steel rather than aluminum to allow smooth movement of the slider fitted around its outer circumference. The endcap is also made of aluminum and has two O-ring grooves in its design to seal the internal volume for pressurization. Both walls are fixed inside the endcap using glue.

The maximum extension length of the shaft is equal to the internal length of the pressure chamber divided by two. This is the case as the single layer of material stored in the pressure chamber turns into a double layer inside the extended shaft, one layer everted and one inverted. For this design, a maximum extension of 150 mm (10% of the average flexible endoscope length) is considered sufficient to proof the concept, resulting in the pressure chamber having an external length of 335 mm.

##### Slider

The slider is designed to have a H7 tolerance fit (+0.02 mm) around the inner pressure chamber wall to prevent leakage from the internal volume. Furthermore, a groove is cut in its body for the placement of an x-ring seal. The slider is made from bronze. Bronze is commonly used in combination with stainless steel for sliding constructions due to its high toughness, low friction with other metals and easy machinability. At the front, the slider has two notches. The notch on the inside is for the

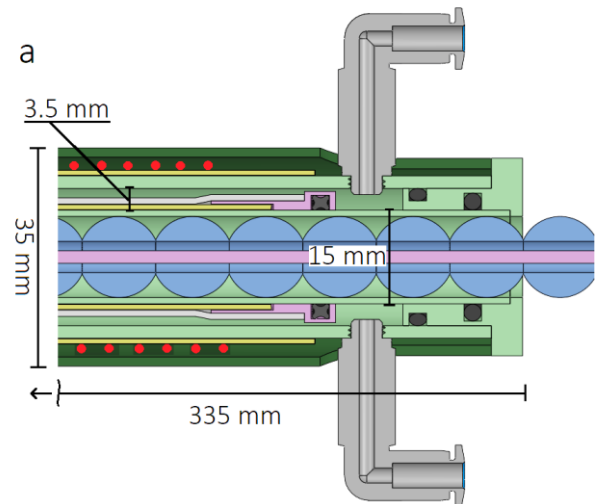


Figure 4.6: Longitudinal section view of the handle and its most important dimensions, additionally showing shaft material stored in and around the pressure chamber. Housing colors: Pressure chamber (light green), slider (light pink), handle (dark green) and seal rings (black).

attachment of the shaft's layer of fibers and the notch on the outside is for the placement of the shaft's inverted rubber tube. Glue is used for attachment of both layers.

##### Handle

Finally a larger circular tube is placed around the pressure chamber and fixed to the endcap using m4 screws. This is done to shield the spring (stored around the outside of the pressure chamber) and to allow attachment of the design to a table using brackets. The attachment of the endcap to the handle inadvertently fixes it to the ground, preventing it from shooting out the end of the pressure chamber during pressurization. The handle is made from aluminum and has an external diameter of 35 mm with a wall thickness of 1.5 mm.

#### 4.3. INITIAL PROTOTYPE

##### Component acquisition

To evaluate the proof of concept design, an initial prototype is constructed. An overview of the prototype components is given in Table 4.1. Off-the-shelf parts were ordered from their suppliers. The beads, inverted-tube, fibers, spring, pressure chamber walls and handle were ordered to size and a post-processing step was applied to them. The remaining parts are fabricated from raw materials using various production methods. The technical drawings used for the post-processing and the custom fabrication can be found in Appendix A.

### Component production and post processing

The rubber inverted tube (Figure 4.7) is obtained from a flattened bicycle tire that is cut to length. The resultant tube was cheap and possessed the desired external diameter, wall thickness and radial stretchability. The steel fibers (Figure 4.8) were cut to length and small amounts of metal glue was applied to the ends of each fiber to prevent their 7x7 strand configuration from unraveling. The cap and brackets (required for the fixation of the prototype to a flat surface) (Figure 4.9 and 4.10) were 3D-printed using a method called Digital Light Processing (DLP). This method of printing offers a high precision and smooth surface quality production of the geometrically complex shapes. The 3D-printing method used a liquid polymer with properties similar to polypropylene, named R5, that gives the cap a low coefficient of friction with its surrounding components. Machining is chosen for production of the pressure chamber parts (Figure 4.11 and 4.12) and the slider (Figure 4.13) as it allows processing of strong and stiff materials to high tolerance fitting, which is required for a pressure chamber.

### Assembly

Assembly of the prototype, partly shown in Figure 4.14, started with temporarily placing the 50 steel fibers in a tight ring around a tube (with the same diameter as the internal pressure chamber wall), using tape. The circular layer of fibers was then glued to a notch in the slider. Once dried, the tape was removed and the fibers staid in a circular layer around the slider. The rubber tube was assembled over the layer of fibers and also glued to the slider. The resultant assembly of the slider with two shaft layers was then placed around the internal wall of the pressure chamber.

To assembly the pressure chamber, the grooves in the pressure chamber endcap were fitted with an O-ring after which the two pressure chamber walls were slid over the endcap and glued in place. This results in the slider and the two shaft layers being neatly stored between the two pressure chamber walls. The front of the flexible tube (sticking out of the pressure chamber) is everted and stretched over a notch in the outer wall and glued in place. This encloses the internal volume. The two pressure inlet valves were screwed into the external wall to complete the pressure chamber.



Figure 4.7: Rubber Inverted tube, cut to size.



Figure 4.8: Steel fibers, cut to size and glued at the ends to prevent fraying of their 7x7 strand configuration.



Figure 4.9: 3D-printed Cap.



Figure 4.10: 3D-printed mounting brackets for the Housing

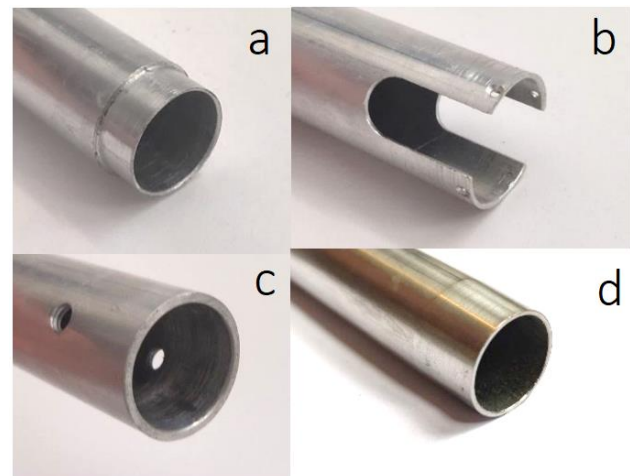


Figure 4.11: Pictures of the various housing tubes after post-processing. a) anterior side of the external wall. b) posterior side of the Handle. c: posterior side of the external wall. d: Internal Wall.



Figure 4.12: aluminum endcap.



Figure 4.13: Bronze slider.





Figure 4.14: Assembly of the initial prototype in five steps from left to right until the point where the fibers were unable to evert around the tip of the inverted tube.

To finish the shaft, the fibers (now sticking out of the inverted tube at the front) were everted around the tube and guided along the outside of the pressure chamber after which the spring is slid around them. The everted fibers are kept in place around the pressure chamber wall with a thin layer of tape at the posterior end. Next, the beads were placed around a string and kept in place by a knot at either end. The string of beads was placed inside the central luminal space of the pressure chamber.

To finish the assembly, the cap was glued to the front of the spring and the string of beads, keeping it in place on the apex of the inverted tube. The housing was placed around the outside of the design and was connected to the endcap using four M4 screws. When using the prototype, the pressure inlet valves were connected to a pneumatic system using tubes. The housing was connected to two mounts which can be attached to a table top using screws.

Table 4.1: overview of the components required for the construction of the prototype. Mentioning for each part, their number, name, method of production or purchase, material, supplier and quantity. P.P. = Post Production

| Table of Components          |                  |                  |                 |                  |      |
|------------------------------|------------------|------------------|-----------------|------------------|------|
| #                            | Part Name        | Production       | Material        | Supplier         | Qty. |
| <b>A: Tip</b>                |                  |                  |                 |                  |      |
| 1                            | Cap              | 3D Print         | Liq. Polymer R5 | Demo             | 1    |
| <b>B: Shaft</b>              |                  |                  |                 |                  |      |
| 2                            | Beads            | purchased        | Wood            | Hobbyshop        | 35   |
| 3                            | Inverted Tube    | purchased + P.P. | Rubber          | DeWolf Delft     | 1    |
| 4                            | Jamming Fibers   | purchased + P.P. | Steel: #1.4401  | Engelman         | 50   |
| 5                            | Spring           | Extruded         | Spring Steel    | Roveron          | 1    |
| <b>C: Housing</b>            |                  |                  |                 |                  |      |
| 6                            | P.C. Inner Wall  | purchased + P.P. | RVS             | Kokkelink        | 1    |
| 7                            | P.C. Outer Wall  | purchased + P.P. | Aluminium       | Salomons Metalen | 1    |
| 8                            | Slider           | Machining        | Bronze          | Demo             | 1    |
| 9                            | P.C. Endcap      | Machining        | Aluminium       | IWS              | 1    |
| 10                           | Inlet Valve      | purchased        | -               | Festo            | 2    |
| 11                           | O-Ring           | purchased        | Rubber          | Gamma            | 2    |
| 12                           | X-Ring           | purchased        | Rubber          | Eriks            | 1    |
| 13                           | Handle           | purchased + P.P. | Aluminium       | Salomons Metalen | 1    |
| <b>D: Experimental Setup</b> |                  |                  |                 |                  |      |
| D1                           | Mounting Bracket | 3D-Print         | Liq. Polymer R5 | Demo             | 2    |
| <b>E: Assembly</b>           |                  |                  |                 |                  |      |
| E1                           | M4 Screw         | purchased        | RVS             | Demo             | 4    |
| E2                           | M3 Set Screw     | purchased        | RVS             | Demo             | 2    |
| E3                           | M6 Screw         | purchased        | RVS             | Demo             | 4    |

### Initial prototype shortcomings & Design changes

During assembly and initial testing and evaluation of the initial prototype, two shortcomings were identified in the proof of concept design:

1. The bending stiffness of the steel fibers was too large for them to evert at the tip because their resultant minimum bending diameter was larger than the 7.5 mm available in the design;
2. The frictional resistance to shaft extension increased more rapidly with the internal pressure than the forward force that drives the shaft extension due to an increase of the frictional normal force on the inner pressure chamber wall.

To overcome these shortcomings, two design changes are implemented in the design. The first design change is that the beads around the central string are removed from the design. This reduces the frictional resistance to apical extension. Even though this design change allows the shaft to encroach on the central luminal space, the lumen remains accessible from the posterior end of the design and can be manually enlarged after extension if desired. The second change is a redesign of the intermediate layer of fibers so that the fibers can both evert at the tip (within the available radial space) and overcome the frictional resistance to apical extension. In the redesign process of the intermediate fiber layer several different tests and design iterations were gone through to find the best configuration and material properties for the fibers in the intermediate layer. The most relevant tests and iterations are discussed in the following segments, culminating in the final version of the design proposed in this thesis in Section 4.4. The flexible extending endoscope propulsion mechanism reverted to as the “Flextendoscope”.



### Preliminary redesign test: Steel tube layer

First a test was conducted to check whether the rubber inverted tube would be able to extend if the frictional resistance no longer increased with the internal pressure level. This was done by replacing the intermediate layer of fibers with a radially stiff steel tube as shown in Figures 4.15a and 4.15b. This resulted in the eversion of the tube at an internal pressure of only 0.6 bar, showing that extension of the design was possible if the frictional resistance is overcome.

### Iteration 1: Layer of nylon ribbons

In this first iteration of the intermediate layer of fibers, shown in Figures 4.15c and 4.15d, the original steel fibers were replaced by 8 nylon ribbons. The coefficient of friction between the nylon ribbons and pressure chamber was already slightly lower (0.4) than between the original steel fibers and pressure chamber (0.5 – 0.8). Additionally, the ribbons had virtually no stiffness in bending due to their geometrical properties. This allowed them to smoothly evert at the tip. However, the thinness of the ribbons resulted in the radially expanding tube bulging between the threads of the spring, locking it in place and stopping the extension. Making them unsuitable for the final design

### Iteration 2: Layer of Dyneema fibers

In this second iteration, shown in Figures 4.15e and 4.15f, the nylon ribbons were replaced by 68 Dyneema fibers with a diameter of 0.65 mm. Dyneema is a strong artificial fiber that is highly flexible in bending and has a low friction coefficient with steel of around 0.2. Due to a high flexibility, the Dyneema fiber cables were able to smoothly evert around the tip. Moreover, the thickness of the fibers was sufficient to prevent the radially expanding tube from bulging between the threads of the spring. However, the friction between the Dyneema cable ring and the stainless steel pressure chamber wall was still found to be too high.

### Iteration 3: Manual extension forces

In the second iteration the frictional resistance was still found to increase more rapidly with the internal pressure level than the forward propulsion force. At this point in the design it is no longer likely that the frictional coefficient can be substantially

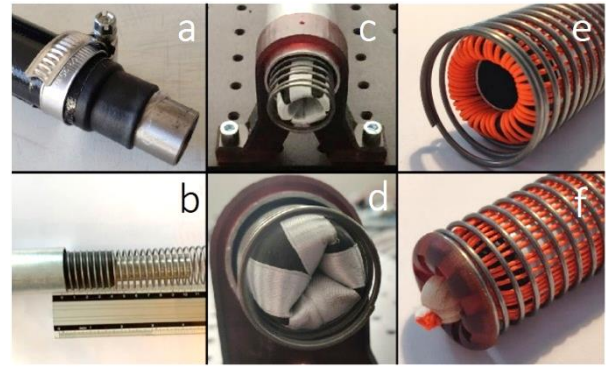


Figure 4.15: test and design iterations for the intermediate shaft layer. a & b): Radially stiff steel tube as intermediate layer. c & d): Eight thin nylon ribbons as intermediate layer. e & f: 65 Dyneema fibers as intermediate layer.

lowered such that the frictional resistance will be overcome. This means that the current design will not be able to extend when solely relying on the internal balance of forces that results from an increase of the internal pressure level. To finally overcome the frictional resistance in the third iteration, the intermediate layer of Dyneema fibers (that was proposed in the second iteration) is reconfigured such that it can be used to manually apply an additional forward force to the internally stored shaft material. This manual force has to be applied to the internally stored shaft material from the posterior end of the design (outside the colon of a hypothetical patient).

To do so, the intermediate shaft layer of 68 Dyneema fibers is split into three groups as shown in Figure 4.16. The first group consists of 65 fibers and maintains its original functionality and arrangement around the shaft. The second group consists of 3 fibers, which are also attached to the slider (through holes in the slider wall) as shown in

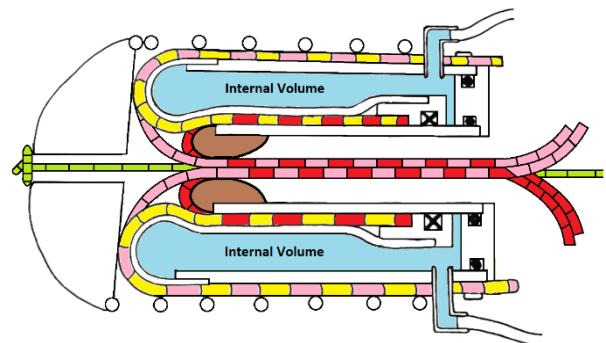
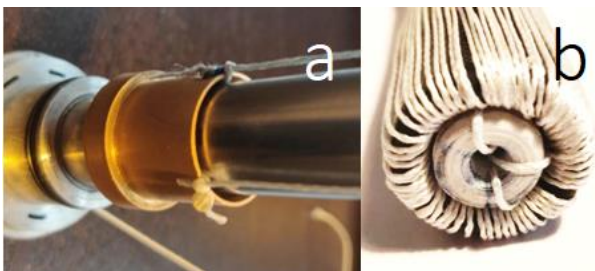


Figure 4.16: Longitudinal section-view of the final prototype design in which the redesigned elements are highlighted. Yellow: fiber group 1 consisting of 65 fibers for frictional reduction and fiber jamming. Red: fiber group 2 consisting of 3 fibers for the application of Manual pulling forces to the slider. Pink: fiber group 3 consisting of 3 fibers for the application of manual pulling forces to the tip. Brown: fiber guide.

Figure 4.17-a and are guided along the pressure chamber wall to the apex of the inverted tube. However, at the apex these 3 cables are inverted through the central lumen of the design to the posterior end instead of being everted around the shaft. At the posterior end, the three fibers are attached to a handle. A manual force can now be transferred through the three fibers to the slider by pulling on the handle. This drives the slider forwards and pushes the shaft material out of the pressure chamber so that it can evert at the tip. The third group of fibers in the intermediate layer also consists of three fibers. These fibers are added to the everted side of the shaft between the everted rubber tube and the spring. From there, they are inverted at the tip and also guided through the central luminal space to the posterior end. By manually pulling on these fibers, a backwards pushing force is applied at the apex of the inverted tube, allowing it to reinvert and retract the shaft.

To keep this required manual force application low in magnitude the internal pressure has to be kept as low as possible to prevent an unnecessary increase of the internal frictional resistance. The minimum pressure (at which the design can extend) is the pressure where the inverted and everted layer of the rubber tube are fully separated with an established layer of air between them. This requires a slight radial expansion of the everted layer. The pressure at which this occurs is determined during evaluation in Chapter 5.

A fiber guide, shown in Figure 4.16 (brown) and Figure 4.17-b (white), is placed at the front of the pressure chamber inside the central luminal space. The shape of the guide smoothens the inversion of the fibers through the central luminal space. This reduces the friction and wear of the manual pulling cables and thus lowers the magnitude of the manual pulling force required to extend the shaft.



*Figure 4.17: a) Connection of the three manual pulling fibers to the slider. b) tip of the design showing fiber group 1 everting outward and fiber group 2 inverting into the cable guide.*

#### 4.4. FLEXTENDOSCOPE

In conclusion, the final version of the flexible endoscope propulsion mechanism design, that is proposed in this thesis is shown in Figures 4.18-a to 4.18-e and from this point in the report referred to as the “Flextendoscope” (a contraction of the words flexible extending endoscope). It contains all the functions and components of the original design concept as discussed in Chapter 3 and Sections 4.1 and 4.2 of this chapter, with the exception of the central luminal beads (which are removed, as discussed in Section 4.3) and the intermediate layer of fibers which is implemented in the redesigned form proposed in Iteration 3 (Section 4.3). The performance of the Flextendoscope prototype is evaluated in the next chapter.

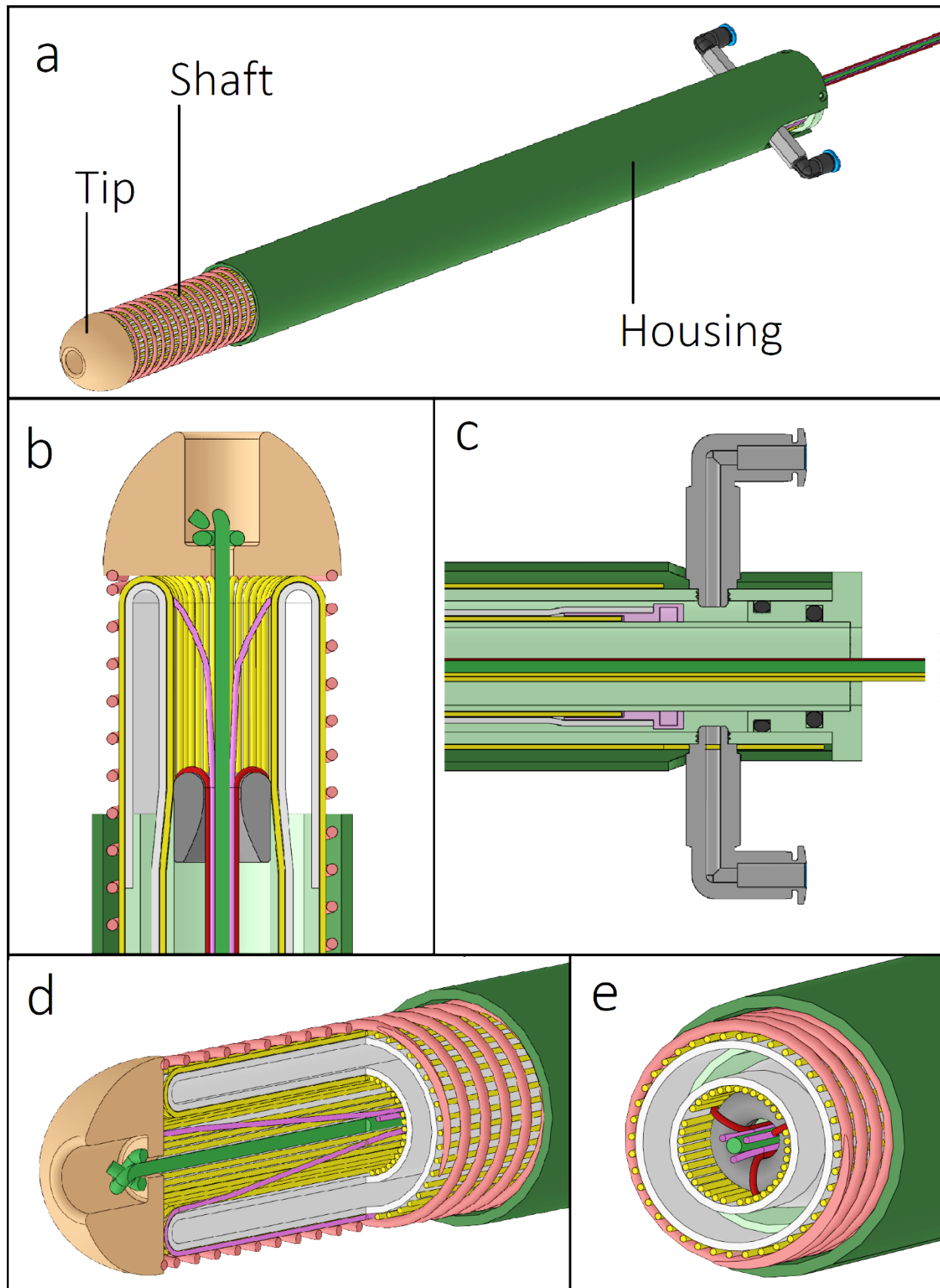


Figure 4.18: The Flextendoscope final design. a) 3d overview of the Flextendoscope. b) Longitudinal section view of the Flextendoscope shaft. c) Longitudinal section view of the Flextendoscope housing. d) Multidirectional 3D section view of the Flextendoscope shaft. e) Radial section view of the Flextendoscope shaft. Components: Cap (orange), Fiber group 1 (yellow), Fiber group 2 (dark red), Fiber group 3 (dark pink), Fiber guide (brown), String (green), Inverted rubber tube (beige), spring (red), Pressure chamber (light green), handle (dark green), Slider (light pink), O ring (black).

# 5 EVALUATION

## 5.1. EXPERIMENTS

### 5.1.1. EXPERIMENTAL GOAL

In this chapter, two conducted experiments are described that assess the performance and behavior of the Flexendoscope prototype through evaluation of its two main functions (apical extension and variable shaft stiffness). The goal of the first experiment is to evaluate the performance and behavior of the apical extension function. The goal of the second experiment is to evaluate the variable stiffness function of the shaft by creating a force-deflection curve (or bending stiffness curve) at multiple internal pressure levels. A research question is proposed for each experiment:

1. To what extent are the distance of extension, extension velocity and the minimally required pulling force of the apical extension function influenced by the internal pressure level?
2. To what extent is the resistance to deformation in bending influenced by the radial deflection distance and internal pressure level?

### 5.1.2. EXPERIMENTAL METHODS

#### Experimental Facility:

In this section, the experimental setup, shown in Figure 5.1, is discussed. During both experiments the prototype is rigidly connected to an optics breadboard (Thorlabs), using M6 bolts, and placed horizontally on a table. A raised platform is fixed in front of the Flexendoscope prototype, level with the bottom of the shaft. This results in a flat surface for the shaft to extend over. Two rulers of millimeter precision are fixed on top of the raised platform. The first ruler is positioned parallel to the prototype to indicate the position of the tip in axial direction. The second ruler is positioned perpendicular to the prototype to indicate the radial position of the tip. One camera (ONEPLUS-6) is mounted horizontally on a tripod above the prototype, to continuously record the position of the prototype's tip and shaft during both experiments.

During the first experiment, a second camera (iPhone 7 plus) is mounted vertically at the

posterior end of the prototype to record the output of the force gauge. Moreover, the group of fibers used to manually extend the prototype are guided over a pulley and connected to an 50N analog force gauge (Sando SN-50), which measures the magnitude of the inputted manual force. Extra weights can be added to increase the 50N limit of the force gauge. For the second experiment the force gauge is connected to the prototype tip, perpendicular to the shaft to record the resistance to deformation.

The prototype is connected to a pressure regulation system, shown in Figure 5.2. The system generates a high air pressure (up to 4 bar) using an electric compressor (SPARMAX TC-610H). The high pressure is transformed into a stable and adjustable lower pressure (up to 2 bar) by a pressure regulator (Festo MS4-LFR-1/4-D7-E-R-M-AS) in combination with a digital pressure sensor (AE-SML-20.0) connected to a Multimeter (FLUKE

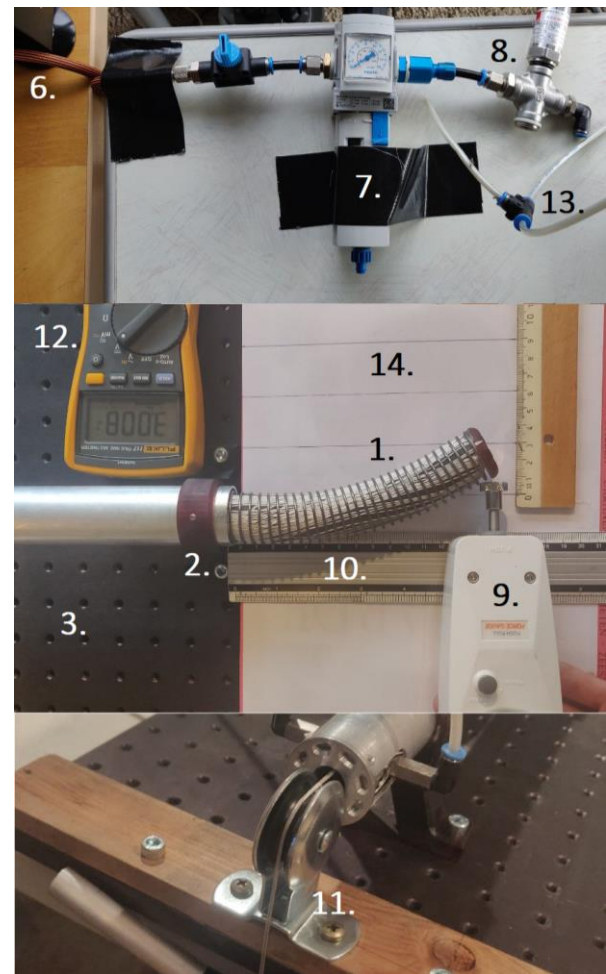


Figure 5.1: An overview of the experimental setup. The numbers indicate the components used in the setup and correspond to the numbers in the component list. Top: Air pressure installation. Middle: The front of the experimental setup Bottom: The back of the experimental setup.



117). The controlled low pressure air is then fed into the prototype.

#### Experimental Setup Components:

1. Proof of concept prototype
2. (2x) Custom Mounting Brackets
3. Optical Breadboard (Thorlabs)
4. (2x) 30 FPS Camera (ONEPLUS-6 & iPhone 7 front camera)
5. (2x) Camera Tripod
6. Air Compressor (SPARMAX TC-610H)
7. 16 Bar Air Pressure Regulator (Festo MS4-LFR-1/4-D7-E-R-M-AS)
8. 2.5 Bar Digital Pressure Sensor (AE-SML-20.0)
9. 50 N Analog Force Gauge (Sando SN-50)
10. (2x) 300 mm Metric Ruler
11. Pulley
12. Multimeter (FLUKE 117 TRUE RMS)
13. Pneumatic tubing (Festo)
14. Raised Platform (white)
15. Optional: 3, 5 & 10 kg Weights

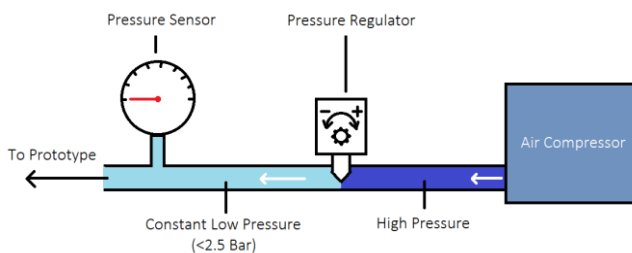


Figure 5.2: Graphical overview of the air pressure system used to regulate the pressure inside the prototype.

#### Experimental Variables:

##### Experiment 1:

In the first experiment, the straight-line extension and retraction distance, velocity and manual pulling force of the prototype are evaluated in terms of the dependent variables:

- Axial position of the tip in mm
- Axial velocity of the tip in mm/s
- Required manual pulling force in N

These dependent variables are evaluated over time for three values of the independent variable:

- Internal pressure in Pa

The three values of the independent variable (internal pressure) will be  $P_{\text{MIN}}$ ,  $P_{\text{MAX}}$  and  $P_{\text{INT}}$ , where  $P_{\text{INT}} = (P_{\text{MIN}} + P_{\text{MAX}})/2$ . The magnitude of  $P_{\text{MIN}}$  &  $P_{\text{MAX}}$  will both be determined in the operational verification test outlined in the experimental protocol below. The initial shaft length and maximum extension will be kept constant at respective levels of 0 and 150 mm.

##### Experiment 2:

During the second experiment the stiffness behavior of the prototype is evaluated and the force-deflection curve is determined through measurement of the dependent variable:

- Radial tip force in N

The dependent variable is evaluated for different values of both of the two independent variables:

- Radial tip deflection in mm
- Internal pressure in kPa

The three values of the radial tip deflection will be 30, 60 and 90 mm, whereas the four values for the internal pressure level will be the atmospheric pressure  $P_{\text{ATM}}$  as well as  $P_{\text{MIN}}$ ,  $P_{\text{MAX}}$  and  $P_{\text{INT}}$ . This results in 12 experimental conditions. The prototype will be kept fully extended at 150 mm for all experimental conditions.

#### Experimental Protocol

##### Operational Verification Test:

Before evaluating the Flexendoscope prototype, an operation verification test is conducted. This short test is carried out to establish that the prototype production and assembly have been completed successfully and that the prototype is sufficiently operational to perform the functions under evaluation. The test is mainly concerned with the presence or formation of leaks in the pressure chamber as well as the breakdown of individual components during the initial pressurization. Furthermore, the test is used to find the minimum and maximum operation pressures. The maximum internal pressure will be taken as the highest pressure under which the prototype can be safely and responsibly extended without the formation of leaks. An ample safety margin will be applied to this value.



During this test, the pressure inside the prototype is slowly increased until the layers of the inverted tube are fully separated at the tip. The prototype is constantly monitored to look for breakages or leaks in the mechanism. If neither are found, the constant pressure level at which the layers are fully separated is denoted as  $P_{MIN}$ . The internal pressure is increased until breakages or leaks occur or until further increase in pressure no longer feels responsible. At that point the test is ceased and the internal is pressure released. The highest value of the internal pressure at which operation was stable is denoted as  $P_{MAX}$ . The intermediate pressure level,  $P_{INT}$ , is calculated by taking the average of the minimum and maximum pressure levels.

#### Experiment 1:

Before starting the first experiment, both camera's are turned on and the prototype is pressurized to the desired level. To start the experiment, the extension fibers are manually pulled (using the attached force gauge) to overcome the internal resistance and initiate the extension process. The prototype is then extended from 0 to 150 mm along a straight line path in axial direction under a constant internal pressure. Both the position of the tip and the applied manual force are recorded at 30 frames per second with the two camera's. After the extension has been completed, the fibers used to manually retract the shaft are guided over the pulley and attached to the force gauge. These retraction fibers are then manually pulled to start the retraction process. Should the force gauge's maximum output of 50N be insufficient to extend or retract the prototype, additional weights are attached between the manual pulling fibers and the force gauge.

After the experiment has been completed, the velocity of the tip can be determined by comparing the tip position and time stamp of two successive frames in the camera recording. This is done using PhysMo (the open source software by dr. Jason Barraclough) as shown in Figure 5.3. The experiment is conducted for all values of the internal pressure. Two repetitive measurements (Trial 1 and Trial 2) are conducted for all the experimental conditions. Based on the measurement data collected from the camera frames, the position, velocity and applied force curves over time are approximated using MATLAB.

#### Experiment 2:

Before starting the second experiment, the shaft is fully extended to a length of 150 mm. The camera is turned on and the prototype is pressurized to the desired pressure level by adjusting the regulator. Once the desired internal pressure level has been achieved, a photo is taken of the initial position. Then the force gauge is attached to the tip, and the tip is deflected in radial direction by pulling the force gauge first to 30 mm, then 60 mm and finally 90 mm in radial direction. At each level of tip deflection, the force required to bend the shaft to that position is denoted and an image is recorded using the camera at each level of deflection. Then, the radial deflection force is unloaded and the prototype is allowed some time to stabilize. After the shaft has stabilized an image is recorded of the final equilibrium position. Finally, the internal pressure is released and the prototype is reset.

The experiment is repeated for all levels of the internal pressure. The collected data is used to approximate a force–deflection curve at each pressure level using MATLAB. Two repetitive measurements (Trial 1 and Trial 2) are conducted for all the experimental conditions.

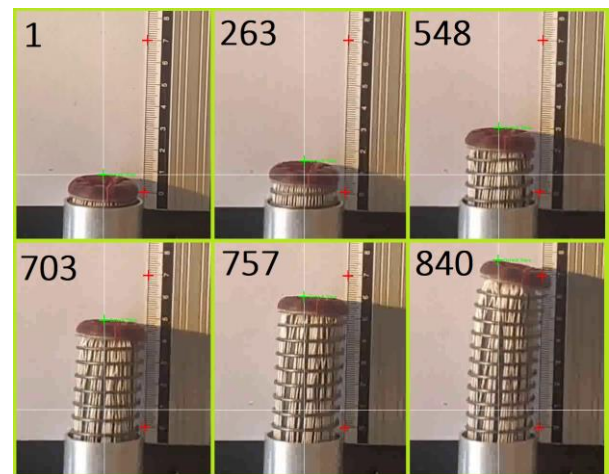


Figure 5.3: Six recorded frames, showing different stages of the prototype elongation during data analysis in the PhysMo motion tracking software. Experiment 1, Trail 1.

## 5.2. RESULTS

### Operational verification test

During the operational verification test, the internal pressure was slowly increased from 0 bar. At around 0.25 bar, initial separation of the inverted and everted layer of the flexible rubber tube was recorded at the tip. Full separation of the inverted tube's two layers occurred around 0.375 bar and was fully established (with a definite layer

of air between the two layers) at 0.5 bar. At this point in the test, the minimally required pressure was recorded at 0.5 bar.

As the pressure increased further, radial expansion of the inverted tube's external layer continued. Contact between the intermediate layer of fibers and spring occurred at an internal pressure level of around 0.7 bar. This signifies the maximum radial expansion of the inverted rubber tube. From 1.25 bar onwards, a slight but definitive leakage was identified in the form of an airflow between the slider and the internal pressure chamber wall. At the pressure of 1.4 bar, the operational verification test was ceased and the maximum internal pressure level,  $P_{MAX}$ , is set to 1 bar. This results in an intermediate pressure level,  $P_{INT}$ , of 0.75 bar.

### Experiment 1: Shaft Extension ( $P_{MIN}$ )

Figure 5.4 shows a plot of the extended shaft length over time during both Trial 1 and Trial 2 as well as the trial average for the internal pressure level  $P_{MIN}$ . For Trial 1, the maximum shaft length was recorded at 70 mm after 24.8 seconds. For Trial 2, the maximum shaft length was recorded at 66 mm after 28 seconds. After reaching maximum length, the rubber tube started folding in on itself at the base of the shaft, rather than everting further at the tip during both trials.

The top graph of Figure 5.5 shows the velocity data of tip during Trial 1 and Trial 2 as well as their accumulative average. Additionally, an exponential function is fitted to the data, showing the trend. For trial 1, the maximum tip velocity was 8.5 mm/s recorded after 18 seconds. For Trial 2, the maximum tip velocity was 7.3 mm/s recorded after 25 seconds.

The bottom graph of Figure 5.5 shows the magnitude of manual force application during Trial 1 and Trial 2 as well as their accumulative average. For Trial 1, the initial manual force (after which elongation commenced) was 96 N, the minimum force was 87.7 N (after 26.2 seconds) and the maximum force was 103 N (after 1.8 seconds). For Trial 2, the initial manual force was 105 N, the minimum force was 87.3 N (after 21.9 seconds) and the maximum force was 119 N (after 6.9 seconds).

### Experiment 1: Retraction ( $P_{MIN}$ )

No retraction of the shaft occurred during either of the two trials at the internal pressure,  $P_{MIN}$ . Instead, the tip of the inverted tube folded in on itself at a manual retraction force of approximately 5N. No further change in the shaft occurred as the manual retraction force was increased up to 50 N after which the experiment was ceased during both trials.

### Experiment 1: $P_{INT}$ and $P_{MAX}$

No shaft extension was recorded during both Trial 1 and Trial 2 at the internal pressure level  $P_{INT}$ . During both trials a maximum manual pulling force of approximately 200 N was recorded after which material failure ensued in the form of a manual extension fiber snapping in both trials. The experiment at the internal pressure level  $P_{INT}$  was ceased after the second material failure in a row.

No shaft extension was recorded at the internal pressure level  $P_{MAX}$  either. Material failure occurred once more at a manual pulling force of an unknown magnitude. At this point it was decided to only conduct one experimental trial at the internal pressure level  $P_{MAX}$ . No retraction trials were conducted for either  $P_{INT}$  or  $P_{MAX}$ .

### Experiment 2

Table 5.1 shows the forces required to deform the prototype shaft in bending up to a radial tip deflection of 30, 60 and 90 mm as well as the equilibrium position after bending for the pressure levels  $P_{ATM}$ ,  $P_{MIN}$ ,  $P_{INT}$  and  $P_{MAX}$ . The table shows the recorded forces during both Trial 1 and Trial 2 as well as their accumulative average. Additionally, Figure 5.6 shows a line plot of the average results at each pressure level.

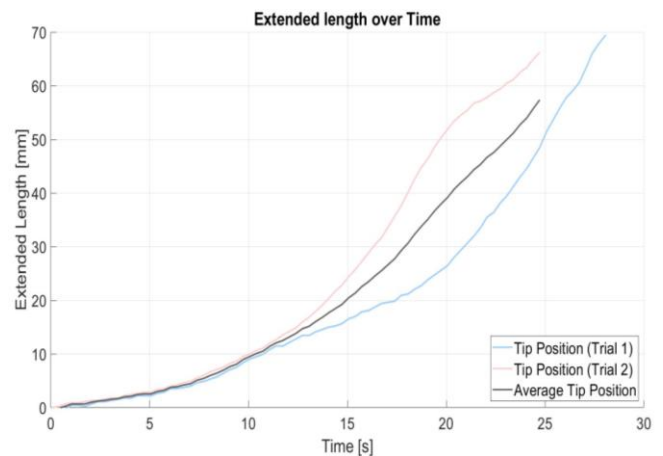


Figure 5.4: Position of the prototype tip over time during extension in Experiment 1.

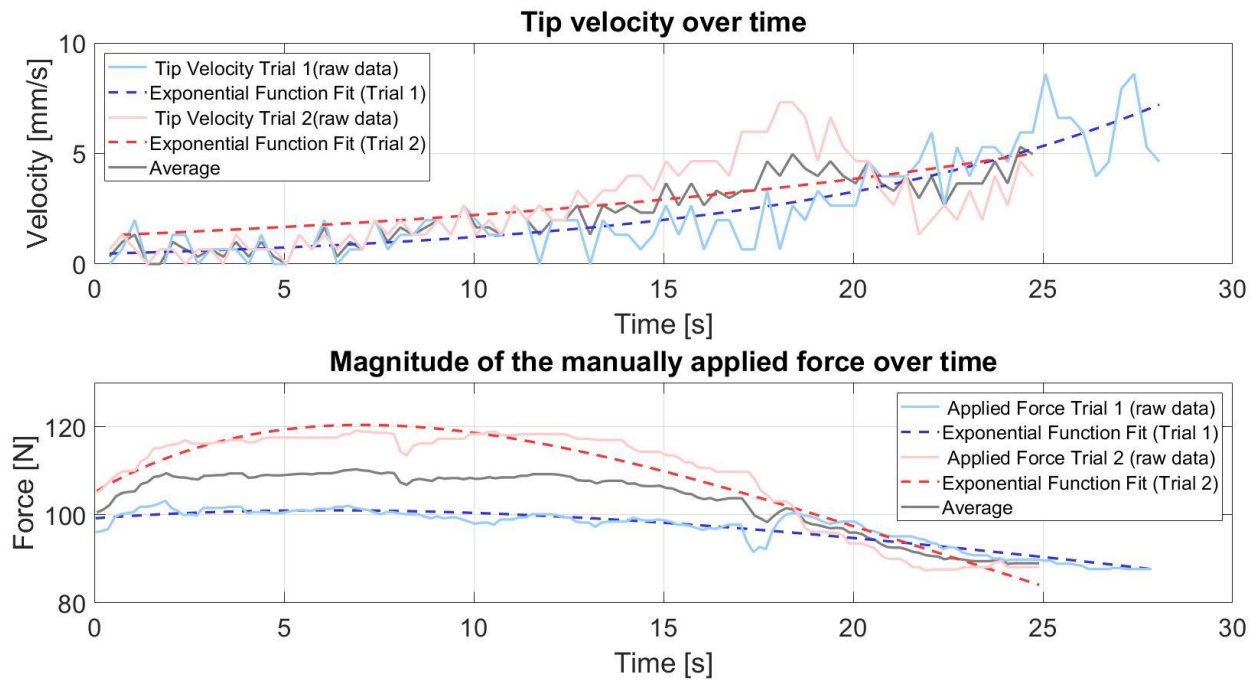


Figure 5.5: Top: Comparison between the tip velocity in Trial 1 and 2 as well as their average. Bottom: Comparison between the manual force applied in Trial 1 and 2 as well as their average.

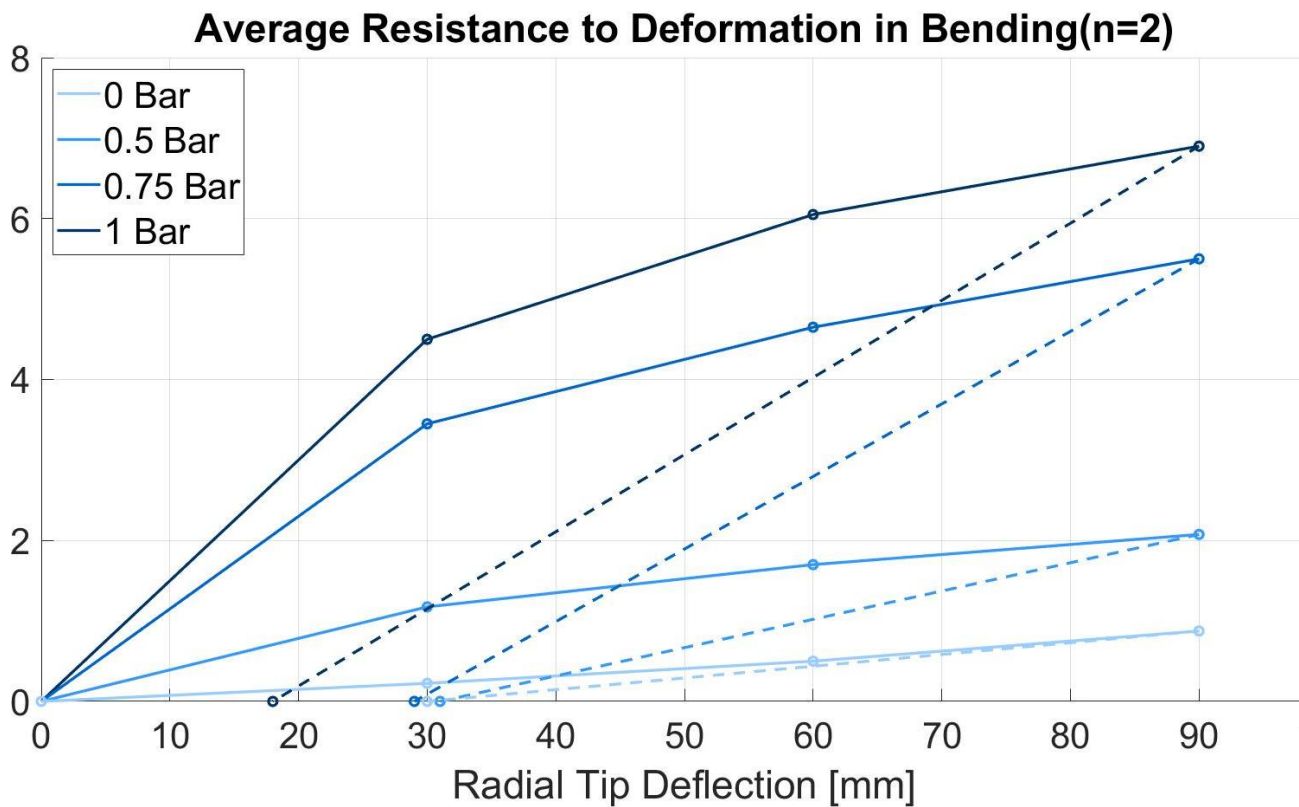


Figure 5.6: Average resistance to deformation in bending with radial tip deflection, in terms of the required radially applied deflection force for four different internal pressure levels.

*Table 5.1: All recorded results of experiment 2.2 and the average of trial 1 and 2. The first three columns show the radially applied force required to deform the shaft in bending through deflection of the tip to 30, 60 or 90 mm respectively. The last column shows the new equilibrium position of the tip in radial direction after deflection to 90 mm and removal of the applied force.*

|                  |         | 30 mm  | 60 mm  | 90 mm  | Equilibrium |
|------------------|---------|--------|--------|--------|-------------|
| PATM             | Trial 1 | 0,35 N | 0,6 N  | 1,1 N  | 30 mm       |
|                  | Trial 2 | 0,1 N  | 0,4 N  | 0,65 N | 30 mm       |
|                  | Average | 0,23 N | 0,50 N | 0,88 N | 30 mm       |
| P <sub>MIN</sub> | Trial 1 | 0,95 N | 1,7 N  | 2,1 N  | 40 mm       |
|                  | Trial 2 | 1,4 N  | 1,7 N  | 2,0 N  | 22 mm       |
|                  | Average | 1,18 N | 1,70 N | 2,08 N | 31 mm       |
| P <sub>INT</sub> | Trial 1 | 3,6 N  | 5,3 N  | 5,6 N  | 35 mm       |
|                  | Trial 2 | 3,3 N  | 4 N    | 5,4 N  | 23 mm       |
|                  | Average | 3,45 N | 4,65 N | 5,50 N | 29 mm       |
| P <sub>MAX</sub> | Trial 1 | 4,3 N  | 6,2 N  | 7,2 N  | 20 mm       |
|                  | Trial 2 | 4,7 N  | 5,9 N  | 6,6 N  | 16 mm       |
|                  | Average | 4,50 N | 6,05 N | 6,90 N | 18 mm       |

### 5.3. DISCUSSION OF THE RESULTS

#### Experiment 1: Maximum shaft extension (P<sub>MIN</sub>)

The prototype shaft extended to less than half (70 m) of its maximum length (150 mm) during both trials of Experiment 1 at pressure level P<sub>MIN</sub> due to internal folding of the rubber inverted tube at the base of the shaft. This internal folding likely occurred due to one of two reasons:

1. the internal pressure P<sub>MIN</sub>, became insufficient to keep the inverted and everted layers of the rubber tube fully separated as their surface area increased;
2. the inverted rubber tube contacted the inner pressure chamber wall through a gap in the intermediate layer of fibers at some point along the stored shaft material.

Both of these reasons would locally change the frictional resistance to sliding of the internally stored rubber tube. This would stop the forward sliding of the stored shaft material at the point of locally increased friction. The manual pulling forces applied to the slider at the back of the stored material would then push all the material between the slider and the point of increased friction onto

itself. New material then no longer arrives at the tip and the apical extension process is ceased.

#### Experiment 1: Retraction

When retracting the prototype shaft during both trials of experiment 1 at pressure level P<sub>MIN</sub>, the shaft axially compressed and folded in on itself. This was likely caused by the frictional resistance to sliding between the stored shaft material and the internal pressure chamber wall being greater in magnitude than the critical compressive buckling load of the inverted-tube at the pressure level P<sub>MIN</sub>. This would cause the inverted-tube to collapse rather than re-invert at the tip and slide back into the storage chamber.

#### Experiment 1: Tip velocity (P<sub>MIN</sub>)

The tip velocity shows a gradual increase and acceleration over time for both trials of Experiment 1 at pressure level P<sub>MIN</sub>. The increase in velocity is less pronounced during Trail 2 than during Trial 1 due to a noticeable drop in tip velocity at around 20 seconds. This drop coincides with a sudden reduction of the applied manual pulling force during Trial 2, which would explain the observed difference. Moreover, the tip velocity shows many sudden variations in magnitude over the entire extension process during both trials. This is likely due to variability of the local frictional resistance experienced by the slider and the stored shaft material as it slides forwards.

#### Experiment 1: Manual Pulling force (P<sub>MIN</sub>)

During both trials of Experiment 1 at the pressure level P<sub>MIN</sub>, the initial manual pulling force required to initiate the extension process was very high (avg: 100.5 N), showing a slight decrease over time (13%) as the shaft extended. The reduction of the required manual force is likely caused by a decrease in length of the (frictionally resistive) internally stored material as well as a decrease of the tip acceleration.

#### Experiment 1: P<sub>INT</sub> and P<sub>MAX</sub>

During all extension trials of experiment 1 at the internal pressure levels P<sub>INT</sub> and P<sub>MAX</sub>, the minimally required manual pulling force is shown to be too high for the structural integrity of the current prototype under evaluation (200 N +). This confirms the theoretical expectation that there is an increase in the required manual pulling force

due to an increase of the frictional resistance with pressure. The frictional resistance increases with pressure due to an increase of the normal force that is applied on the sliding contact area when the flexible inverted tube is compressed.

stresses due to bending of the shaft exceed the frictional resistance of the jamming mechanism.

### Experiment 2: Stiffness increase with pressure

The results of Experiment 2 seem to indicate an increase in bending stiffness with pressure for all pressure levels. The highest average resistance to deformation in bending of 0.88 N under atmospheric pressure ( $P_{ATM}$ ) shows that the prototype shaft is highly compliant when in an unactuated or unpressurized state.

The highest average resistance to deformation in bending of 2.08 N for the minimum extension pressure ( $P_{MIN}$ ) shows that the shaft is still relatively compliant when it apically extends at that internal pressure level.

The most sizable increase in resistance to deformation in bending is shown to occur between  $P_{MIN}$  and  $P_{INT}$ . This sudden increase is associated with the activation of the fiber jamming mechanism due to contact establishment between the inverted tube and intermediate layer of fibers at around 0.7 bar as discussed in the results of the operational verification test in Section 5.2. After the sudden increase between  $P_{MIN}$  and  $P_{INT}$ , a smaller increase is seen between  $P_{INT}$  and  $P_{MAX}$ . This smaller increase is associated with an increase of the normal force in radial direction exerted by the inverted tube on the intermediate layer of fibers.

### Experiment 2: Stiffness increase with deflection

The results of Experiment 2 seem to indicate a further increase in bending stiffness with the distance of tip deflection in radial direction. This is associated with elastic bending behavior, which was likely caused by the properties of the spring around the shaft and axial stretching of the jammed Dyneema fibers in the intermediate shaft layer.

The results also show the occurrence of some hysteresis as the tip does not fully return to its initial position after bending but rather finds a new equilibrium position. The hysteresis indicates a loss of energy in the mechanism which is likely caused by axial slipping of individual Dyneema fibers in the jammed intermediate layer when the internal



## 6 DISCUSSION

### 6.1 OVERVIEW

The analogy drawn between plant roots moving through cracks in soil and flexible endoscopes moving through a human colon has proven very relevant and valuable as a source of inspiration for the design of flexible endoscopes. Eight biological features were identified of which seven are suitable as potential solutions in the development of medical instruments.

Furthermore, the Flexendoscope concept is found to be very promising. The combination of an apical extension mechanism with a variable stiffness mechanism theoretically allows the insertion of a highly compliant shaft into the colon which can still provide the desired high tip rigidity after insertion at the surgical site. The functionality of the current Flexendoscope prototype was, however, slightly less promising. Limitations in the current design prevented the apical extension mechanism from functioning properly achieving only a limited extension length. On the other hand, the results obtained during evaluation of the prototype's variable stiffness mechanism were very desirable, showing considerable stiffening at convenient pressure levels above the apical extension pressure. To improve the design of the Flexendoscope, limitations in the current proof of concept design have to be overcome. Redesign proposals to do so are provided in Section 6.3 of this discussion. Besides these redesign proposals, this thesis also gathered a large amount of knowledge on practicalities of designing and constructing a physical prototype of an flexible, variable stiffness inverted tube mechanism. Overcoming initial hurdles and paving a way for future developments.

If the limitations in the current design can be overcome in future iterations, the Flexendoscope design could ultimately prevent colon stretching as well as shaft buckling and shear force transmission to the colon wall during insertion into the colon.

### 6.2 PROTOTYPE BEHAVIOR

#### Apical extension

Apical extension was achieved only at the lowest evaluated internal pressure,  $P_{\text{MIN}}$ . At this internal pressure level, the functionality was erratic and unreliable since only half the maximum extension was achieved, retraction of the shaft did not occur

and manually applied forces (required for the extension) were very high. Although the current performance of the apical extension function is left wanting, it did show that shaft extension is possible thus validating the proof of concept. Furthermore, the results showed that the behavioral problems of the apical extension function have a common root cause, which is the high frictional resistance to extension within the mechanism and the frictional increase with pressure.

#### Loss of precision in endoscope tip control

The tip velocity showed many sudden variations in magnitude during extension in Experiment 1 due to local variation of the internal frictional resistance. This inconsistency of the frictional resistance to extension is undesirable in a flexible endoscope because it makes the relation between the manual input force and the output tip velocity unreliable. This results in a loss of precision when controlling the propulsion of the tip, which could lead to the transmission of excessive normal forces from the endoscope tip to the colon wall.

#### Loss of force feedback

The high magnitude of the manually applied force, required to initiate shaft extension during both trials of Experiment 1 (avg: 100.5 N), is undesirable for a flexible endoscope. The high magnitude of the input force makes it difficult for a physician to sense small variations in the input force caused by axial resistances at the endoscope tip (up to 13 N as discussed in Chapter 1). This results in a loss of haptic force feedback between the endoscope tip and the physician, which could lead to the transmission of excessive normal forces from the endoscope tip to the colon wall.

#### Internal frictional resistance

If the frictional resistance and its increase with pressure can be overcome in future iterations of the design, the internal pressure during extension could be increased. This would likely prevent internal folding of the inverted tube and allow full extension as well as retraction of the shaft, thus improving performance. Additionally, it would lower the required manual input force and make the relation between the input force and the output tip velocity more reliable. This would improve force feedback and precision control of the endoscope tip respectively.

**Variable stiffness: Threshold pressure**

The threshold pressure (0.7 bar) above which the onset of fiber jamming results in a sudden increase in the resistance to deformation in bending of the Flextendoscope shaft was found to be above the pressure level  $P_{\text{MIN}}$  (0.5 bar), at which the shaft is able to extend. This property of the variable stiffness function is highly desirable for a flexible endoscope as it allows the design to overcome the paradoxical stiffness requirement that forms a limitation for current flexible endoscope designs. The higher threshold pressure allows the shaft of an endoscope to extend through the colon while remaining relatively flexible in bending. Upon arrival of the tip at the location of medical interest, the internal pressure  $P_{\text{MIN}}$  can be increased above the threshold to substantially stiffen the mechanism and facilitate the increased endoscope tip rigidity, which is required to perform a surgical procedure.

**Variable stiffness: Hysteresis**

The prototype shaft has been shown to initially deform elastically in bending until the internal stresses (due to bending) exceed the friction between the jammed fibers in the intermediate shaft layer. When the internal stress exceed the internal friction the fibers start to slide relative to each other. This causes the shaft to deform plastically due to the occurrence of hysteresis and loss of energy in the shaft.

In the author's opinion, this response to bending is very desirable in a flexible endoscope. The initial elastic response allows an endoscope shaft to restore and retain its shape after small deflections in straighter sections of the colon. Moreover, the plastic response caused by energy loss in the shaft reduces the normal force that is transmitted by the endoscope shaft at the contact point with the colon during large deformations in bending.

The plastic deformation is not undesirable in this design (as it would be in conventional endoscope shafts). The newly obtained equilibrium position of the shaft (as a result of the plastic deformation) is undone when the internal pressure is reduced and the previously jammed fibers can be manually rearranged into a straight configuration.

**6.3 DESIGN LIMITATIONS AND RECOMMENDATIONS****Contradictory requirements in the current design**

The current design of the Flextendoscope results in a number of contradictory requirements on some of its components:

1. The intermediate layer of fibers is desired to have a low coefficient of friction with the internal pressure chamber wall and spring to improve extension but also have a high coefficient of friction with the inverted rubber tube to improve fiber jamming efficiency;
2. On the one hand, the inverted intermediate layer of the shaft (currently consisting of Dyneema fibers) is desired to be stiff in radial direction to prevent an increase of the frictional resistance to extension with pressure. On the other hand, the layer is required to evert, for which it has to be flexible in bending and thus compliant in radial direction;
3. On the one hand, the intermediate shaft layer of fibers is required to be highly flexible in bending to evert at the tip. On the other hand, the flexibility of the individual fibers causes them to misalign and create tangential gaps, greatly increasing the frictional resistance to extension and making the layer very difficult to assemble.

These contradictions inhibit the components from functioning optimally, resulting in limitations in the current Flextendoscope design.

**Limitation 1: Internal sliding of the shaft material**

The greatest limitation of the design is the internal sliding of the stored shaft material in the pressure chamber as it results in the frictional resistance to extension, which is the cause of most problems experienced by the apical extension function. In a future rendition of the Flextendoscope design, this forward sliding of the stored inverted tube over the pressure chamber wall can be overcome through internal or external multiplication of the inverted rubber tube in the shaft design as shown in Figures 6.1 and 6.2 respectively. Both these solutions essentially result in a non-sliding surface on the outside of the shaft as well as on the central luminal side of the shaft.

Internal multiplication of the inverted tube, in other words, means placing an additional inverted tube (which is mirrored in orientation) inside the central luminal space of the original inverted tube. This results in both the internal and external wall of the combined inverted tubes becoming stationary as the sliding, inverted shaft material is stored in the center between the two stationary walls. Ensuring that the internally stored sliding shaft material remains in the center of the two inverted tubes will prove to be a major design challenge. Overcoming that challenge comes down to correctly defining the mechanical properties and natural diameters of both the inverted tubes.

External multiplication of the inverted tube results in a shaft that is made up of multiple inverted tubes placed in a circular pattern around a central lumen. This method also ensures that the sliding inverted shaft material is stored in the center of each individual inverted tube, resulting in a stationary wall on both the internal and external side of the shaft.

#### Limitation 2: Sliding of the spring along the colon

The second limitation of the design is that the spring (which serves as the external layer of the shaft) is unable to invert. This causes the spring to slide along the outside of the shaft as it extends. Although this limitation is on purpose, it should be addressed in future iterations as the flexible colon wall could in theory become pinched between the threads of the spring when it slides along the colon wall.

A possible solution to this limitation is replacing the spring with a thin tube (knitted from Dyneema fibers) which is flexible as well as compressible and thus invertible but not radially expandable as shown in Figure 6.3. This would result in a simplified shaft that consists of three invertible layers that can be interconnected at multiple points along the shaft length rather than the three current unconnected layers of the shaft.

#### Limitation 3: Gaps in the inverted layer of fibers

The third limitation in the design is the emergence of tangential gaps between individual fibers in the intermediate shaft layer. This happens because of the small diameter and compressibility of the Dyneema fibers, which allows fibers to cross over each other and misalign rather than form a perfect single layer. The occurrence of these gaps is fully

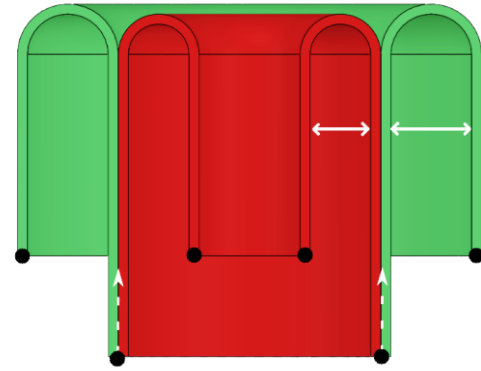


Figure 6.1: Section view of an internally multiplied inverted tube. The external walls of the internal tube (red) and external tube (green) remain stationary whilst the internal walls in the center, where the two tubes meet, slide forwards.

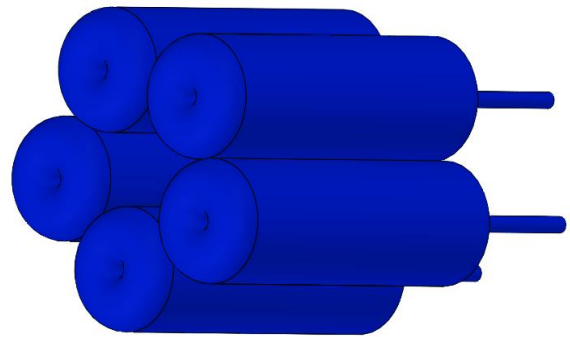


Figure 6.2: 3D view of an externally multiplied configuration of five inverted tubes in a circular pattern to create a shaft with lumen. All the external walls remain stationary and only the center of each individual inverted tube slides.

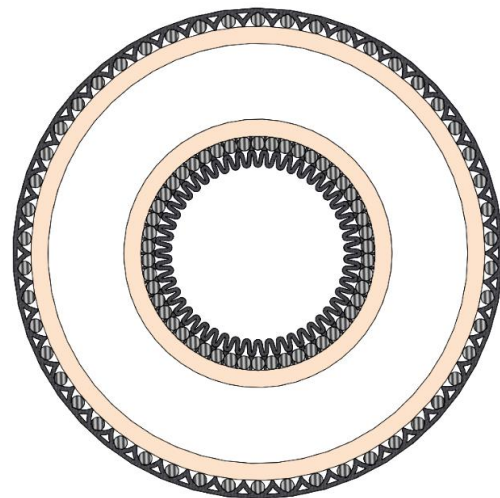


Figure 6.3: Section view of an inverted multilayered tube consisting of an flexible rubber tube (beige), longitudinal Dyneema fibers (light gray) and a woven Dyneema sheath (dark gray). On the internal inverted section the Dyneema sheath is compressed and folded whilst on the external everted section it is smooth and tensioned thereby limiting further radial expansion.

dependent on the precision with which the shaft material is assembled around the internal pressure chamber wall. This makes the current prototype difficult to assemble to a satisfactory degree and makes the performance of the prototype inconsistent.

The design proposal, discussed in the previous limitation (shown in Figure 6.3), could prevent misalignment (caused by the tangential sliding of individual fibers) because the stitches connecting the internal and external layers of that shaft in that design would encapsulate each individual fiber in the intermediate layer in a separate longitudinal pocket. Moreover, the individual fibers should be redesigned to have a diameter of at least 2 mm. This would reduce the number of fibers around the circumference to 22 at most. This greatly simplifies assembly of the intermediate layer and lessens the chance of individual fibers crossing over each other when sliding tangentially.

#### **Limitation 4: Internal shaft material storage**

A fourth limitation of the current design is the inefficiency of the material storage. By storing the shaft material in a single straight line, the storage length needs to be double the maximum obtainable shaft length. In a functional flexible endoscope, this would result in a storage length of 3.6 meters. Future iterations of the Flexendoscope should look into storing shaft material in the same manner as in a garden hose. Even though a garden hose is spooled, its central lumen remains accessible through attachment of the tube end to the core of the spool.

Alternatively, should the shaft redesign consist of multiple inverted tubes as was proposed in Limitation 1 and shown in Figure 6.2, the individual tubes could be stored more efficiently by rolling them tightly around a spool. This would not enclose the central lumen of the shaft but only pinch shut the lumina of the individual inverted tubes.

#### **Limitation 5: Shaft Retraction**

The fifth limitation of the design is that the manual retraction forces are currently applied at the tip of the shaft, which causes the shaft to buckle under the compressive load. In a redesign, the manual pulling force should be applied at the posterior end of the shaft material on what is currently the slider. This was not an option in the current design as

access to the shaft material was blocked off from the posterior side by the pressure chamber end cap. This limitation could be overcome in a future iteration by allowing access to the shaft material from the posterior end through a pressure seal.

#### **Limitation 6: Pneumatic actuation**

The sixth and final limitation of the current design is that it is actuated pneumatically. This would be a limitation for a flexible endoscope when inserted into the colon because air is compressible. In the event of a leak the pressurized air will flow into the colon and expand. This would rapidly inflate the colon and cause complications. In future iterations, the pneumatic actuation should be exchanged with hydraulic actuation. Because water is incompressible, a leak would no longer result in instantaneous expansion of the colon and consequences would likely be less severe.

#### **Downscale shaft diameter**

Although not a limitation, the current external diameter of the flexible endoscope shaft is too wide for use in a real colon. In future iterations, the shaft should be downscaled from 30 mm external diameter to 15 mm at most. A 50% downscale would be relatively straightforward. The dimensions of every component can easily be decreased without complicating their functionality or structural integrity. Scalability of the design is mostly limited by the relatively small dimension of the individual fibers in the intermediate shaft layer. However, as mentioned in limitation 2, the relative dimensions of these individual fibers should be increased by at least a factor three in future designs. Therefore, subsequent downscaling of these fibers should not be problematic.

#### **Include tip steerability**

Tip steerability could be included in future iterations of the Flexendoscope design to ease extension of the tip through a colon bend. Either a currently existing steerable tip can be mounted on the apex of the inverted tube or tip steerability could be custom designed. The author has looked into manners of including custom steerability in the Flexendoscope design through manipulation of specific fibers in the intermediate shaft layer, but this was ultimately considered too complex for the current stage of the design. Including steering in the design is a challenge for two reasons. Firstly,

establishing a controllable mechanical link with the tip is difficult because of the continuous change in distance between tip and handle. Secondly, building steerability into the shaft itself is difficult because the shaft material at the tip is continuously renewed. Some conceptual ideas of steerable Flextendoscope designs can be found in appendix D.

#### 6.4 SCIENTIFIC RELEVANCE AND FUTURE RESEARCH

##### Biological inspiration: Plant root growth

The analogy drawn between plant roots moving through cracks in soil and flexible endoscopes moving through a human colon has proven very relevant and valuable as a source of inspiration for the design of flexible endoscopes. Eight biological features were identified of which seven are suitable as potential solutions in the development of medical instruments. The unique mechanical behavior of growing plant roots has resulted in a new type of minimally invasive propulsion through cavities in the human body. This manner of propulsion can be further explored in the future for use in a variety of medical instruments such as flexible endoscopes or endovascular catheters. The class of inverted tube mechanisms is likely to be the most natural and useful mechanical translation of the apical extension mechanism of plant roots for applications in the medical sector due to their simple, soft and highly flexible nature.

##### Potential of the Flextendoscope design

The conceptual combination of an apical extension mechanism with variable stiffness in the Flextendoscope design has shown to be very promising. The unique combination of the two main functions could ultimately allow the insertion of a highly flexible shaft while still being able to supply a high tip rigidity when required after insertion. This would result in the inherent prevention of colon stretching during insertion of an endoscope as well as a shaft design that is no longer bound by the stiffness trade-off in current flexible endoscopes. Additionally, the switch from posterior push insertion to apical extension inherently prevents shaft buckling and will ultimately also prevent shear transmission to the colon wall due to shaft sliding. The prevention of these implications by the Flextendoscope design could ultimately lead to colonoscopy becoming an

easier, safer and less painful procedure with a higher success rate.

##### Gathered knowledge

A large amount of knowledge on practicalities of designing and constructing a physical prototype of an flexible, variable stiffness inverted tube mechanism was gathered in this thesis. Initial hurdles were overcome in the development of a physical proof of concept prototype, paving the way for future innovations.

##### Focus of future redesigns

Further developments of the Flextendoscope design should focus on eliminating the internal frictional resistance and look into overcoming the contradictory requirements currently enforced on components within the design. This process can be kickstarted by evaluating the recommendations and design proposals in Section 6.2.

##### Other fields of application

The Flextendoscope design can also be relevant to applications outside the medical sector such as the exploration of ducts, vents, tubes and rubble or the penetration of granular soils for the taking of samples or construction of underground pipes and cable networks.



## 7 CONCLUSION

The goal of this thesis was to design and evaluate a proof of concept propulsion mechanism for the insertion of a flexible endoscope into the human colon. The reason for redesigning the method of insertion was to overcome the limitations found in state of the art flexible endoscope designs and to prevent the medical implications that they bring about during current colonoscopic procedures. This would ultimately make colonoscopy safer and less painful for the patient as well as make the procedure less specialistic to perform.

As inspiration for the design, an analogy was drawn between plant roots moving through cracks in soil and flexible endoscopes moving through the human colon. The analogy was found to be very relevant and useful, resulting in eight biological features of which seven were suitable as a potential solution in the development of a flexible endoscope. Of these seven suitable solutions, apical extension and variable stiffness became the main functions of the proposed design. The focus of the design process on these two functions ultimately culminated a final design of a flexible, extending endoscope named the Flextendoscope.

The Flextendoscope consisted of an inverted tube mechanism combined with a fiber jamming mechanism which enable the apical extension and variable stiffness of the design respectively. Both functions were actuated through an increase of the pneumatic pressure in the mechanism. The concept of the Flextendoscope design is found to be very promising as it theoretically allows the insertion of a highly compliant shaft into the colon which can still provide the desired high tip rigidity after insertion at the surgical site.

Although the prototype evaluation validated the feasibility of the proof of concept design, the performance of the apical extension function was of limited success. Due to internal frictional problems, the prototype shaft was only able to extend under the lowest evaluated pressure, 0.5 bar, requiring high manual input forces up to 119 Newton. Moreover, the prototype was not able to retract after the extension. On the other hand, the performance of the variable stiffness function was found to be very desirable. The bending stiffness of the prototype was found to increase with both pressure level and distance of radial deflection, showing initial elastic deformation followed by

plastic deformation and hysteresis. It showed considerable stiffening at a convenient threshold pressure of 0.7 bar, slightly above the apical extension pressure.

To improve the performance of the physical prototype limitations in the Flextendoscope design have to be overcome. Initial redesign proposals are provided in the thesis to pave the way for future developments. If the current limitations caused by the internal frictional resistances are overcome the Flextendoscope concept has the potential to prevent colon stretching, buckling and shear force transmission to the colon wall during insertion of a flexible endoscope. The prevention of these implications by the Flextendoscope design could ultimately lead to colonoscopy becoming an easier, safer and less painful procedure with a higher success rate.

# BIBLIOGRAPHY

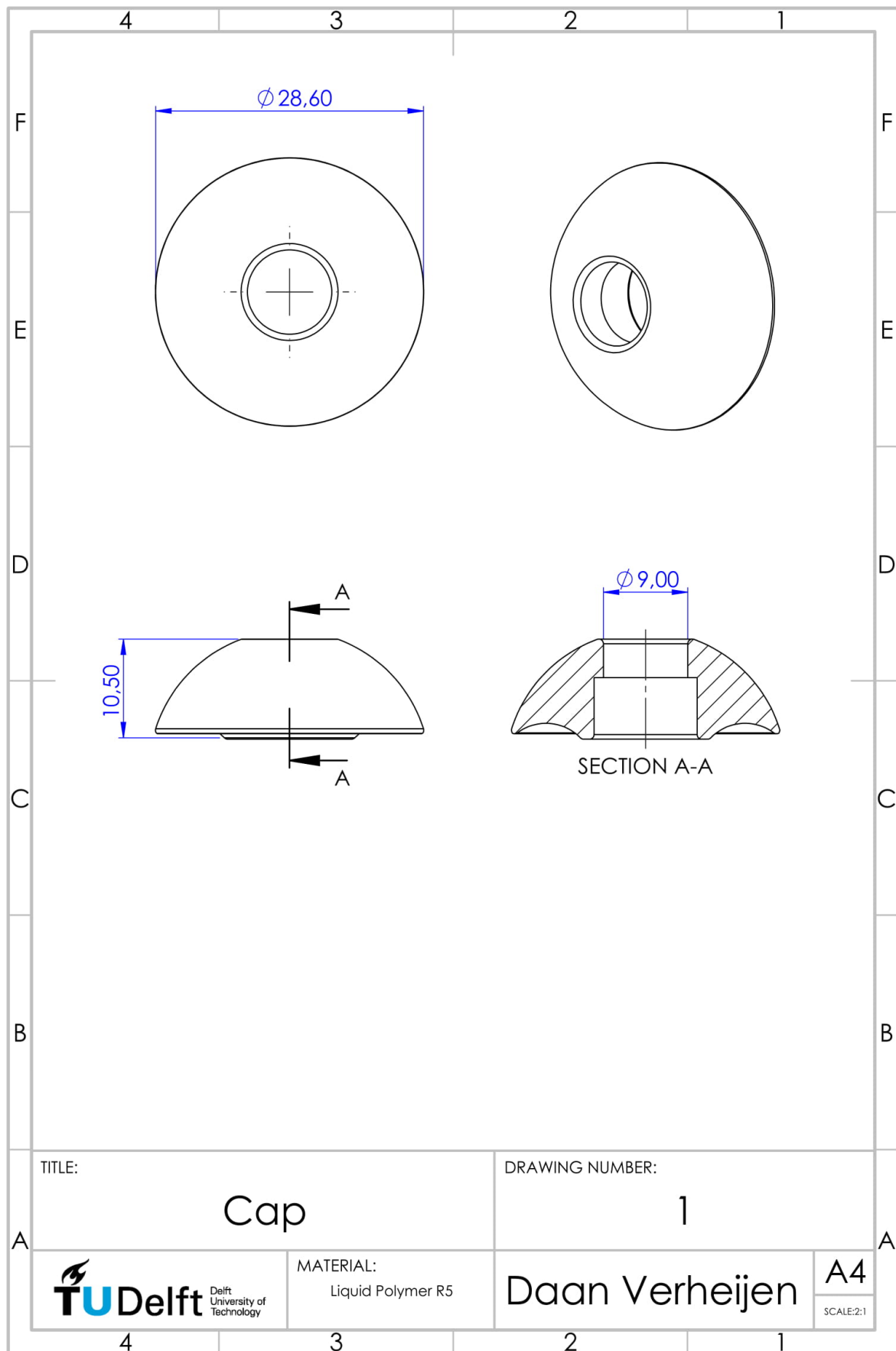
- [1] J. Moreira-Pinto, *et al.*, "Natural orifice transluminal endoscopy surgery: A review", *World Journal of Gastroenterology*, Vol. 17, pp. 3795-3801, 2011.
- [2] A.J. Loeve, "Shaft-guidance for flexible endoscopes", TU Delft repository: <http://repository.tudelft.nl/>, pp. 101-124, 2012.
- [3] Rozeboom, E.D., Ruiter, J.G., Franken, M. *et al.* Single-handed controller reduces the workload of flexible endoscopy. *J Robotic Surg* 8, 319–324 (2014).
- [4] Marieb, E. and Hoehn, K., 2016. *Human Anatomy & Physiology*. 10th ed. Harlow: Pearson Education Limited, pp.450-505, 717-791.
- [5] Loeve AJ, Fockens P, Breedveld P. Mechanical analysis of insertion problems and pain during colonoscopy: why highly skill-dependent colonoscopy routines are necessary in the first place and how they may be avoided. *Can J Gastroenterol*. 2013;27(5):293-302.
- [6] Appleyard MN, Mosse CA, Mills TN, Bell GD, Castillo FD, and Swain CP, "The measurement of forces exerted during colonoscopy," *Gastrointestinal Endoscopy*, vol. 52, pp. 237-240, 2000.
- [7] A. Ali, *et al.*, "Steerable catheters in cardiology: classifying steerability and assessing future challenges", *IEEE transactions on biomedical engineering*, Vol. 63, pp. 679-693, 2016.
- [8] A. Ali, *et al.*, "Catheter steering in interventional cardiology: Mechanical analysis and novel solution", *Journal of Engineering in Medicine*, Vol. 233, pp. 1207-1218, 2019.
- [9] P. Breedveld, *et al.*, "A new, easily miniaturized steerable endoscope", in *IEEE Engineering in Medicine and Biology Magazine*, Vol. 24, pp. 40-47, 2005.
- [10] L.J. Clark, *et al.*, "How do roots penetrate strong soil?", *Plant and Soil*, Vol. 255, pp. 93-104, 2003.
- [11] E. Kolb, *et al.*, "Physical root-soil interactions", *Physical Biology*, Vol. 14, pp. 1-40, 2017.
- [12] B.J. Atwell, "Response of roots to mechanical impedance", *Environmental and experimental botany*, Vol. 33, pp. 27-40, 1993.
- [13] A. Sadeghi, *et al.*, "A novel growing device inspired by plant root soil penetration behaviors", *PLoS ONE*, Vol. 9, 2014.
- [14] A.M. Abdalla, *et al.*, "The mechanics of root growth in granular media", *Journal of Agricultural Engineering Research*, Vol. 14, pp. 236-248, 1969.
- [15] S. Ruiz, *et al.*, "The mechanics and energetics of soil penetration by earthworms and plant roots – higher rates cost more", *Vadose Zone Journal*, Vol. 16, pp. 77-109, 2017.
- [16] J.H. Trevor, "The dynamics and mechanical energy expenditure of the polychaetes *Nephtys cirrosa*, *Nereis diversicolor* and *Arenicola marina* during burrowing", *Estuarine and Coastal Marine science*, Vol. 6, pp. 605-619, 1978.
- [17] P. Slade, *et al.*, "Design of a soft catheter for low-force and constrained surgery", *IEEE/RSJ International Conference on Intelligent Robots and Systems (IROS)*, pp. 174-180, 2017.

- [18] K. Jin, *et al.*, How do roots elongate in a structured soil?, *Journal of Experimental Botany*, Volume 64, Issue 15, November 2013, pp. 4761–4777
- [19] A. Glyn Bengough, Kenneth Loades, Blair M. McKenzie, Root hairs aid soil penetration by anchoring the root surface to pore walls, *Journal of Experimental Botany*, Volume 67, Issue 4, February 2016, pp. 1071–1078.
- [20] A. Sadeghi, *et al.*, “Robotic mechanism for soil penetration inspired by plant root”, IEEE/International conference on robotics and automation (ICRA), pp. 3457-3462, 2013.
- [21] J.D. Greer, *et al.*, “Obstacle-Aided navigation of a soft growing robot”, IEEE/International conference on robotics and automation (ICRA), pp. 4165-4172, 2018.
- [22] J.D. Greer, *et al.*, “A soft, steerable continuum robot that grows via tip extension”, *Soft robotics*, Vol. 6, pp. 95-108, 2019.
- [23] E.W. Hawkes, *et al.*, “A soft robot that navigates its environment through growth”, *Science robotics*, Vol. 2, pp. 1-7, 2017.
- [24] J. Luong, *et al.*, “Eversion and retraction of a soft robot towards the exploration of coral reefs”, IEEE/International conference on soft robotics (RoboSoft) COEX, pp. 801-807, 2019.
- [25] A. Sadeghi, *et al.*, “Towards self-growing soft robots inspired by plant roots and based on additive manufacturing technologies”, *Soft robotics*, Vol. 4, pp. 211-223, 2017.
- [26] H. Dehgahni, *et al.*, “Design and preliminary evaluation of a self-steering, pneumatically driven colonoscopy robot”, *Journal of Medical Engineering & Technology*, Vol. 41, pp. 223-236, 2017.
- [27] T.K. Morimoto, *et al.*, “Toward the design of personalized continuum surgical robots”, *Annals of Biomedical Engineering*, Vol. 46, pp. 1522-1533, 2018.
- [28] A.J. Loeve, D.H. Plettenburg, P. Breedveld, J. Dankelman., “Endoscope Shaft-Rigidity Control Mechanism: FORGUIDE”, *IEEE Trnas Biomed Eng*, vol. 59 pp. 542-551, 2012.

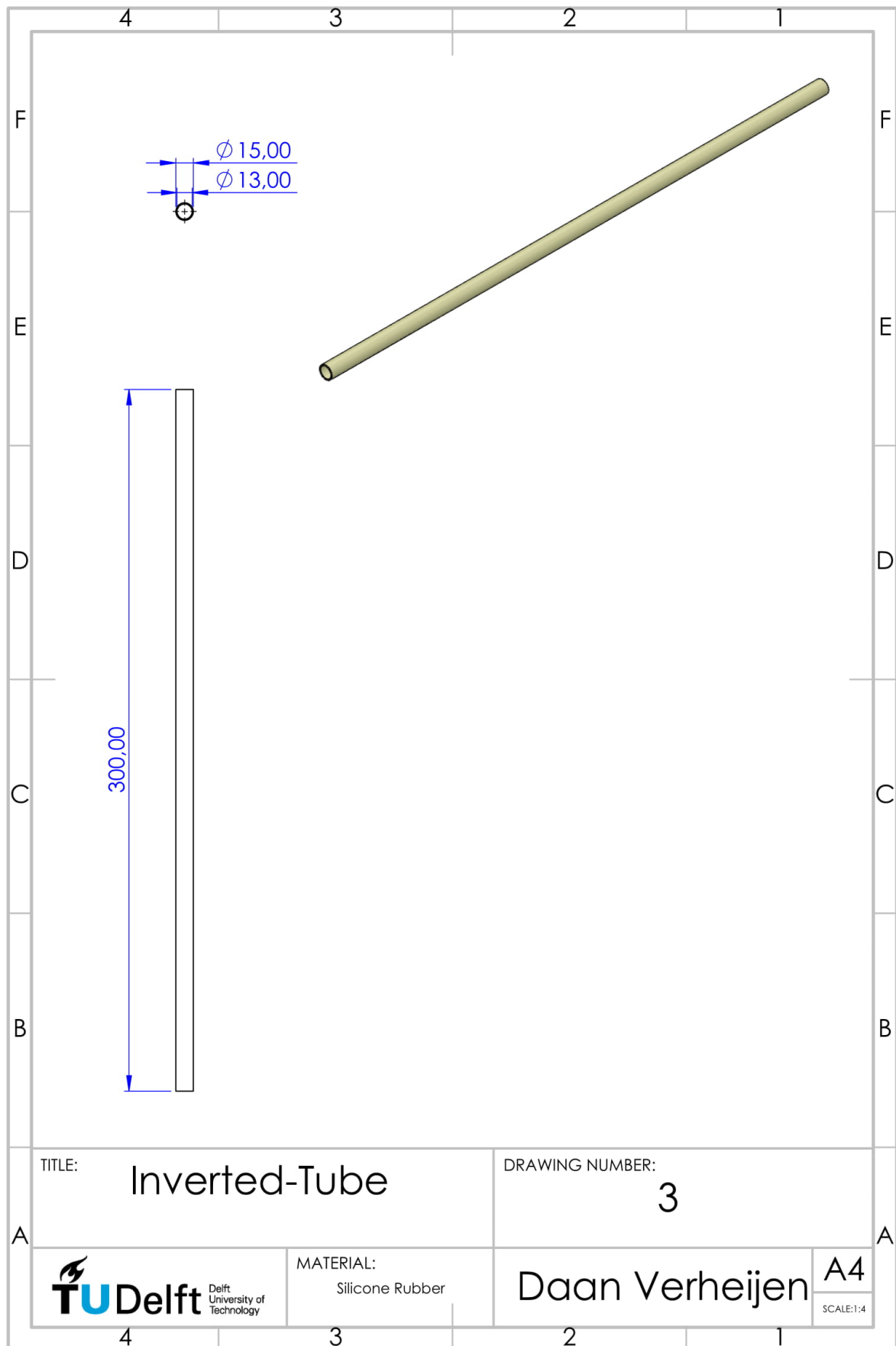
# A

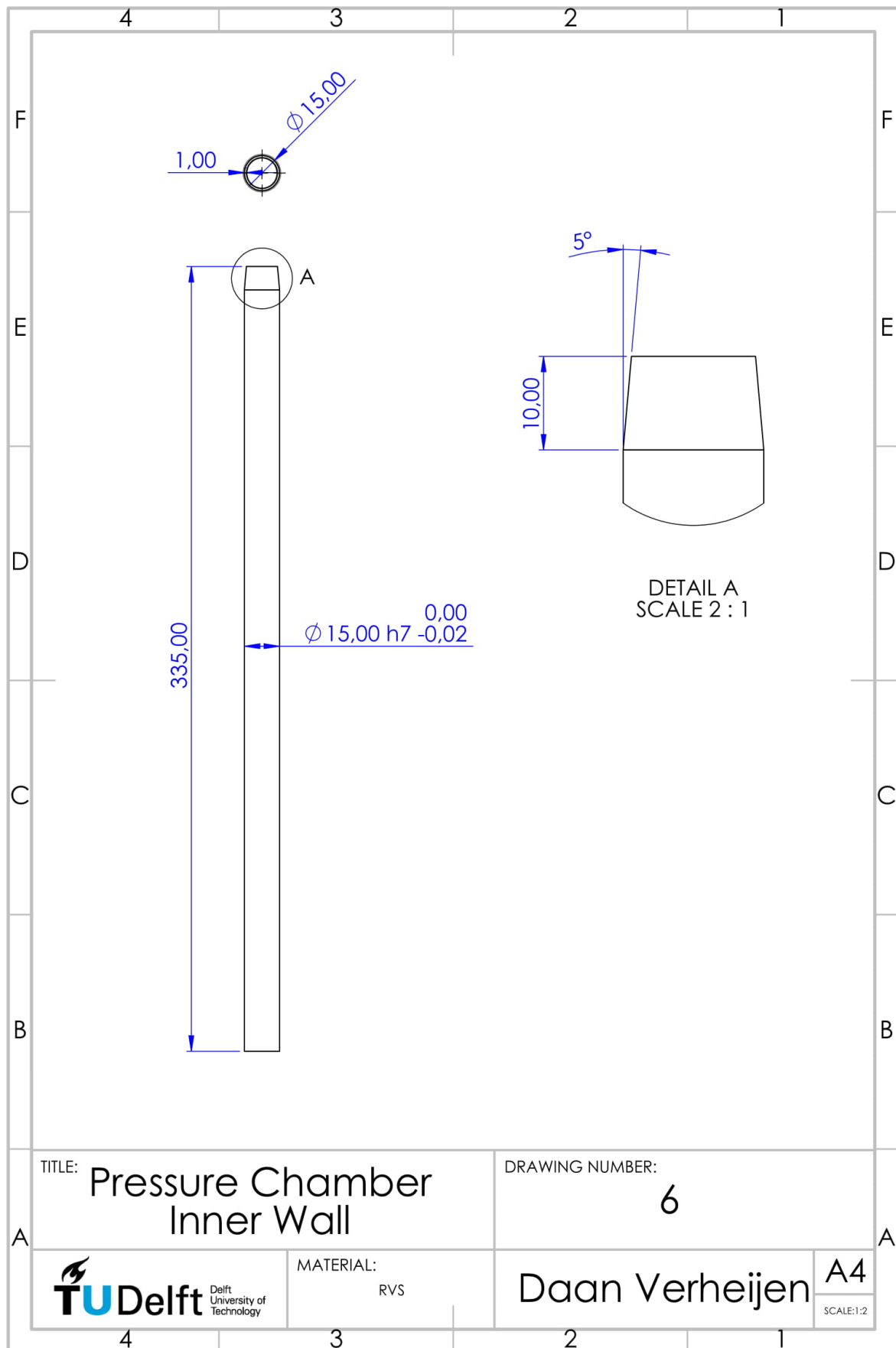
## APPENDIX: TECHNICAL DESIGN DRAWINGS

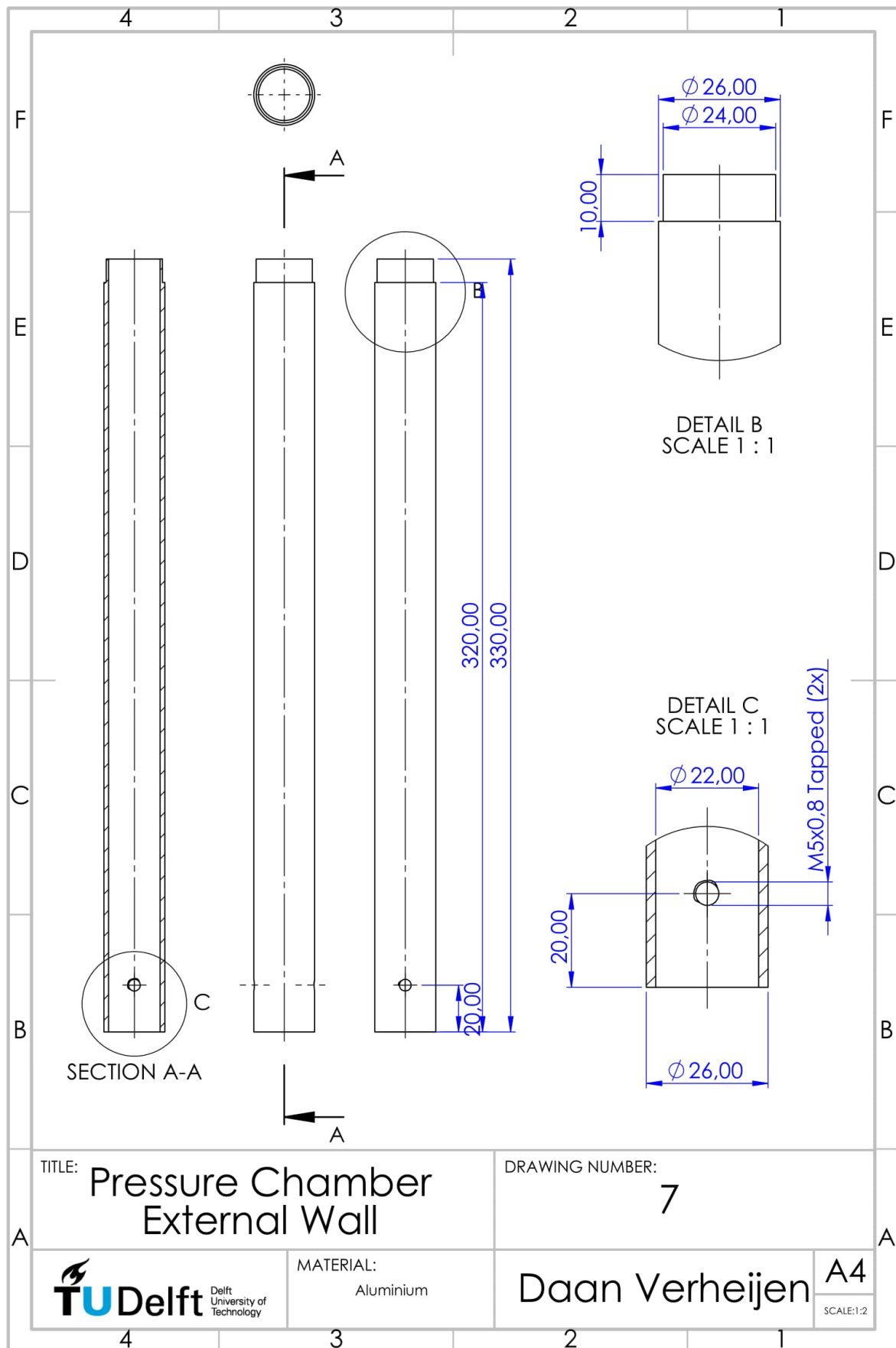
| Partslist             |                  |                  |                  |          |
|-----------------------|------------------|------------------|------------------|----------|
| Part #                | Part Name        | Production       | Supplier         | Quantity |
| A: Tip                |                  |                  |                  |          |
| 1                     | Cap              | 3D Print         | Demo             | 1        |
| B: Shaft              |                  |                  |                  |          |
| 3                     | Inverted-Tube    | Rubber Extrusion | n / a            | 1        |
| C: Housing            |                  |                  |                  |          |
| 6                     | P.C. Inner Wall  | purchased + P.P. | Salomons Metalen | 1        |
| 7                     | P.C. Outer Wall  | purchased + P.P. | Salomons Metalen | 1        |
| 8                     | Slider           | Machining        | n / a            | 1        |
| 9                     | P.C. Endcap      | Machining        | n / a            | 1        |
| 13                    | Handle           | purchased + P.P. | Salomons Metalen | 1        |
| D: Experimental Setup |                  |                  |                  |          |
| D1                    | Mounting Bracket | 3D-Print         | Demo             | 2        |

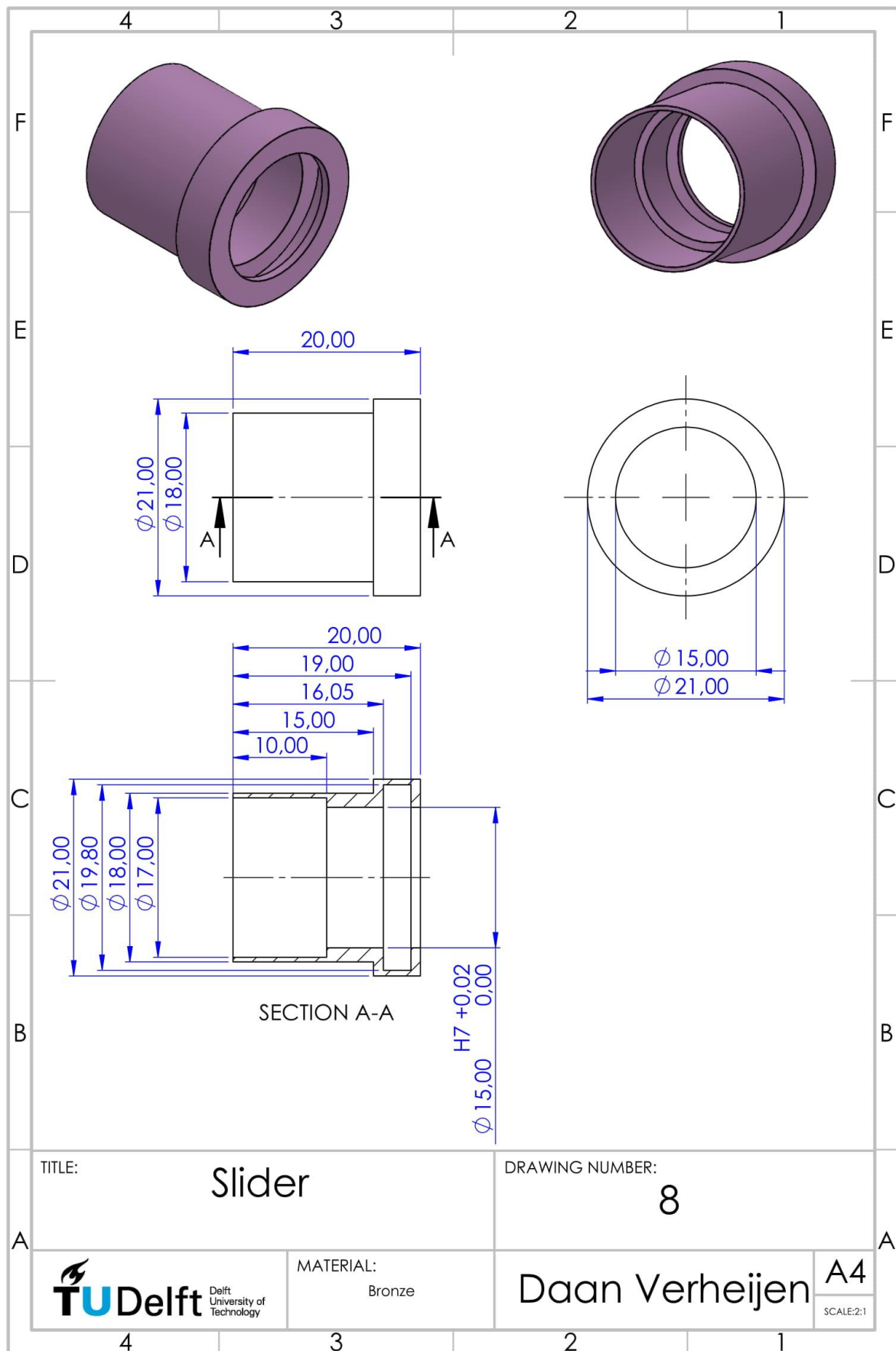


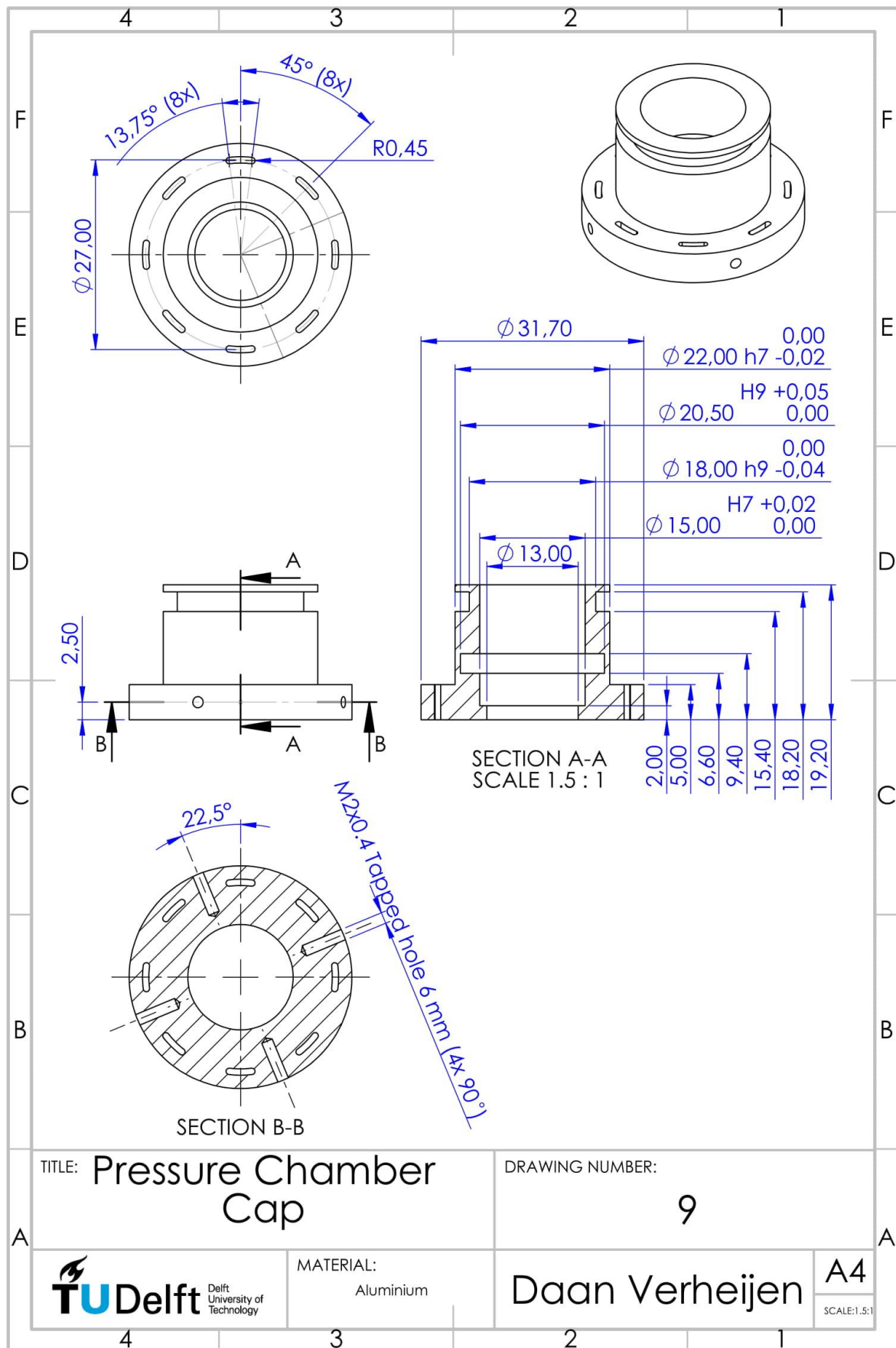




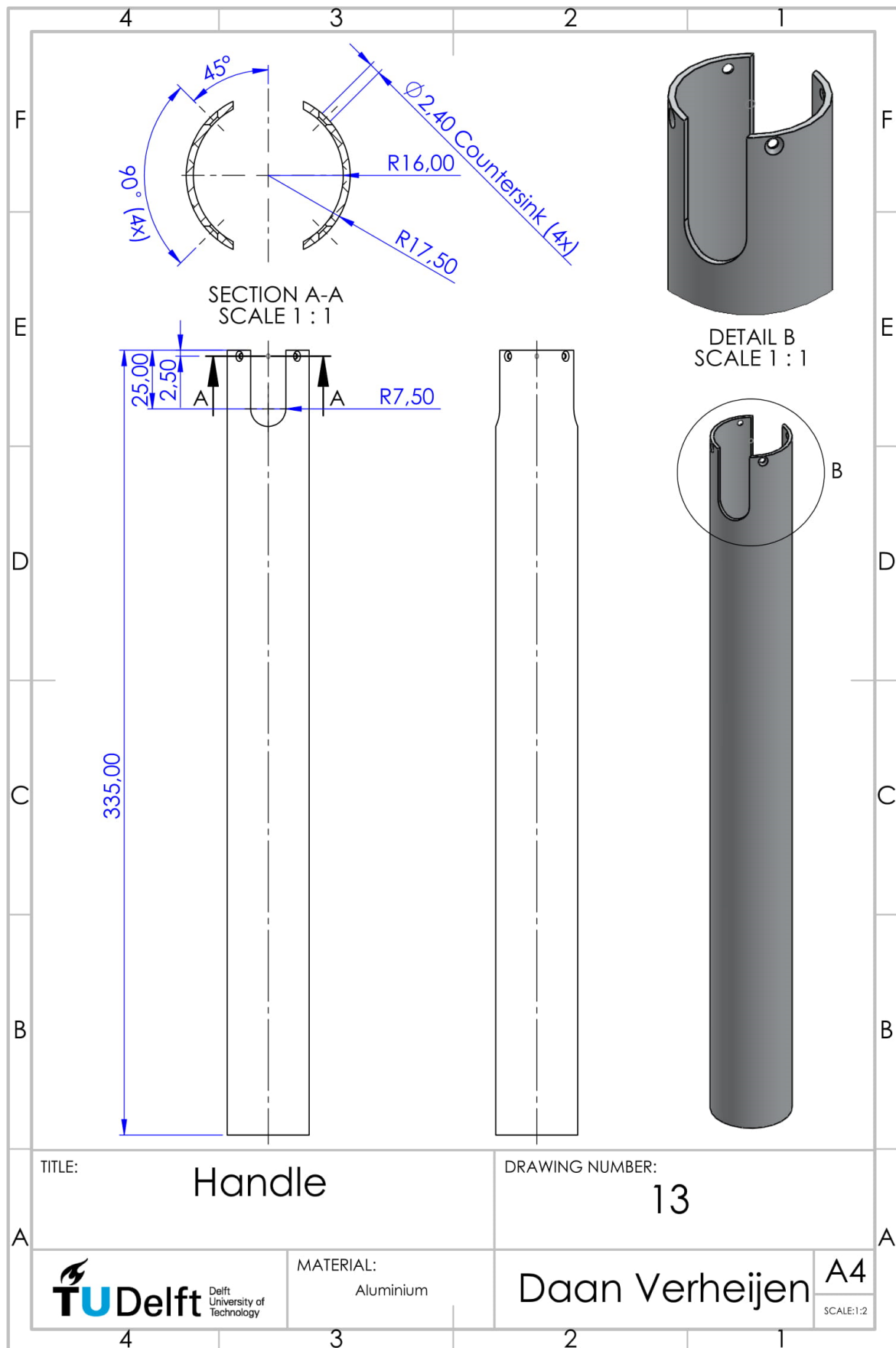


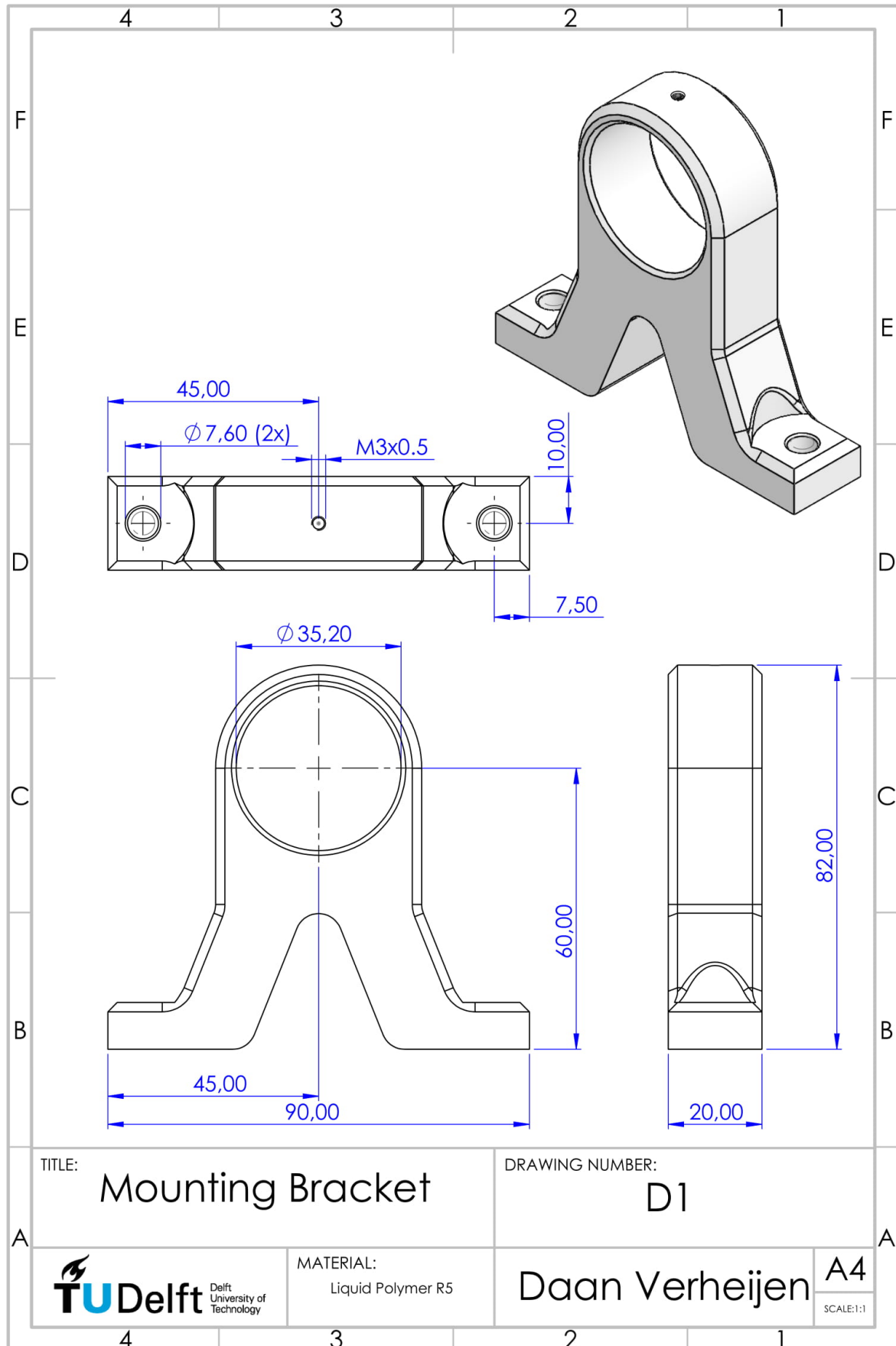












# B

## APPENDIX: MATLAB DATA ANALYSIS SCRIPTS

### Experiment 1

```
% Data Analysis of the Experiment 1: Extension and Retraction
clear all, close all, clc

%% Experimental Data Import from Excell
%Data of Trial 1 Camera 1 (T2C1)
T2C1_raw = xlsread('T2C1_plotdata'); %framenumber, timestamp, x(abs), Y(abs), X(m), Y(m)
T2C1_raw(840,:) = T2C1_raw(839,:) + (T2C1_raw(839,:)-T2C1_raw(838,:)); %add 1 frame
T2C1_raw(841,:) = T2C1_raw(840,:) + (T2C1_raw(840,:)-T2C1_raw(839,:)); %add 1 frame
T2C1_t = T2C1_raw(1:10:end,2);
T2C1_pos = T2C1_raw(1:10:end,6)*10; %only consider every 10th frame (3fps) to smoothen data (dt = 0.33 sec)

for i = 2:length(T2C1_pos)
    T2C1_vel(i-1) = (T2C1_pos(i)-T2C1_pos(i-1))/(T2C1_t(i) - T2C1_t(i-1,:)); %v = (p2-p1)/(t2-t1)
end

save('T2C1_vel','T2C1_vel')
save('T2C1_t','T2C1_t')
lambda0_T2C1 = [1 70.0]';
lambda0_T2C2 = [0.005 0.8]';

%Data of Trial 1 Camera 2 (T2C2)
T2C2_raw = xlsread('T2C2_data'); %frame,timestamp,force
T2C2_t = T2C2_raw(1:5:end,2);
T2C2_F = T2C2_raw(1:5:end,3);
save('T2C2_t','T2C2_t')
save('T2C2_F','T2C2_F')

%Data of trial 2 Camera 1 (T3C1)
T3C1_raw = xlsread('T3C1_data'); %framenumber, timestamp, x(abs), Y(abs), X(m), Y(m)
T3C1_t = T3C1_raw(1:10:end,2);
T3C1_pos = abs(T3C1_raw(1:10:end,5))*10; %only consider every 10th frame (3fps) to smoothen data (dt = 0.33 sec)

for i = 2:length(T3C1_pos)
    T3C1_vel(i-1) = (T3C1_pos(i)-T3C1_pos(i-1))/(T3C1_t(i) - T3C1_t(i-1,:)); %v = (p2-p1)/(t2-t1)
end

save('T3C1_vel','T3C1_vel')
save('T3C1_t','T3C1_t')
lambda0_T3C1 = [-0.05 80.0]';
lambda0_T3C2 = [0.005 0.8]';

%Data of Trial 2 Camera 2 (T3C2)
T3C2_raw = xlsread('T3C2_data'); %frame,timestamp,force
T3C2_t = T3C2_raw(1:5:end,2);
T3C2_F = T3C2_raw(1:5:end,5);
save('T3C2_t','T3C2_t')
save('T3C2_F','T3C2_F')

%% Position, Velocity and Force Analysis (TRIAL 1)
% Position (Trial 1)
figure(1)
hold on
plot(T2C1_t,T2C1_pos,'color',[153/255 204/255 255/255],'Linewidth',2)
axis([0 30 0 70])
grid on
title('Extended length over Time (Trial 1)','FontSize',30)
xlabel('Time [s]','FontSize',25)
ylabel('Extended Length [mm]','FontSize',25)
legend('Tip Position','Location','Southeast','FontSize',25)
set(gca,'FontSize',25);

% Velocity (Trial 1)
```

```

figure (2)
lambda1_T2C1 = fminsearch(@expfitfun_T2C1,lambda0_T2C1);
[residual_T2C1,beta_T2C1,f2v] = expfitfun_T2C1(lambda1_T2C1);
axis([0 30 0 10])
grid on
title('Tip velocity over time (Trial 1)','FontSize',25)
xlabel('Time [s]','FontSize',20)
ylabel('Velocity [mm/s]','FontSize',20)
legend('Tip Velocity (raw data)','Exponential Function Fit','Location','Northwest','FontSize',20)
set(gca,'FontSize',20);

% Force (Trial 1)
figure(2)
lambda1_T2C2 = fminsearch(@expfitfun_T2C2,lambda0_T2C2);
[residual_T2C2,beta_T2C2,f2f] = expfitfun_T2C2(lambda1_T2C2);
axis([0 30 80 120])
grid on
title('Magnitude of the manually applied force over time (Trial 1)','FontSize',25)
xlabel('Time [s]','FontSize',20)
ylabel('Force [N]','FontSize',20)
legend('Applied Force (raw data)','Exponential Function Fit','Location','Northeast','FontSize',20)
set(gca,'FontSize',20);

%% Position, Velocity and Force Analysis (TRIAL 2)
% Position (Trial 2)
figure(3)
hold on
plot(T3C1_t,T3C1_pos,'color',[255/255 204/255 204/255],'Linewidth',2) %run2 cleaned position data
axis([0 30 0 70])
grid on
title('Extended length over Time (Trial 2)','FontSize',30)
xlabel('Time [s]','FontSize',25)
ylabel('Extended Length [mm]','FontSize',25)
legend('Tip Position','Location','Southeast','FontSize',25)
set(gca,'FontSize',25);

% Velocity (Trial 2)
figure (4)
lambda1_T3C1 = fminsearch(@expfitfun_T3C1,lambda0_T3C1);
[residual_T3C1,beta_T3C1,f4v] = expfitfun_T3C1(lambda1_T3C1);
axis([0 30 0 10])
grid on
title('Tip velocity over time (Trial 2)','FontSize',25)
xlabel('Time [s]','FontSize',20)
ylabel('Velocity [mm/s]','FontSize',20)
legend('Tip Velocity (raw data)','Exponential Function Fit','Location','Northwest','FontSize',20)
set(gca,'FontSize',20);

% Force (Trial 2)
figure(4)
lambda1_T3C2 = fminsearch(@expfitfun_T3C2,lambda0_T3C2);
[residual_T3C2,beta_T3C2,f4f] = expfitfun_T3C2(lambda1_T3C2);
axis([0 30 80 130])
grid on
title('Magnitude of the manually applied force over time (Trial 2)','FontSize',25)
xlabel('Time [s]','FontSize',20)
ylabel('Force [N]','FontSize',20)
legend('Applied Force (raw data)','Exponential Function Fit','Location','Northeast','FontSize',20)
set(gca,'FontSize',20)

%% Compare the Tip Position during Trial 1 and 2
for i = 1:length(T3C1_pos)
    Pos_avg(i) = (T2C1_pos(i) + T3C1_pos(i))/2;
end

figure(5)
hold on
plot(T2C1_t,T2C1_pos,'color',[153/255 204/255 255/255],'Linewidth',2) %run1 cleaned position data
plot(T3C1_t,T3C1_pos,'color',[255/255 204/255 204/255],'Linewidth',2) %run2 cleaned position data
plot(T3C1_t,Pos_avg,'color',[96/255 96/255 96/255],'Linewidth',2)
axis([0 30 0 70])
grid on
title('Extended length over Time','FontSize',25)
xlabel('Time [s]','FontSize',20)
ylabel('Extended Length [mm]','FontSize',20)
legend('Tip Position (Trial 1)','Tip Position (Trial 2)','Average Tip Position','Location','Southeast','FontSize',20)

```

```

set(gca,'FontSize',20);

%% Compare the Tip Velocity during Trial 1 and 2
for i = 1:length(T3C1_vel)
    V_avg(i) = (f2v(1).YData(i) + f4v(1).YData(i))/2;
end

f6 = figure(6);
hold on
f61 = subplot(2,1,1);
f6_avgV = plot(T3C1_t(2:end),V_avg,'color',[128/255 128/255 128/255],'Linewidth',2);
f2vc = copyobj(f2v,f61);
f4vc = copyobj(f4v,f61);
axis([0 30 0 10])
grid on
title('Tip velocity over time','FontSize',25)
xlabel('Time [s]','FontSize',20)
ylabel('Velocity [mm/s]','FontSize',20)
legend([f2vc(1),f2vc(2),f4vc(1),f4vc(2),f6_avgV],' Tip Velocity Trial 1(raw data)','Exponential Function Fit (Trial 1)',' Tip Velocity Trial 2(raw data)','Exponential Function Fit (Trial 2)','Average','Location','Northwest','FontSize',15)
set(gca,'FontSize',20);

%% Compare the Applied Force during Trial 1 and 2
for i = 1:length(T3C2_F)
    F_avg(i) = (f2f(1).YData(i) + f4f(1).YData(i))/2;
end

figure (6)
hold on
f62 = subplot(2,1,2);
f6_avgF = plot(T3C2_t,F_avg,'color',[128/255 128/255 128/255],'Linewidth',2);
f2fc = copyobj(f2f,f62);
f4fc = copyobj(f4f,f62);
grid on
axis([0 30 80 130])
title('Magnitude of the manually applied force over time','FontSize',25)
xlabel('Time [s]','FontSize',20)
ylabel('Force [N]','FontSize',20)
legend([f2fc(1),f2fc(2),f4fc(1),f4fc(2),f6_avgF],' Applied Force Trial 1 (raw data)','Exponential Function Fit (Trial 1)',' Applied Force Trial 2 (raw data)','Exponential Function Fit (Trial 2)','Average','Location','Northeast','FontSize',15)
set(gca,'FontSize',20);

```

## Experiment 2

% Data Analysis of the Experiment 2: Bending Stiffness

clear all, close all, clc

%Data Input

```

D_P0 = [0,30,60,90,30;0,30,60,90,30;0,30,60,90,30]; %Deflection at P0, run1 ; run2 ; avg
D_Pmin = [0,30,60,90,40;0,30,60,90,22;0,30,60,90,31];%Deflection at Pmin, run1 ; run2 ; avg
D_Pint = [0,30,60,90,35;0,30,60,90,23;0,30,60,90,29];%Deflection at Pint, run1 ; run2 ; avg
D_Pmax = [0,30,60,90,20;0,30,60,90,16;0,30,60,90,18];%Deflection at Pmax, run1 ; run2 ; avg

F_P0 = [0,0.35,0.6,1.1,0;0,0.1,0.4,0.65,0;0,0.225,0.5,0.875,0]; %Force at P0, run1 ; run2 ; avg
F_Pmin = [0,0.95,1.7,2.1,0;0,1.4,1.7,2.05,0;0,1.175,1.7,2.075,0]; %Force at Pmin, run1 ; run2 ; avg
F_Pint = [0,3.6,5.3,5.6,0;0,3.3,4,5.4,0;0,3.45,4.65,5.5,0]; %Force at Pint, run1 ; run2 ; avg
F_Pmax = [0,4.3,6.2,7.2,0;0,4.7,5.9,6.6,0;0,4.5,6.05,6.9,0]; %Force at Pmax, run1 ; run2 ; avg

```

```

figure(1)
subplot(2,2,1)
hold on
grid on
fr1 =
plot(D_P0(1,:),F_P0(1,:), 'r',D_Pmin(1,:),F_Pmin(1,:), 'b',D_Pint(1,:),F_Pint(1,:), 'k',D_Pmax(1,:),F_Pmax(1,:), 'g', 'LineWidth',1.2);
set(fr1(1),'color',[153/255 204/255 255/255]);
set(fr1(2),'color',[51/255 153/255 255/255]);
set(fr1(3),'color',[0/255 102/255 204/255]);
set(fr1(4),'color',[0/255 51/255 102/255]);
axis([0 100 0 8])
xlabel('Radial Deflection [mm]')
ylabel('Deflection Force [N]')
title('Resistance to Deformation in Bending, Run 1')
legend('0 Bar','0.5 Bar','0.75 Bar','1 Bar','Location','Southeast')

```



```

subplot(2,2,2)
hold on
grid on
fr2 =
plot(D_P0(2,:),F_P0(2,:), 'r',D_Pmin(2,:),F_Pmin(2,:), 'b',D_Pint(2,:),F_Pint(2,:), 'k',D_Pmax(2,:),F_P
max(2,:), 'g', 'LineWidth',1.2);
set(fr2(1), 'color', [153/255 204/255 255/255]);
set(fr2(2), 'color', [51/255 153/255 255/255]);
set(fr2(3), 'color', [0/255 102/255 204/255]);
set(fr2(4), 'color', [0/255 51/255 102/255]);
axis([0 100 0 8])
xlabel('Radial Deflection [mm]')
ylabel('Deflection Force [N]')
title('Resistance to Deformation in Bending, Run 2')
legend('0 Bar','0.5 Bar','0.75 Bar','1 Bar','Location','Southeast')

subplot(2,2,[3,4])
hold on
grid on
f2_34l =
plot(D_P0(3,1:4),F_P0(3,1:4), 'r',D_Pmin(3,1:4),F_Pmin(3,1:4), 'b',D_Pint(3,1:4),F_Pint(3,1:4), 'k',D_P
max(3,1:4),F_Pmax(3,1:4), 'g', 'LineWidth',2);
f2_34p =
plot(D_P0(3,:),F_P0(3,:), 'ro',D_Pmin(3,:),F_Pmin(3,:), 'bo',D_Pint(3,:),F_Pint(3,:), 'ko',D_Pmax(3,:),
F_Pmax(3,:), 'go', 'LineWidth',2);
f2_34dl = plot(D_P0(3,4:5),F_P0(3,4:5), 'r--',D_Pmin(3,4:5),F_Pmin(3,4:5), 'b--
',D_Pint(3,4:5),F_Pint(3,4:5), 'k--',D_Pmax(3,4:5),F_Pmax(3,4:5), 'g--', 'LineWidth',2);
set(f2_34l(1), 'color', [153/255 204/255 255/255]);
set(f2_34l(2), 'color', [51/255 153/255 255/255]);
set(f2_34l(3), 'color', [0/255 102/255 204/255]);
set(f2_34l(4), 'color', [0/255 51/255 102/255]);
set(f2_34p(1), 'color', [153/255 204/255 255/255]);
set(f2_34p(2), 'color', [51/255 153/255 255/255]);
set(f2_34p(3), 'color', [0/255 102/255 204/255]);
set(f2_34p(4), 'color', [0/255 51/255 102/255]);
set(f2_34dl(1), 'color', [153/255 204/255 255/255]);
set(f2_34dl(2), 'color', [51/255 153/255 255/255]);
set(f2_34dl(3), 'color', [0/255 102/255 204/255]);
set(f2_34dl(4), 'color', [0/255 51/255 102/255]);
axis([0 100 0 8]);
xlabel('Radial Deflection [mm]')
ylabel('Deflection Force [N]')
title('Resistance to Deformation in Bending, Run Average')
legend('0 Bar','0.5 Bar','0.75 Bar','1 Bar','Location','Southeast')

figure(2);
f3 = gca;
hold on
f2_34lc = copyobj(f2_34l,f3);
f2_34pc = copyobj(f2_34p,f3);
f2_34dlc = copyobj(f2_34dl,f3);
axis([0 100 0 8])
grid on
xlabel('Radial Tip Deflection [mm]', 'FontSize',25)
ylabel('Radial Tip Force [N]', 'FontSize',25)
title('Average Resistance to Deformation in Bending(n=2)', 'FontSize',30)
legend([f2_34lc(1),f2_34lc(2),f2_34lc(3),f2_34lc(4)], '0 Bar','0.5 Bar','0.75 Bar','1
Bar','Location','Northwest', 'FontSize',25)
set(gca, 'FontSize',25);

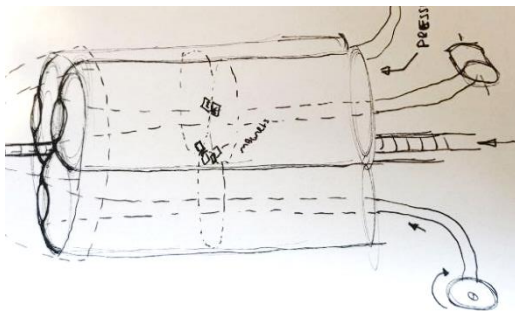
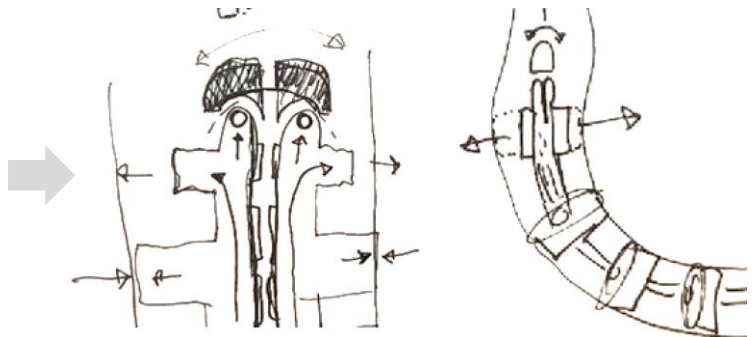
```

# C

## APPENDIX: CONCEPT DESIGN IDEATION

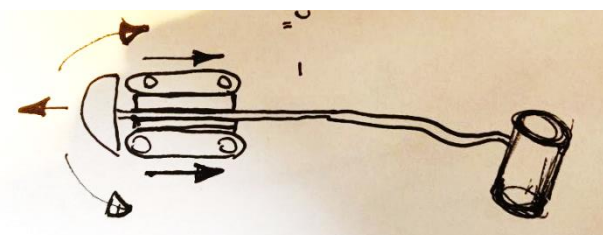
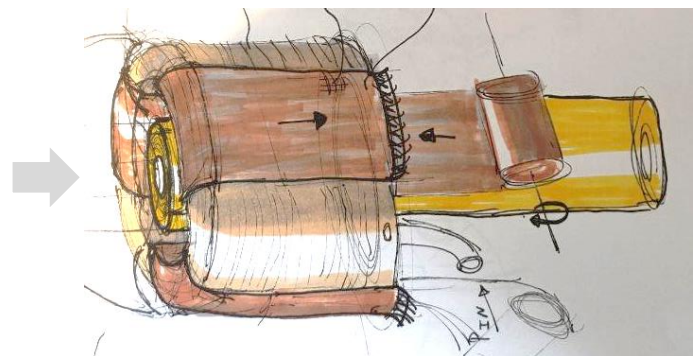
In this appendix some flexible endoscope propulsion mechanism design ideas, varying in their level of detailing, are shown. Most were created during the initial ideation phase prior to the concepts generated in Chapter 3. Some ideas resemble the chosen Flextendoscope whilst other differ completely. Each idea is supplemented with a short general explanation of the idea. They are included here in the hope that they may spark inspiration and creativity for future designs.

A Flexible Inverted tube with radially expandable segments, allowing it to “attach” itself to tubes with varying diameters, increasing the rigidity of its tip by shortening the unsupported length.

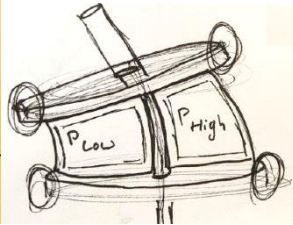
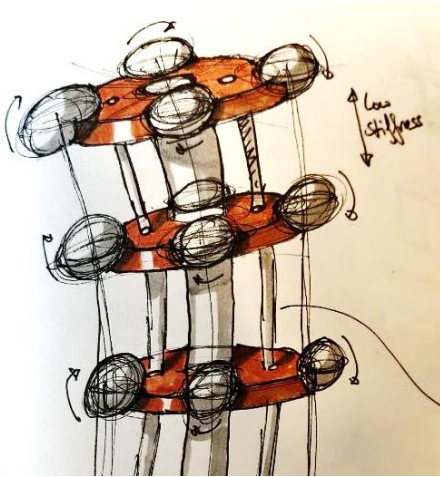


A Shaft consisting of three individually actuated inverted tubes with a lumen in the center. They remain attached to each other as they evert with magnetic strip along their length. Steering is theoretically possible by varying the everted lengths of the individual tubes relative to each other.

A long, compressed, donut shaped, balloon with multiple ribbons everting around it as it elongates to control the length of the elongation and the external diameter. Varying the respective length of the ribbons could hypothetically allow steering control over the elongation.

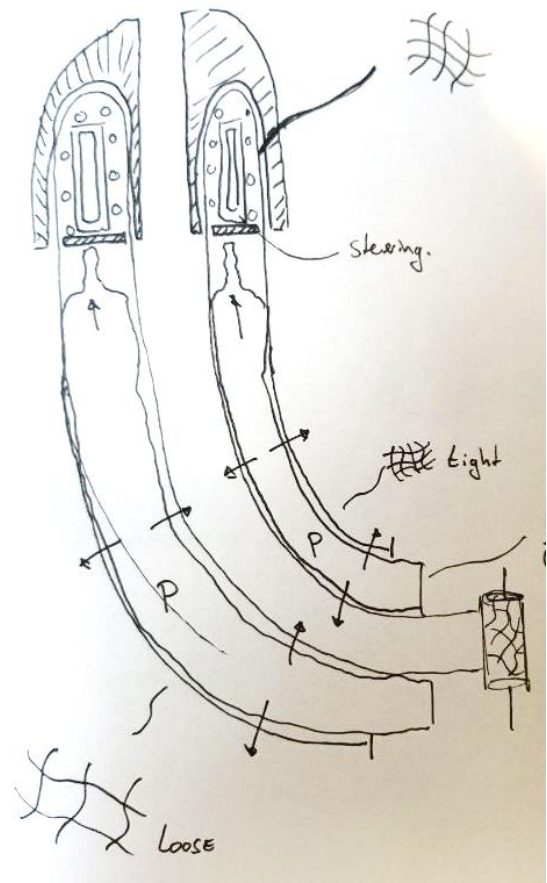


An actuated donut shaped tip continually everts and inverts in on itself, creating a forward rolling motion. This pushes the inverted tube around it forward, elongating the design as the tubing rolls off the posterior spool.

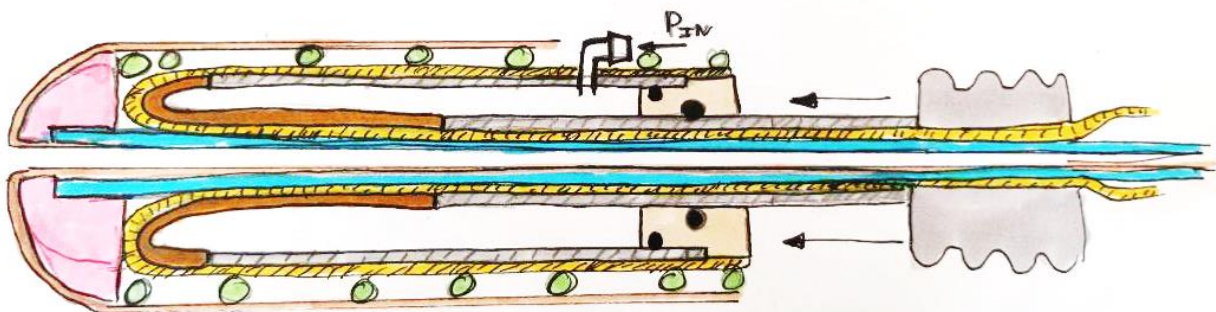


A central lumen with horizontal platforms attached along its length. The individual platforms are orientable relative to each other using multiple (individually expandable) pneumatic chambers. Thus enabling steering of the shaft. Ball bearings are attached to the platforms to prevent friction upon contact with surfaces.

An Inflatable donut shaped balloon with a steel wire mesh tube everted around it. The forward expansion of the balloon drives the eversion to the steel mesh tubing. The configuration of the meshing changes from loose large diamonds to small tightknit diamonds during the eversion. A custom steerable tip is placed on the front of the expanding balloon.



A design similar to the Flextendoscope but with a manual "plunger" (light gray) that is attached to the inverted tube (orange) instead of the slider. The plunger can be pushed to actuate the elongation of the design.

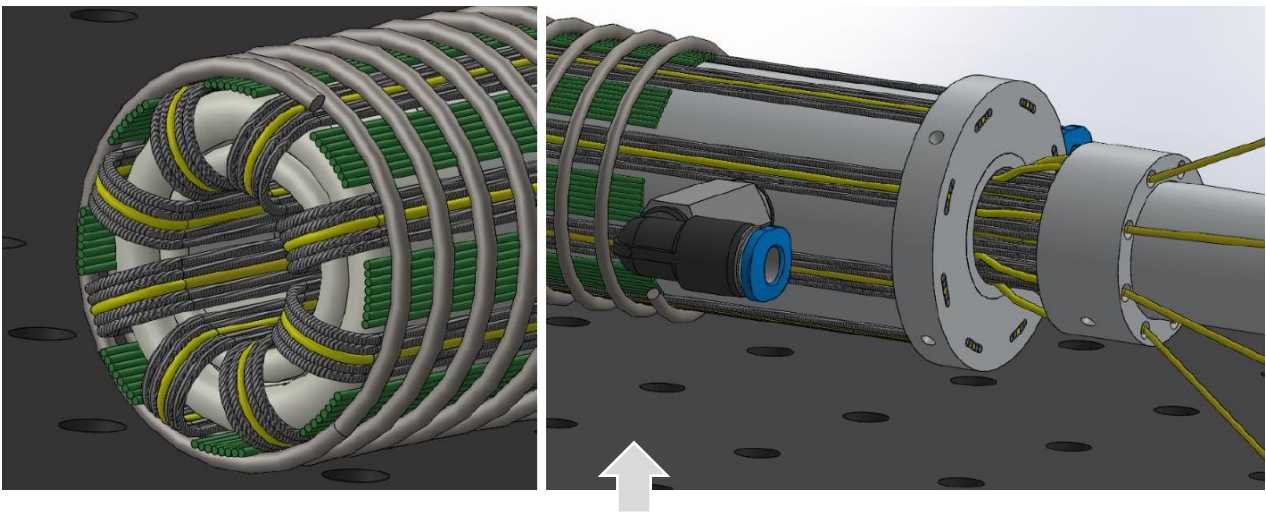


# D

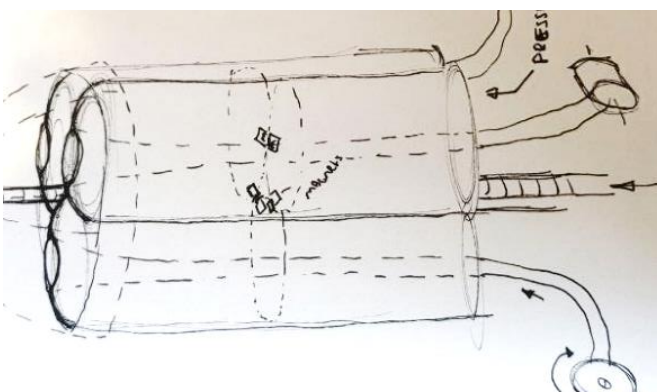
## APPENDIX:

### STEERABLE FLEXTENDOSCOPE CONCEPTS

This appendix contains some concept ideas of how the Flextendoscope design might be made steerable. Some of the ideas are worked out in more detail than others.



The design could be made steerable by separating eight cables (yellow) positioned equally spaced around the circumference of the intermediate shaft layer. By actively varying the length of these eight cables relative to each other (using small actuators) the direction of the eversion process might be controlled.



By placing multiple inverted tubes around the circumference of the shaft and individually controlling their everted lengths the direction of the shaft as a whole can be controlled.

The design could be made steerable at the front by placing a custom steerable tip on top of or inside the inverted tube. In this example the custom tip consist of two springs, one inside the other, with three hydraulic segments inside the circumferential space between the two springs. By changing the volume of the hydraulic segments relative to each other the springs can be bend in any direction and to a varying degree, enabling steering.

